The Role of 11β-Hydroxysteroid Dehydrogenase Type 1 in Bile Acid Homeostasis

Inauguraldissertation

zur

Erlangung der Würde eines Doktors der Philosophie

vorgelegt der

Philosophisch-Naturwissenschaftlichen Fakultät

der Universität Basel

von

Carlos Alberto Penno

aus Fraiburgo, Brasilien

Basel, 2013

Genehmigt von der Philosophisch-Naturwissenschaftlichen Fakultät

auf Antrag von

Prof. Dr. Alex Odermatt

Prof. Dr. Michael Arand

Basel, den 26.03.2013

Prof. Dr. Jörg Schibler

Dekan

TABLE OF CONTENTS

1. ABBREVIATIONS

11β-HSD1	11β-hydroxysteroid dehydrogenase type 1
7-oxoLCA	7-oxolithocholic acid
7-oxoDCA	7-oxodeoxycholic acid
BA(s)	Bile acid(s)
BACS	Bile acid-CoA synthase
CA	Cholic acid
CDCA	Chenodeoxycholic acid
FXR	Farnesoid X receptor
GC(s)	Glucocorticoid(s)
GR	Glucocorticoid receptor
GRE	Glucocorticoid response elements
G-7-oxoLCA	Glyco-7-oxolithocholic acid
H6PDH	Hexose-6-phosphate dehydrogenase
NADPH	Nicotinamide adenine dinucleotide phosphate
NRF2	Nuclear factor (erythroid-derived 2)-like 2
PGC1α	Peroxisome proliferator-activated receptor-γ coactivator-1α
T-BAs	Tauro-conjugated bile acids
T-7-oxoLCA	Tauro-7-oxolithocholic acid
VLCS	Very long-chain coenzyme A synthetase
VLCSH2	Very long-chain acyl-CoA synthetase homolog 2
WT	Wild-type

2. SUMMARY

Bile acids (BAs) are important modulators of metabolic functions such as lipid, triglyceride and glucose homeostasis. Intrahepatic accumulation of BAs is known to cause liver injury in cholestatic conditions, where normal trans-hepatic BA flow is impaired due to pathological conditions or induced by toxic drugs. Therefore, it is important to understand the mechanisms of BA homeostasis regulation and to identify novel players and characterize their functions. The main goal of the present work was to investigate the impact of altered hepatic glucocorticoid activation by the enzyme 11β-hydroxysteroid dehydrogenase type 1 (11β-HSD1) on BA homeostasis and to unravel the mechanisms of adaptations in a scenario of impaired 11β-HSD1 function. In order to achieve this goal, we developed and validated an ultra-performance liquid chromatography tandem mass spectrometry (UPLC-MS/MS) method for the quantification of a total of 24 BAs, including 11 unconjugated, 6 glycine-conjugated and 7 taurine-conjugated BAs, in biological matrices (serum/plasma and tissues) and cell culture supernatants. This method was validated and applied in a side project in which potential time-dependent changes of BAs in plasma from sham-operated and uninephrectomized male Sprague-Dawley rats were investigated. Several primary and secondary BAs were transiently elevated one week after uninephrectomy, followed by normalization thereafter. Using liver microsomal preparations and recombinant enzyme we then tested whether 11β-HSD1, in addition to its well-known role in the conversion of inactive to active glucocorticoids, is able to reduce 7-oxo BAs. We found that human 11β-HSD1 reduces the secondary BA 7-oxolithocholic acid (7-oxoLCA) mainly to chenodeoxycholic acid (CDCA) and to lesser amount to ursodeoxycholic acid (UDCA). 11β-HSD1 exclusively catalyzed the oxoreduction of 7-oxoLCA, in contrast to its role in the interconversion of glucocorticoids. The enzyme also metabolized 7-oxoLCA-glycine and -taurine conjugates. Furthermore, we compared 7-oxoLCA metabolism by human 11β-HSD1 with that of other species, including canine, guinea-pig, rat, mouse and hamster and we observed species-specific differences. While recombinant mouse and rat 11β-HSD1 converted 7-oxoLCA to equivalent amounts of CDCA and UDCA, the

hamster and canine enzymes were stereoselective, producing mainly CDCA similar to the human enzyme. Surprisingly, guinea-pig 11β-HSD1 did not reduce 7-oxoLCA. The analysis of circulating BA profiles of several species confirmed earlier observations by other investigators, that 7-oxoLCA and its glycine-conjugated (G-7-oxoLCA) metabolite are abundant BAs in guinea-pigs compared with other species. These findings suggest that the lack of 11β-HSD1 oxoreductase activity on 7-oxoLCA in guinea-pigs is responsible for its elevated circulating levels. Next, we hypothesized that 7-oxoLCA might be a biomarker of impaired 11β-HSD1 activity. Analysis of BAs in serum from liver-specific 11β-HSD1 deficient mice revealed 18-, 47- and 7-fold elevation of 7-oxoLCA, its taurine and glycine conjugates compared with wild-type mice, respectively. In addition, 7-oxoLCA and its taurine conjugate were 2- and 6-fold elevated in liver from liver-specific 11β-HSD1 deficient mice. Moreover, BA profiles in serum and liver of liver-specific 11β-HSD1 deficient mice indicated a disturbed BA homeostasis. Circulating and intrahepatic levels of several unconjugated BAs species were up to 16-fold significantly elevated in liver-specific 11β-HSD1 deficient compared with wild-type mice. To pinpoint the molecular mechanism of altered BAs profiles, gene expression analysis was performed. The results suggest FXR-dependent decrease of BA synthesis, a compensatory effect to counteract the intrahepatic accumulation of BAs. In addition, the enzymes responsible for BA conjugation with coenzyme A, an intermediate step in BAs amidation, named *VLCS* and *VLCSH2* displayed significantly lower expression levels in liver from liver-specific 11β-HSD1 deficient compared with wild-type mice. The decreased BA conjugating machinery in the liver of liver-specific 11β-HSD1 deficient mice may account for the elevated intrahepatic levels of unconjugated BAs observed. Moreover, the expression of *OATP4*, a basolateral BA transporter responsible for the uptake of unconjugated BAs from the circulation into hepatocytes presented reduced expression levels and may account for the significant elevation of several circulating unconjugated BAs found in liver-specific 11β-HSD1 deficient mice.

In conclusion, we demonstrated an important role of 11β-HSD1 in the oxoreduction on 7-oxoLCA and provided evidences that 7-oxoLCA its taurine conjugate are functional biomarkers of impair 11β-HSD1 activity. Circulating concentrations of these 7-oxo BAs may find application in the assessment of the therapeutic efficacy of 11β-HSD1

inhibitors. Moreover, we described for the first time the impact of intrahepatic glucocorticoid regeneration deficiency on BA homeostasis in mice. Our findings indicate that 11β-HSD1 is an important modulator of BAs homeostasis, and potential disturbances of BA homeostasis must be taken into account when assessing the safety of 11β-HSD1 inhibitors, with particular attention to cholestatic patients and patients receiving combined therapeutic regimens with drugs known to induce liver injury.

3. INTRODUCTION

A short historical overview of the research on BAs with a focus on their physiological properties is presented. Then, the biochemistry of BA metabolism, including pathway of synthesis, conjugation and transporters will be discussed briefly, followed by an overview of the key modulators of BA homeostasis. Finally, the goals and objective of this PhD thesis will be introduced.

3.1 BILE ACID RESEARCH, A HISTORICAL OVERVIEW

BAs are together with cholesterol, phospholipids and bilirubin the main components of bile (Trauner and Boyer 2003). Although, it took until 1848 when Prof Adolph Strecker finally succeeded in isolating the two most abundant acids taurocholic acid and glycocholic acid from ox-gall, the research on bile constituents started at much earlier stage with the research of Prof Leopold Gmelin, Prof Luis Jacques Thénard and Prof Jöns Jacob Berzelius (Wieland 1928). In 1885, Prof Mylius discovered choleic acid, an acid very similar in composition to desoxycholic acid (DCA), which was discovered later in 1886 (Wieland 1928). It was found, however, that choleic acid was not a new chemical entity, but an association of fatty acids such as stearic acid, palmitc acid, oleic acid to desoxycholic acid (Wieland 1928). The association of fatty acids with desoxycholic acid was of such intensity that no dissociation into constituents occurred during salt formation or dissolution (Wieland 1928). These additive properties of desoxycholic acid were further elucidated in following experiments and showed they were not restricted to fatty acids, but it was found that hydrocarbons, alcohols, esters, and phenols could also bind to desoxycholic acid (Wieland 1928). Moreover, the alkali salts of desoxycholic acid, and also those of cholic acid and its conjugates are able to absorb lipophilic substances such as cholesterol, naphthalene, camphor, alkaloids and others (Wieland 1928). These initial studies provided the basis for the assumption of a potential physiological role of the bile to enable the diffusion of insoluble substances through the intestinal cells, by emulsifying them as soluble choleinates (Wieland 1928). In 1927, Prof Heinrich Otto Wieland was awarded the Nobel Prize in Chemistry for his

work on BAs, which clarified the mechanism by which bile plays a role in the absorption of food in the intestine and for performing structural studies of BAs.

3.2 BILE ACID METABOLISM

3.2.1 SYNTHESIS AND CONJUGATION

BAs are synthesized from cholesterol in the liver and secreted from hepatocytes into the bile canaliculi and thereafter stored in the gall bladder (Thomas, Pellicciari et al. 2008). Importantly, the pathway for BA synthesis is the primary pathway for cholesterol catabolism and approximately 500 mg of cholesterol are converted into BAs every day by the adult liver (Russell 2003; Thomas, Pellicciari et al. 2008). After food intake, BAs are delivered into the lumen of the small intestine where they act as emulsifiers of dietary lipids, cholesterol and fat-soluble vitamins, which are incorporated into lipoproteins and transported to the liver (Russell and Setchell 1992). About 95% of BAs delivered to the small intestine are reabsorbed in the gut and only approximately 5% eliminated by the faeces (Russell 2003). The BAs eliminated are resynthesized in the liver through a pathway that involves at least 17 different enzymes (Russell 2003). The final products of this pathway are known as primary BAs: cholic acid (CA) and chenodeoxycholic (CDCA) acid in rats and humans, and β-muricholic acid in mice. After reaching the intestine, the chemical diversity of the BA pool is extensively broadened by the actions of anaerobic bacteria, which convert BAs into several secondary and tertiary compounds, hence guarantee a repertoire of hydrophobic entities needed for a complete solubilisation of nutrients (Hylemon and Harder 1998). BA synthesis involves several steps, which can be distinguished as follows: 1) modification of the ring structure of cholesterol, 2) further modifications to the ring structure, 3) oxidation and shortening of the side chain, and 4) conjugation of the BA with an amino acid (Russell 2003) (please refer to Figure 1 for a simplified scheme of BA biosynthesis). There are two pathways through which cholesterol is fluxed to form BAs: 1) the classic pathway (neutral, accounting for 75% of total BA pool) and 2) the alternative pathway (acidic, accounting for the remaining 25% of BAs) (Russell and Setchell 1992; Russell 2003). The two main products of this pathway are CA and CDCA (Russell 2003). Cholesterol

7α-hydroxylase is the first and rate-limiting enzyme of the classical pathway and is responsible for most of total BA synthesis (Ishibashi, Schwarz et al. 1996; Schwarz, Lund et al. 1996), whereas sterol-27-hydroxylase is the first enzyme of the alternative pathway. Interestingly, 27-hydroxylase can also hydroxylate cholesterol at carbons 24 and 25 to from 24- and 25-hydroxycholesterol, respectively (Lund, Björkhem et al. 1993) (Schwarz, Russell et al. 1998; Schwarz, Russell et al. 2001). Thereafter, oxysterols are 7α-hydroxylated by the CYP7B1 oxysterol 7α-hydroxylase (Martin, Reiss et al. 1997; Schwarz, Lund et al. 1997) or by CYP39A1, which remains a liver microsomal enzyme poorly characterized (Russell 2003).

Ring structure modifications take place on 7α-hydroxylated intermediates derived from cholesterol and 7α-hydroxylated oxysterols which are converted into their 3-oxo, Δ4 forms by microsomal 3β-hydroxy-Δ5-C27-steroid oxidoreductase (HSD3B7) (Russell 2003). The reaction involves isomerization of the double bond from the 5 to the 4 position and the oxidation of the 3β-hydroxyl to a 3-oxo group (Wikvall 1981; Furster, Zhang et al. 1996). The products of the last reaction can enter two routes: 1) the intermediate may be 12α-hydroxylated by microsomal CYP8B1 leading to CA formation (Li-Hawkins, Gafvels et al. 2002) and 2) the intermediate might escape 12α-hydroxylation and will be 5β-reduced by AKR1D1 (Δ4-3-oxosteroid 5β-reductase, a member of the aldo-keto reductases family) (Russell 2003) to form CDCA (Russell 2003). The last reaction of ring modification involves reduction of the 3-oxo group to an alcohol in the alpha stereoconfiguration and is catalyzed by 3α-hydroxysteroid dehydrogenase (AKR1C4) (Usui, Okuda et al. 1994), another member of the aldo-keto reductase family. The products of reactions of ring structure modification subsequently undergo progressive oxidation and shortening of the sterol side-chain. The first reaction in this series is catalyzed by 27-hydroxylase, which hydroxylates carbon 27, then oxidizes it to an aldehyde and subsequently to a carboxylic acid (Andersson, Davis et al. 1989; Dahlbäck and Holmberg 1990; Pikuleva, Babiker et al. 1998). These oxidized BA intermediates exit the mitochondria and are subsequently activated to their coenzyme A derivatives before side chain cleavage via peroxisomal β-oxidation. The first reaction is catalyzed by BA coenzyme A ligase (also known as BA coenzyme A

synthetase, BACS). This reaction can be accomplished by two enzymes: 1) very long-chain coenzyme A synthetase (VLCS) (a 620 amino acid protein of the endoplasmic reticulum and peroxisome and 2) very long-chain acyl-coenzyme A synthetase homolog 2 (VLCSH2) (Steinberg, Mihalik et al. 2000; Mihalik, Steinberg et al. 2002; Inoue, Yu et al. 2004). After activation of intermediates through BA ligase, the 25(R) isomers are converted into their 25(S) isomers by 2-methylacylcoenzyme A racemase, an enzyme localized in mitochondria and peroxisomes (Amery, Fransen et al. 2000; Kotti, Savolainen et al. 2000). Following this reaction, the products are next further dehydrogenated by FAD-containing peroxisomal branched chain acyl-coenzyme A oxidase to form 24,25-trans-unsaturated products (Russell 2003). There are two acyl-coenzyme A oxidases in humans and mice (ACOX1 and ACOX2). Interestingly, human and mouse are catalytically similar, whereas the rat enzymes have different substrate specificities (Van Veldhoven, Vanhove et al. 1992). The next step in the biosynthesis of BAs involves hydration and oxidation at the Δ24 bond and is catalyzed by the D-bifunctional protein (a complex peroxisomal enzyme of 736 amino acids) (Baes, Huyghe et al. 2000). The final step in the oxidation of the side chain is performed by peroxisomal thiolase 2, which cleaves the C24-C25 bond to form propionyl-coenzyme A and a C24-coenzyme A BA intermediate (Kannenberg, Ellinghaus et al. 1999).

The final stage of BA biosynthesis involves the amidation usually of glycine and taurine, to carbon 24. This reaction is catalyzed by peroxisomal BA coenzyme A: amino acid N-acyltransferase enzyme (Solaas, Ulvestad et al. 2000). Conjugation is an efficient process as more than 98% of BAs synthesized in liver are amidated (Russell 2003). Interestingly, there are species-dependent differences as to the substrates of the N-acyltransferase enzyme between human and mice. While the human enzyme accepted BA coenzyme A thioester, taurine and glycine, the mouse enzyme displayed a preference to taurine (Falany, Johnson et al. 1994; Falany, Fortinberry et al. 1997). The conjugation of BAs increases their amphipathicity thus enhancing their solubility, and also making them impermeable to cells membranes (Meier 1995).

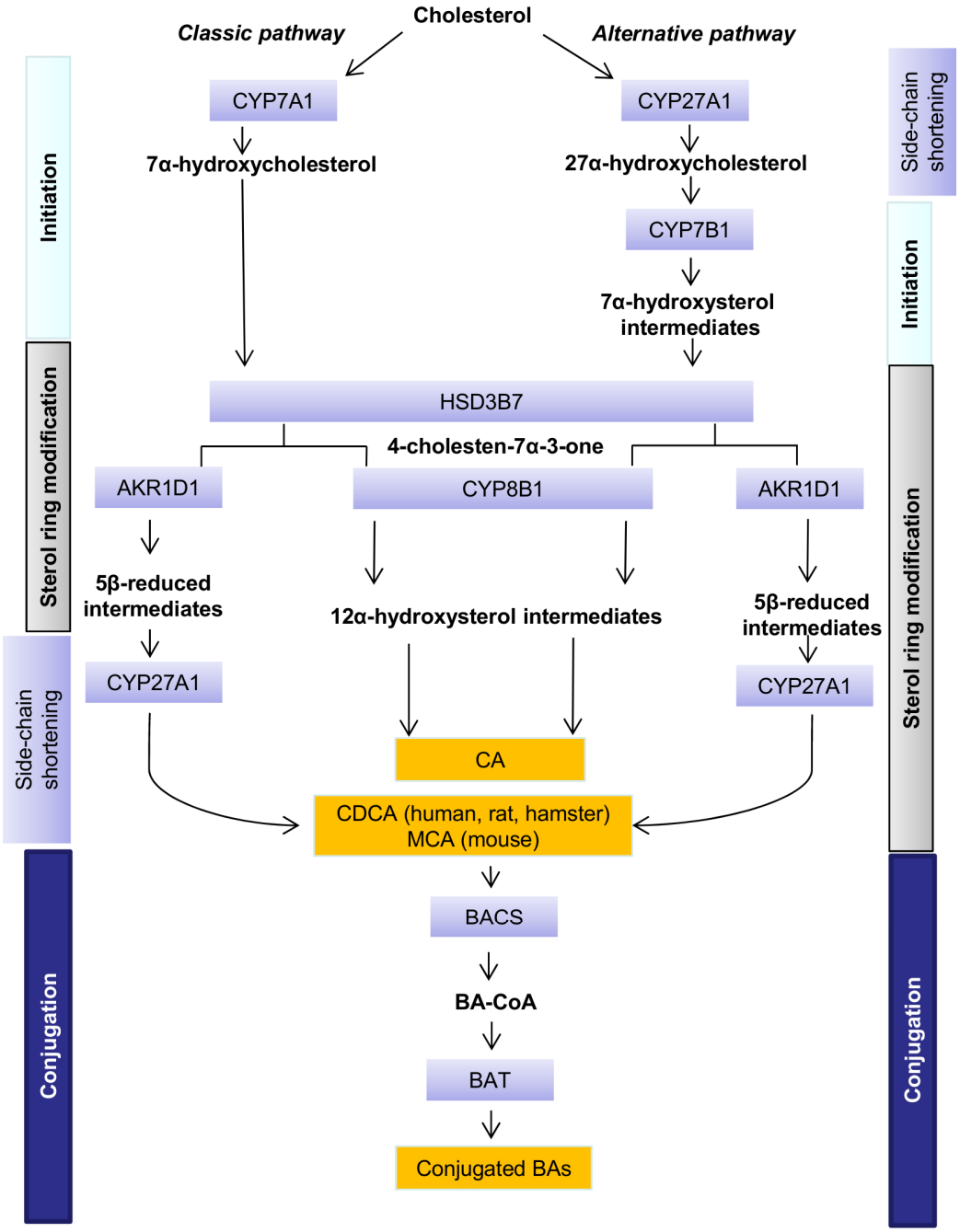

Figure 1. Simplified scheme of the BA synthesis pathway. Adapted from (Thomas, Pellicciari et al. 2008).

3.2.2 BILE ACID TRANSPORT SYSTEMS

Owing to the fact that conjugated and free BAs are not able to cross membranes (Russell 2003), dedicated transport systems are required to enable BA flow into an out of cells.

3.2.2.1 HEPATIC TRANSPORTERS

The active transport of BAs from blood into the bile represents the major driving force for bile flow (Trauner and Boyer 2003). The hepatocyte is a polarized cell with basolaterol (sinusoidal) and apical (canalicular) membrane domains (Figure 2). Overall, BA transporters in the liver include those involved on BA uptake, hepatocyte efflux and canalicular efflux. Hepatic uptake transport starts at the basolateral membrane, which faces the portal blood plasma via the fenestrae of the sinuidal endothelial cells and the space of Disse. After uptake into hepatocytes, BAs diffuse to the canaliculi for subsequent excretion. This step is considered the rate-limiting step of bile secretion since transport occurs against a high concentration gradient into the bile (Trauner and Boyer 2003). It is generally assumed that BA concentrations within hepatocytes are in the micromolar range, whereas canalicular concentration are as much as 1000-fold higher (Stieger, O´Neil et al. 1992).

Hepatic uptake transporters: The uptake of BAs occurs against a 5- to 10-fold concentration gradient between the portal blood and the hepatocyte and is mediated by two mechanism, sodium-dependent and independent systems (Nathanson and Boyer 1991). Under normal conditions, BAs are removed from portal blood predominantly by zone 1 (periportal) hepatocytes (Jones, Hradek et al. 1980; Groothuis, Hardonk et al. 1982). In this zone, the major hepatic uptake system includes the high-affinity Na+-dependent BA transporter NTCP (*SCLA1*) and a family of multi-specific organic anion transporters (OATPs; *SCL21A*) that are able to mediate Na+-independent BA uptake. The major uptake transporters are introduced as follows:

1) Sodium-dependent uptake via NTCP: The Na+-dependent system is responsible for the uptake of >80% of conjugated taurocholate and <50% of unconjugated cholate (Kullak-Ublick, Stieger et al. 2000; Meier and Stieger 2002). Due to the

fact that BAs are extensively conjugated, NTCP is the most relevant sodium-dependent BA uptake system (Hagenbuch, Scharschmidt et al. 1996). The transporter is localized exclusively at the basolateral membrane of differentiated mammalian hepatocytes and its expression is restricted to hepatocytes (Ananthanarayanan, Ng et al. 1994; Stieger, Hagenbuch et al. 1994). It transports all physiological BAs (e.g. taurocholate, glycocholate, taurodeoxycholate, tauroursodeoxycholate), although its transport activity is highest for the conjugated dihydroxy and trihydroxy BAs (Meier, Eckhardt et al. 1997; Kullak-Ublick, Stieger et al. 2000; Meier and Stieger 2002).

2) Sodium-independent uptake via OATPs. In contrast to sodium-dependent BA uptake, the OATPs consist of several different gene products, are sodium-independent and display specificity for a large range of substrates not only including conjugated and free BAs, but also bromosulfophthalein (BSP), bilirubin, 4,4′-diisothiocyanostilbene-2,2′-disulfonic acid (DIDS), cardiac glycosides, steroids, linear and cyclic peptides, mycotoxins, organic cations, and various pharmaceuticals such as paravastatin (Meier, Eckhardt et al. 1997; Kullak-Ublick, Stieger et al. 2000; Meier and Stieger 2002; Trauner and Boyer 2003). Nevertheless, it is generally accepted that sodium-independent transport systems are quantitavely not as significant as sodium-dependent uptake. (Kullak-Ublick, Stieger et al. 2000). OATP1 is a basolateral transporter not only expressed in the liver, but also on the apical membrane of the kidney proximal tubular cells, and choroid plexus epithelial cells (Bergwerk, Shi et al. 1996; Angeletti, Novikoff et al. 1997). Functionally, OATP1 transports taurocholic acid, cholic acid, glycocholic acid, taurochenodeoxycholic acid, tauroursodeoxycholic acid, taurodeoxycholic acid, taurohyodeoxycholic acid and also a wide range of other substrates (Meier, Eckhardt et al. 1997; Kullak-Ublick 1999; Kullak-Ublick, Stieger et al. 2000; Meier and Stieger 2000; Meier and Stieger 2002). Studies using oocytes injected with total rat liver mRNA revealed that OATP1 is responsible for 80% of sodium-independent taurocholate uptake (Hagenbuch, Scharschmidt et al. 1996). In contrast to OATP1, OATP2 is expressed in the retina, in endothelial cells of the

blood-brain barrier and on the basolateral membrane of hepatocytes and on epithelial cells in the choroid plexus (Gao, Stieger et al. 1999; Reichel, Gao et al. 1999; Soroka, Lee et al. 2001). OATP2 is predominantly expressed in perivenous/pericentral hepatocytes, in contrast to OATP1 whose expression is homogenously distributed throughout the liver (Kakyo, Sakagami et al. 1999; Reichel, Gao et al. 1999). With regard to substrate specificity, OATP2 is similar to OATP1, with similar affinities to BAs such as taurocholate and cholate. The third family member is OATP4, which similarly to OATP1 and 2 is a multi-specific transporter including taurocholate and several other substrates (Cattori, Hagenbuch et al. 2000); however, a role in the transport of unconjugated BAs has also been proposed (Csanaky, Lu et al. 2011).

Basolateral efflux transporters: They are responsible to remove BAs from the hepatocyte back into sinusoidal blood and are induced under cholestatic conditions. Major transporters in this category belong to the multidrug resistance subfamily such as MRP3, MRP4, and also organic solute transporter - OSTα/β. Originally, it was believed that MRP3 plays a role in BA efflux. It was then demonstrated that MRP3 knockout mice have no differences in serum BA concentrations and hepatic injury after bile duct ligation compared with wild-type controls (Belinsky, Dawson et al. 2005; Zelcer, Wetering et al. 2006). Moreover, human MRP3 transports BAs only with low affinity (Akita, Suzuki et al. 2002). On the other hand, evidence pointed out that MRP4 might have a protective role on hepatocytes due to the fact that cholestasis induced by bile duct ligation in MRP4 knockout mice resulted in aggravated liver toxicity as compared with bile duct ligated wild-type controls (Mennone, Soroka et al. 2006). Moreover, upon cholestatic conditions MRP4 expression was shown to be elevated in human and rat livers (Denk, Soroka et al. 2004; Gradhand, Lang et al. 2007).

The contribution of organic solute transporters-α/β (OST) to the adaptive response to cholestatic liver injury has been examined by OST-α gene deletion in mice (Soroka, Mennone et al. 2010). Surprisingly, OST-α deficiency resulted in a substantial attenuation of cholestatic hepatic injury, which was mediated by an elevated urinary excretion of BAs concomitantly with an increased expression levels of MRP3 and MRP4

in the liver (Soroka, Mennone et al. 2010). Although these findings suggest a participation of OST-α/β in hepatic BA transport, further studies are warranted to elucidate their physiological relevance in this organ (Kock and Brouwer 2012).

Canalicular efflux transport: BA transport is carried out by ATP-dependent proteins of the ABC transporter superfamily, e.g. multidrug-resistance proteins (MDRs) and MRPs. Major transporters in this category includes the bile salt export pump (BSEP), P-glycoprotein (P-gp, MDR1a/1b) and the multidrug resistance protein 2 (MRP2). BSEP is considered the major canalicular bile salt transport system and is expressed exclusively in the canalicular membrane of hepatocytes (Kock and Brouwer 2012). BSEP presents a narrow substrate spectrum and is thus primarily responsible for the transport of monoanionic, conjugated BAs such as taurochenodeoxycholic acid, taurocholic acid, taurodeoxycholic acid, and glycocholic acid. In humans, BSEP deficiency results in progressive familial intrahepatic cholestasis type 2 (PFIC2), a fatal liver disease with greatly reduced bile flow (Strautnieks, Bull et al. 1998). However, in mice BSEP knockout leads to nonprogressive, persistent intrahepatic cholestasis manifested by significantly less severity than PFIC2, suggesting an alternative BA canalicular efflux transport in mice compensates for the loss of BSEP. These findings led to the discovery that multidrug resistance (MDR) transporters such as MDR1a and MDR1b can compensate for the loss of BSEP in mice (Wang, Salem et al. 2001; Wang, Chen et al. 2009). Moreover, MDR1a was shown to transport BAs in mice; however, with a lower affinity (Lam, Wang et al. 2005). On the other hand, MDR2-null mice exhibited similar BA excretion into bile compared with wild-type mice suggesting a minor role in BA transport. Nevertheless, its importance on biliary excretion of phospholipids in the canalicular membrane suggests a role in protecting the biliary tree from BA toxicity by forming mixed phospholipid-BA micelles (Elferink, Tytgat et al. 1997).

MRP2 is an organic anion transporter expressed in the apical (canalicular) membrane of hepatocytes, involved in the transport of bile salt sulfates conjugate such as taurolithocholate-3-sulfate, but not monoanionic bile salts such as taurocholate (Gerk and Vore 2002). MRP2 is involved also in the biliary transport of other endogenous

substrates such as glutathione, bilirubin glucuronide and a broad range of exogenous compounds (Jemnitz, Heredi-Szabo et al. 2010).

3.2.2.2 INTESTINAL TRANSPORTERS

After reaching the intestine, BAs are extensively reabsorbed and transported back to the liver via the enterohepatic circulation. It is generally accepted that the BA transport in the enterocytes consists of three major components: 1) apical uptake of conjugated BAs in terminal ileum via a sodium-dependent mechanism; 2) intracellular BA transport in the enterocytes mediated via cytosolic BA-binding protein (IBABP) and 3) anion exchange mechanism for the basolateral efflux of BAs from enterocytes.

Apical transport: Apical transport in the enterocyte occurs via mainly three mechanisms: 1) passive diffusion of unconjugated BAs in small and large intestine; 2) uptake of BAs in the terminal ileum via a sodium-dependent mechanism and 3) sodium-independent anion exchange mechanism in proximal jejunum (Klaassen and Aleksunes 2010). The well characterized ASBT (Apical sodium bile acid transporter, *SLC10A2*) is expressed on the apical surface of ileal enterocytes and transports conjugated and unconjugated BAs, with higher affinity for dihydroxy BAs such as CDCA and DCA compared with trihydroxy BAs such as cholate, taurocholate, and glyco-cholate (Craddock, Love et al. 1998). Faecal BA excretion is increased in ASBT-null mice, leading to a reduced total BA pool (Dawson, Haywood et al. 2003). Moreover, several loss-of-function mutations in the ASBT gene cause primary BA malabsorption that is characterized by diarrhea, fat malabsorption, and malnutrition (Wong, Oelkers et al. 1995; Oelkers, Kirby et al. 1997).

After transport across the enterocyte membrane, BAs are bound to IBABP, which belongs to a family of intracellular lipid-binding proteins that reversibly bind BAs and other lipids (Trauner and Boyer 2003). Its expression is limited to the ileum, with low expression found in cholangiocytes (Lin, Kramer et al. 1990). However, further studies, including the generation of IBABP-null mice, would shed light on the physiological importance for BA homeostasis.

Apical efflux transporter in the intestine: MDR1a/Pgp is expressed at the apical surface of enterocytes (Panwala, Jones et al. 1998) and plays a role in effluxing drugs from enterocytes back into the intestinal lumen and thereby affecting absorption of orally administration medication (Klaassen and Aleksunes 2010). Similar, to the liver, MRP2 exerts apical efflux transport of BAs in enterocytes.

Basolateral efflux transporters in the intestine: Similar to the liver, OST-α and OST-β are responsible to efflux BAs and other substrates such as conjugated steroids across the basolateral membrane in the intestine (Seward, Koh et al. 2003). OST-α-null mice presented with hypertrophy of the small intestine and a reduced BA pool, reduced serum BAs, reduced cholesterol and triglycerides levels, and exhibited several compensatory gene expression changes, including higher intestinal, hepatic and renal MRP3 and lower CYP7A1 expression levels (Ballatori, Fang et al. 2008). Furthermore, combined loss of OST-α and MRP3 in female OST-α/MRP3-null mice results in disrupted transileal transport of taurocholic acid (Rao, Haywood et al. 2008). The current known substrates of OST-α/β includes the major species of BAs such as glycine and taurine conjugates of cholic acid, deoxycholic acid, chenodeoxycholic acid, and ursodeoxycholic acid (Ballatori, Christian et al. 2005).

3.2.2.3 RENAL TRANSPORTER

BAs which escape first-pass clearance by the liver (10 to 50%, depending on the BA species) are filtered at the glomerulus and reabsorbed in the proximal convoluted tubule (Wilson, Burckhardt et al. 1981). Under normal conditions, urinary BA losses are 1-2% of total renal BA input; however, renal elimination of sulfated and glucuronidated BAs become an important adaptive mechanism under cholestatic situations (Trauner and Boyer 2003). Similar to the ileocytes, renal proximal tubule epithelium expresses the ASBT and OST-α/β (Ballatori, Christian et al. 2005), which guarantee the efficient renal influx of BA back into the circulation. On the other hand, apical efflux transporters such as MRP2, MRP4 and MDR1b are mainly responsible for renal secretion of chemical into urine (Klaassen and Aleksunes 2010).

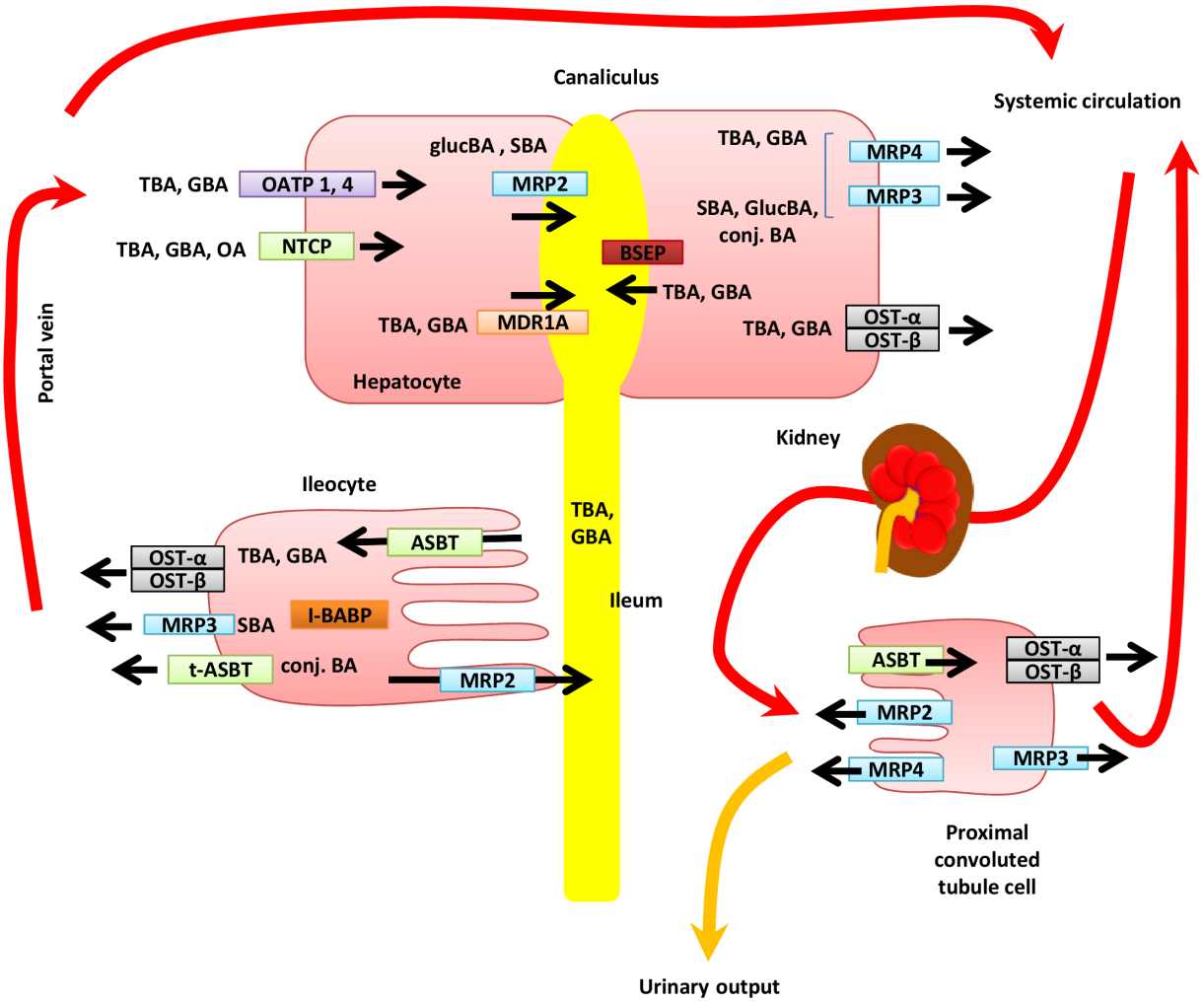

Figure 2. Overview of the bile acid transport system in hepatocytes, ileocytes and tubule cells is shown. Arrows indicate BA flow. glucBA: glucoronidated-BA, SBA: sulfated-BA; TBA: tauro-BA; GBA: glyco-BA. (Adapted from (Thomas, Pellicciari et al. 2008)).

3.2.3 Biotransformation of BAs

During the enterohepatic circulation, primary BAs escaping ileal transport, approximately 400-800 mg/day, are substrates for intense bacterial biotransformation and structural modification by the action of facultative and anaerobic bacteria to give rise to secondary BAs, therefore broadening their chemical structures and properties (Ridlon, Kang et al. 2006). Biotransformation reactions consists mainly of deconjugation by bile salt hydrolases (BSH), hydroxyl group dehydrogenation/epimerization at position

3-, 7- and 12- by hydroxysteroid dehydrogenases (HSDs) and dehydroxylation at position 7α- and 7β- (Ridlon, Kang et al. 2006). Epimerization is the reversible change in stereochemistry from α to β (or vice versa) with the generation of stable oxo-bile acid intermediates (Ridlon, Kang et al. 2006). 3α/β-HSDs specifically catalyze the reversible, stereo-specific oxidation/reduction between 3oxo- and 3α- or 3β-hydroxy BAs and seem to favour the 3α-position (Macdonald, Hutchison et al. 1983). On the other hand, 7α-/7β- and 12α-/12β-HSDs catalyze the reversible, stereospecific oxidation/reduction of the 7α-/7β- and 12α-/12β- hydroxyl groups of BAs, respectively (Ridlon, Kang et al. 2006). The action of these enzymes increases the amount of β-hydroxylated BAs, which reach the liver via the enterohepatic circulation; however, they do not accumulate owing to their efficient epimerization (Ridlon, Kang et al. 2006). In the human colon, several bacterial strains, including *Escherichia coli*, *Bacteroides fragilis* and *Bacteroides intestinalis* express 7-HSDs that generate 7-oxoDCA from CA and 7-oxoLCA from CDCA and UDCA (Macdonald, Williams et al. 1975; Fukiya, Arata et al. 2009). In spite of these reactions, it is generally assumed that 7α-dehydroxylation is the most important bacterial bile salt biotransformation in the human colon due to the fact that secondary BAs such as DCA and LCA predominate in human faeces and owing to the inability of human liver to 7α-hydroxylate these secondary BAs back to their respective primary forms (Ridlon, Kang et al. 2006).

3.2.4 MAJOR REGULATORS OF BA HOMEOSTASIS

3.2.4.1 FARNESOID X RECEPTOR (FXR)

BAs modulate their own biosynthesis from cholesterol through mechanism of feedback regulation, which is controlled by the entero-hepatic system. Possibly, the first layer of regulation involved in this intricate regulatory mechanism involves the FXR. FXR is an intracellular BA sensor controlling BA homeostasis through orchestrating enterohepatic recycling, transport and biosynthesis of BA, thus allowing the organism to maintain a constant BA pool and to mediate hepatic protective responses to counteract BA accumulation in pathophysiological and toxicological situations (Thomas, Pellicciari et al. 2008; Klaassen and Aleksunes 2010). FXR is not exclusively expressed in the liver.

The intestine, the kidney and the adrenal cortex are also organs of abundant FXR expression (Bookout, Jeong et al. 2006). Some conjugated and free BAs are endogenous ligands that activate FXR, among them CDCA and its conjugates present the most potent affinity in the range of EC50 of 4.5 – 10 μM (figure 3) (Makishima, Okamoto et al. 1999; Parks, Blanchard et al. 1999; Wang, Chen et al. 1999). After activation, FXR induces the expression of the short heterodimer partner (SHP-1, NR0B2), an atypical nuclear receptor capable of interfering with the activity of several nuclear receptors such as the liver receptor homologue 1 (LRH1, *NR5A2*) and liver X receptor-α (LXR-α, *NR1H3*) to repress the expression of *CYP7A1* and *CYP8B1*, two main enzymes in the biosynthesis of BAs (Figure 3) (Goodwin, Jones et al. 2000; Zhang and Chiang 2001; Brendel, Schoonjans et al. 2002; Båvner, Sanyal et al. 2005). At the same time, hepatic FXR activation increases BA conjugation (Pircher, Kitto et al. 2003) and canalicular efflux by inducing the transcription of BSEP, MDR2 and MRP2 thus promoting bile flow and preventing accumulation of toxic BAs in the liver (Eloranta and Kullak-Ublick 2005). In addition, FXR decreases hepatic BA uptake by down-regulating *NTCP* gene expression in isolated hepatocytes (Denson, Sturm et al. 2001). Therefore, FXR-null mice develop increased hepatic necrosis due to intrahepatic cholestasis, which demonstrates the importance of FXR mediated BA homeostasis (Zollner, Fickert et al. 2003; Cui, Aleksunes et al. 2009). In the intestine, FXR promotes expression of the ileal BA binding protein (I-BABP, *FABP6*), basolateral BA transporters OST-α/β, ASBT expression in mouse and human ileum, and fibroblast growth factor 19 (FGF19 or FGF15 in mouse), which subsequently through an autocrine and SHP-independent mechanism represses *CYP7A1* gene in the liver (Holt, Luo et al. 2003; Houten and Auwerx 2004; Moschetta, Bookout et al. 2004; Inagaki, Choi et al. 2005; Sinha, Chen et al. 2008). Surprisingly, a recent study suggests that FGF19 autocrine signalling from the intestine plays a dominant role in FXR mediated *CYP7A1* gene repression over the FXR-SHP pathway, while FXR/SHP pathway was important for supressing *CYP8B1* (Kong, Wang et al. 2012). Further studies are needed to clarify the contribution of each pathway in supressing BA synthesis. Overall, the collective effect of BA-mediated FXR is to prevent accumulation of toxic BA accumulation by stimulating BA efflux in the canaliculus and preventing BA uptake from the portal blood. In addition, BA

accumulation in the enterocytes activates FXR, which in turn represses BA absorption and biosynthesis (Thomas, Pellicciari et al. 2008).

3.2.4.2 PREGNANE-X RECEPTOR (PXR)

The role of PXR in regulating BA synthesis was identified by using the PXR agonist pregnenolone 16α-carbonitrile (PCN) which repressed hepatic *CYP7A1* (Mason and Boyd 1978). In follow-up studies, these initial findings were confirmed by using PXR-deficient mice in which PCN-mediated repression of *CYP7A1* is absent (Staudinger, Goodwin et al. 2001). Other known direct agonists for human and murine PXR are lithocholic acid (LCA) and 5β-Cholestan-3α, 7α, 12α-triol (Goodwin, Jones et al. 2000). The effect of PXR on *CYP7A1* repression seems to be mediated by HNF4α and PGC1α, which are required for *CYP7A1* gene transcription (Bhalla, Ozalp et al. 2004). On the other hand, activation of PXR in intestinal cells was shown to induce FGF15 expression and a PXR response element is found in *FGF15* (Wistuba, Gnewuch et al. 2007). Interestingly, a recent study showed that PXR-null mice fed a lithogenic diet had a higher susceptibility to develop cholesterol gallstones, an effect which may be related to decreased *CYP7A1* gene expression, and consequently a reduced BA pool (He, Nishida et al. 2011). Moreover, PXR induces CYP3A enzymes, which are responsible for BA hydroxylation, BA conjugating enzymes such as SULT2A1 and UGTs, transporters such as MRP2 and OATP2, which strongly suggests that PXR activation is part of the organism´s adaptive response to reduce the burden of excessive BA levels and counteract BA toxicity (Staudinger, Goodwin et al. 2001; Kliewer and Willson 2002). Supporting this notion is the fact that PXR-null mice are more susceptible to hepatotoxicity of LCA, bile duct ligation and numerous experimental forms of cholestasis (Staudinger, Goodwin et al. 2001; Stedman, Liddle et al. 2005). In humans, rifampicin treatment has been used to reduce pruritus associated with cholestasis, an effect believed to be mediated by PXR (Hofmann 2002).

3.2.4.3 VITAMIN D RECEPTOR (VDR)

Several lines of evidence revealed that the VDR may act as an intestinal BA sensor, which protects the intestine from BA toxicity. BAs, particularly LCA, is an endogenous

VDR ligand, besides 1α,25-dihydroxyvitamin D3 (Makishima, Lu et al. 2002). Examples of functions of VDR in intestinal cells include the induction of CYP3A, SULT2A1, MRP3 and ASBT (Thummel, Brimer et al. 2001; Chen, Ma et al. 2003; Chatterjee, Echchgadda et al. 2005; McCarthy, Li et al. 2005). Similarly, in human hepatocytes treatment with VDR agonists induces the expression of VDR target genes, including *CYP3A*, *CYP2B* and *CYP2C*; however, further studies are needed to elucidate the role of VDR in the liver. In culture hepatocytes and using VDR-null mice, there is evidence suggesting that VDR agonists are able to repress *CYP7A1* expression, possibly through the FGF15 pathway since FGF15-null mice failed to repress *CYP7A1* upon 1α,25-dihydroxyvitamin D3 treatment (Han and Chiang 2009; Schmidt, Holmstrom et al. 2010). Despite these observations, the role of VDR in repressing BA synthesis is still controversial and further studies are needed to clarify its physiological and potential pharmacological applications (Nishida, Ozeki et al. 2009).

3.2.4.4 NUCLEAR FACTOR-E2-RELATED FACTOR 2 (NRF2)

Nrf2 is a transcription factor member of the basic leucine zipper family and is a crucial mediator of an adaptive response to counteract oxidative stress (Moi, Chan et al. 1994; Klaassen and Reisman 2010). Nrf2 binds to antioxidant response elements (AREs) in the regulatory regions of target genes and activates the transcription of genes involved in detoxification such as NAD(P)H quinone oxidorecutase 1 (Nqo1), heme oxidase-1, glutathione-S-transferase, and the glutathione synthesis enzymes glutamate cysteine ligases (Weerachayaphorn, Mennone et al. 2012). Moreover, increased hepatic expression of Nrf2-dependent *Nqo-1* is seen in cholestasis following bile duct ligation (BDL) in mice, suggesting its activation during cholestasis (Weerachayaphorn, Mennone et al. 2012). Nevertheless, Nrf2-null mice do not exhibit more severe hepatic injury after BDL, which could be explained by the decreased expression of *CYP7A1*, *CYP8B1* and *ASBT*, and increased *CYP3A11*, *BSEP* and *OST-α* mRNA expression levels. (Weerachayaphorn, Mennone et al. 2012). These findings suggest an important role of Nrf2 in the regulation of BA homeostasis in liver and intestine.

3.2.4.5 GLUCOCORTICOID RECEPTOR AND 11B -HYDROXYSTEROID DEHYDROGENASE TYPE 1

The glucocorticoid receptor (GR) is a ubiquitously expressed nuclear receptor, which regulates a plethora of physiological processes (Odermatt and Gumy 2008; Ramamoorthy and Cidlowski 2013). The GR is essential for the modulation of the immune system, lipid synthesis, carbohydrate metabolism, stress response, the maintenance of electrolyte concentrations, blood pressure, appropriate brain functions, neuronal functions and cellular growth and differentiation (Odermatt and Gumy 2008; Odermatt and Nashev 2010). It is estimated that up to 10-20% of all genes in a higher organism is modulated by glucocorticoids promoting time- and tissue-specifically gene expression networks which fine-tune metabolic processes (John, Johnson et al. 2009; Ramamoorthy and Cidlowski 2013). The importance of appropriate function of GR can be illustrated by the fact the GR-null mice die after birth and untreated adrenalectomy is lethal (Cole, Blendy et al. 1995). Endogenous glucocorticoids (e.g., cortisol, corticosterone) and their synthetic analogs (e.g. dexamethasone, prednisolone, budesonide) activate GR leading to GR homodimerization and nuclear translocation (Ramamoorthy and Cidlowski 2013). Synthetic glucocorticoids are widely used to treat inflammatory and autoimmune diseases, including asthma, rheumatoid arthritis and numerous allergic reactions; however, long-term treatment with glucocorticoids are associated with hyperglycemia, liver steatosis, hyperlipidemia and insulin resistance through the activation of hepatic gluconeogenesis (Andrews and Walker 1999; Lemke, Krones-Herzig et al. 2008). Nevertheless, GR also modulates BA homeostasis in humans, which can be illustrated by the fact that Cushing´s patients and patients with chronic active hepatitis upon short-term glucocorticoids therapy with prednisolone presented increased serum BAs (Yamanishi, Nosaka et al. 1985; Lu, Zhang et al. 2012). In animals models GR-mediated effects on BA handling is recapitulated by dexamethasone treatment in mice and rats, which present higher circulating BA levels as compared with control groups (Lu, Zhang et al. 2012; Rosales, Romero et al. 2013). Dexamethasone treatment has been shown to increase *CYP7A1*, *CYP8B1*, *BSEP*, *MRP3* and *MRP4*, while down-regulates *MDR1a* and *SHP* gene expression levels in the liver of mice (Lu, Zhang et al. 2012). Interestingly, dexamethasone mediated BA

changes were blunted in FXR-null mice, suggesting that active FXR is essential for the GR-mediated effects in *SHP* expression and thus BA homeostasis (Lu, Zhang et al. 2012). Furthermore, it was shown that the GR physically interacts with FXR and represses its transcriptional activity by recruiting C-terminal binding protein (CtBP) upon dexamethasone treatment (Lu, Zhang et al. 2012). Interestingly, silencing of CtBP *in vivo* using adenoviral vectors normalized hepatic BA contents upon glucocorticoids treatment and also *SHP*, *CYP7A1* and *CYP8B1* expression levels (Lu, Zhang et al. 2012). Although, the mechanism of FXR repression by GR seems to be the major effect of glucocorticoids on BA homeostasis, the direct repression or induction of target genes involved in BA homeostasis by the GR has also been shown (Lu, Zhang et al. 2012). Moreover, the GR also play a role in hepatic and ileal BA uptake by transactivating the human *NTCP* and *ASBT*, respectively (Jung, Fantin et al. 2004; Eloranta, Jung et al. 2006; Rose, Díaz et al. 2011). In addition, GR activation induces ileal and hepatic *OST-α/β* expression in humans and rodents (Khan, Chow et al. 2009). In spite of these findings, the pharmacological approach with synthetic glucocorticoids for the elucidation of interactions between glucocorticoids and BA homeostasis is highly artificial since synthetic glucocorticoids have different properties compared with endogenous glucocorticoids. Depending on their concentrations, they may influence the activities of other nuclear receptors (Pascussi, Drocourt et al. 2000; Pascussi, Gerbal-Chaloin et al. 2000). Moreover, differences regarding study design, treatment duration and animal models explain large variations and controversy emerging from these studies. In this context, Rosales et al. reported that although glucocorticoids treatment in rats induced *BSEP*, *MRP2* and *CYP27A1*, genes coding for *FXR*, *GR*, *SHP*, *NTCP*, *MRP4*, *CYP7A*1 and *BAT* were down-regulated (Rosales, Romero et al.). The observations by Rosales et al. are in contradiction with those of Rose et al. who reported opposite effects of dexamethasone treatment regarding to circulating BAs concentrations in mice (Rose, Díaz et al. 2011). In addition, Cheng et al. have shown that although *NTCP* is up-regulated upon dexamethasone treatment in mouse liver (Cheng, Buckley et al. 2007), *BSEP* expression was not influenced, findings which are in conflict with to that of other investigators (Lu, Zhang et al. 2012; Rosales, Romero et al.). Experimental protocol, animal strain, treatment regimens and different drugs are likely to be responsible for

these discrepancies. On the other hand, *in vitro* liver models may offer a more robust alternative system to study the role of glucocorticoids on BA homeostasis. Nevertheless, culture conditions might largely influence the results. With this regard, Turncliff et al. supplied 100 nM of dexamethasone (DEX) to sandwich-cultured rat hepatocytes and reported that DEX had no effect on *OATP1a1*, *MRP3*, *MDR1a/b* or *BSEP* expression levels (Turncliff, Meier et al. 2004). Intriguingly, *NTCP* expression was down-regulated, contrasting previous reports (Eloranta, Jung et al. 2006).

Glucocorticoid action in organs and cells are not solely determined by the circulating concentration of active steroids, yet another layer of regulation is the one performed by enzymes modulating the ratio of active/inactive (cortisol/cortisone) metabolites and thus determine intracellular availability of active metabolites. The enzymes responsible for the interconversion of glucocorticoids are known to belong to the short-chain dehydrogenase/reductase (SDR) family, which comprise 73 genes in humans (Odermatt and Nashev 2010). 11β-HSD1 (*SDR26C1*) is a member of the SDR superfamily and responsible for glucocorticoid (cortisol) regeneration in metabolically active tissues such as liver, adipose and skeletal muscle (Odermatt and Nashev 2010). A considerable number of researchers used animal models of overexpression and knockout of 11β-HSD1 to provide evidence for an association between the development of metabolic diseases and excessive glucocorticoid exposure (Tomlinson and Stewart 2007). In addition, treatment with selective 11β-HSD1 inhibitors of transgenic and diet-induced rat models of obesity, type 2 diabetes and atherosclerosis demonstrated beneficial outcomes of several metabolic parameters (Tomlinson and Stewart 2007; Odermatt and Nashev 2010). Currently, several pharmaceutical companies have on-going programs in pursuit of selective inhibitors; however, several questions regarding the safety of such inhibitors have arisen due to “alternative” functions of 11β-HSD1, which include the metabolism of several endogenous and exogenous compounds such as 7-hydroxy- and 7-keto-DHEA, 7-oxygenated pregnenolone, 7-ketocholesterol, 7-ketoepiandrosterone, 7-keto-5-androstane-3,17-diol, 7-oxoLCA, metyrapone, p-nitroacetophenone, p-nitrobenzaldehyde, ketoprofen, oracin, triadimefon and the tobacco carcinogen nicotine-derived nitrosamine ketone (NNK) (Odermatt and Nashev

2010; Odermatt, Da Cunha et al. 2011). Taking this into consideration, we investigated in this work the role of 11β-HSD1 in BA homeostasis since 11β-HSD1 regenerates glucocorticoids in hepatocytes and thus may modulate the transcriptional activity of GR-dependent genes including those responsible for the fine-tuning BA homeostasis. In addition, this work raises further safety questions regarding therapeutic interventions with 11β-HSD1 inhibitors which need to take into consideration the impact on BA homeostasis. To the best of our knowledge, this is the first work addressing these questions. In the course of this thesis, we have also discovered a novel role of 11β-HSD1 in BA homeostasis, i.e. the metabolism of the secondary BA 7-oxoLCA, thus extending our knowledge of the functions of this enzyme with regard to BA homeostasis. 7-oxoLCA and its conjugates, deprived of apparent major physiological functions and toxicity may serve as biomarker of 11β-HSD1 inhibition in clinical and preclinical studies.

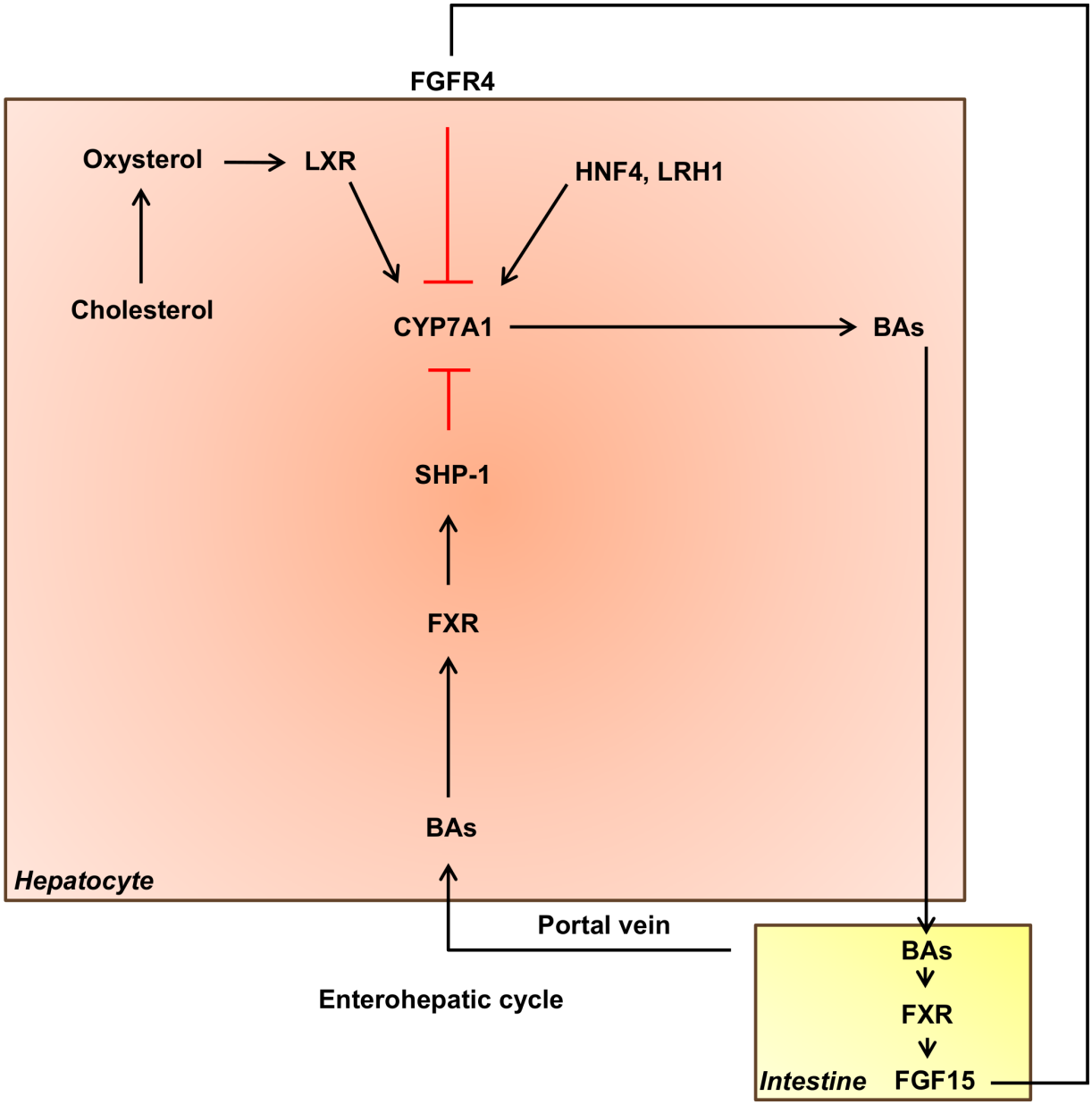

Figure 3. Mechanism of regulation of BA homeostasis by BAs, nuclear receptors and transcriptional factors (adapted from (Thomas, Pellicciari et al. 2008).

4. HEPATIC REDUCTION OF THE SECONDARY BILE ACID 7-OXOLITHOCHOLIC ACID IS MEDIATED BY 11B-HYDROXYSTEROID DEHYDROGENASE 1.

Alex Odermatt*, Thierry Da Cunha*, Carlos A. Penno*†, Charlie Chandsawangbhuwana‡, Christian Reichert*, Armin Wolf†, Min Dong† and Michael E. Baker‡

* Division of Molecular and Systems Toxicology, Department of Pharmaceutical Sciences, University of Basel, Basel, Switzerland,

† Preclinical Safety, Novartis Institute for Biomedical Research, Basel, Switzerland

‡ Department of Medicine, University of California, San Diego, La Jolla, CA, U.S.A

In this study we characterized a new function of 11β-HSD1 in the metabolism of the secondary BA 7-oxoLCA acid using in vitro assays.

BJ www.biochemj.org

Biochem. J. (2011) **436**, 621–629 (Printed in Great Britain) doi:10.1042/BJ20110022

Hepatic reduction of the secondary bile acid 7-oxolithocholic acid is mediated by 11β-hydroxysteroid dehydrogenase 1

Alex ODERMATT*[1], Thierry DA CUNHA*, Carlos A. PENNO*†, Charlie CHANDSAWANGBHUWANA‡, Christian REICHERT*, Armin WOLF†, Min DONG† and Michael E. BAKER‡

*Division of Molecular and Systems Toxicology, Department of Pharmaceutical Sciences, University of Basel, Klingelbergstrasse 50, CH-4056 Basel, Switzerland, †Preclinical Safety, Novartis Institute for Biomedical Research, CH-4009 Basel, Switzerland, and ‡Department of Medicine, 0693 University of California, San Diego, 9500 Gilman Drive, La Jolla, CA 92093-0693, U.S.A.

The oxidized bile acid 7-oxoLCA (7-oxolithocholic acid), formed primarily by gut micro-organisms, is reduced in human liver to CDCA (chenodeoxycholic acid) and, to a lesser extent, UDCA (ursodeoxycholic acid). The enzyme(s) responsible remained unknown. Using human liver microsomes, we observed enhanced 7-oxoLCA reduction in the presence of detergent. The reaction was dependent on NADPH and stimulated by glucose 6-phosphate, suggesting localization of the enzyme in the ER (endoplasmic reticulum) and dependence on NADPH-generating H6PDH (hexose-6-phosphate dehydrogenase). Using recombinant human 11β-HSD1 (11β-hydroxysteroid dehydrogenase 1), we demonstrate efficient conversion of 7-oxoLCA into CDCA and, to a lesser extent, UDCA. Unlike the reversible metabolism of glucocorticoids, 11β-HSD1 mediated solely 7-oxo reduction of 7-oxoLCA and its taurine and glycine conjugates. Furthermore, we investigated the interference of bile acids with 11β-HSD1-dependent interconversion of glucocorticoids. 7-OxoLCA and its conjugates preferentially inhibited cortisone reduction, and CDCA and its conjugates inhibited cortisol oxidation. Three-dimensional modelling provided an explanation for the binding mode and selectivity of the bile acids studied. The results reveal that 11β-HSD1 is responsible for 7-oxoLCA reduction in humans, providing a further link between hepatic glucocorticoid activation and bile acid metabolism. These findings also suggest the need for animal and clinical studies to explore whether inhibition of 11β-HSD1 to reduce cortisol levels would also lead to an accumulation of 7-oxoLCA, thereby potentially affecting bile acid-mediated functions.

Key words: bile acid, glucocorticoid, 11β-hydroxysteroid dehydrogenase, liver, metabolism, 7-oxolithocholic acid.

INTRODUCTION

Bile acids play an essential role in the processing and uptake of dietary lipids and fat-soluble vitamins, and in the elimination of cholesterol and toxic lipophilic compounds from the body. Impaired regulation of the composition and concentration of bile acids and bile salts has been associated with hepatobiliary and digestive diseases [1]. Thus it is important to identify the proteins involved in the maintenance of bile acid homoeostasis.

Bile acids are synthesized from cholesterol by CYP (cytochrome P450)-mediated oxidative type I biotransformation reactions. In addition to CYP enzymes, oxidoreductases and peroxisomal oxidases are involved in bile acid synthesis [2]. The major bile acids present in human bile are CDCA (chenodeoxycholic acid) (35–50 %), its 12-hydroxylated derivative CA (cholic acid) (30–45 %) and DCA (deoxycholic acid) (10–20 %), the bacterial 7-deoxy metabolite of CA (for structures, see Figure 1) [3,4]. Several type II biotransformation reactions of bile acids occur in the liver. Unconjugated bile acids, either newly synthesized or reaching the liver after bacterial deconjugation via the enterohepatic circulation [5], are subjected to reamidation with taurine and glycine, and, to a lesser extent, by sulfation and glucuronidation. In some species, the liver catalyses the CYP-mediated rehydroxylation of the secondary bile acids DCA and LCA (lithocholic acid), which are formed from CA and CDCA through 7-dehydroxylation by bacterial enzymes in the colon during the enterohepatic circulation [5]. Furthermore, hepatic enzymes convert iso- or 3-oxo bile acids into the preferred 3α-hydroxy derivatives and 7-oxo bile acids into the 7α- and 7β-hydroxy forms [6]. Whereas several hydroxylating CYPs and conjugating liver enzymes have been identified and characterized, the enzyme(s) involved in the hepatic oxidoreduction of 7-oxo bile acids remained unknown.

In the human colon, several bacterial strains, including *Escherichia coli*, *Bacteroides fragilis* and *Bacteroides intestinalis*, express 7α-HSD (7α-hydroxysteroid dehydrogenase) enzymes that generate 7-oxoDCA (7-oxodeoxycholic acid) from CA, and 7-oxoLCA (7-oxolithocholic acid) from CDCA and UDCA (ursodeoxycholic acid) [7,8]. The gut microbiota also contains hydroxysteroid dehydrogenases that catalyse the epimerization of 7α- to 7β-hydroxy bile acids with the generation of a stable oxo-bile acid intermediate [9–11], thus contributing to the formation of the UDCA found in bile and faeces. The secondary bile acids DCA and LCA, as well as the 7-oxo bile acids 7-oxoDCA and

Abbreviations used: CA, cholic acid; CDCA, chenodeoxycholic acid; CDC-Gly, chenodeoxycholylglycine; CDC-Tau, chenodeoxycholyltaurine; CYP, cytochrome P450; DCA, deoxycholic acid; DMEM, Dulbecco's modified Eagle's medium; ER, endoplasmic reticulum; FXR, farnesoid X receptor; G6P, glucose 6-phosphate; G6S, glucose 6-sulfate; HEK, human embryonic kidney; H6PDH, hexose-6-phosphate dehydrogenase; 7α-HSD, 7α-hydroxysteroid dehydrogenase; 11β-HSD, 11β-hydroxysteroid dehydrogenase; i.v., intravenous; LC, liquid chromatography; LCA, lithocholic acid; MRM, Multiple Reaction Monitoring; 7-oxoDCA, 7-oxodeoxycholic acid; 7-oxoLCA, 7-oxolithocholic acid; 7-oxoLC-Gly, 7-oxolithocholylglycine; 7-oxoLC-Tau, 7-oxolithocholyltaurine; SDR, short-chain dehydrogenase/reductase; UDCA, ursodeoxycholic acid; UDC-Gly, ursodeoxycholylglycine; UDC-Tau, ursodeoxycholyltaurine.

[1] To whom correspondence should be addressed (email alex.odermatt@unibas.ch).

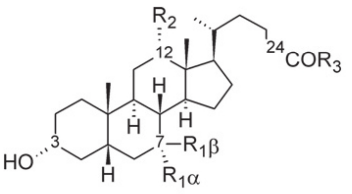

	R_1	R_2	R_3
CA	αOH	αOH	OH
CDCA	αOH	H	OH
UDCA	βOH	H	OH
DCA	H	αOH	OH
LCA	H	H	OH
7-oxoLCA	=0	H	OH
7-oxoLC-Tau	=0	H	$NHCH_2CH_2SO_3H$
7-oxoLC-Gly	=0	H	$NHCH_2COOH$

Figure 1 Structures of bile acids

7-oxoLCA, are eliminated by the faeces. However, a substantial fraction of these secondary bile acids is not excreted, but reabsorbed in the distal intestine and transported back to the liver.

Early studies on the metabolism of radiolabelled 7-oxoLCA in rats with bile fistulas indicated the preferential formation of UDCA and lower amounts of CDCA and its metabolites [12]. Later, Fromm et al. [13] reported the preferential conversion of radiolabelled 7-oxoLCA into CDCA, with approximately 10% UDCA after a single hepatic passage following i.v. (intravenous) administration in humans. Similarly, 7-oxoLC-Gly (7-oxolithocholylglycine) and 7-oxoLC-Tau (7-oxolithocholyltaurine) were converted into the 7α-hydroxy epimer. After small intestinal infusion, 7-oxoLCA was metabolized primarily to CDCA as observed after i.v. injection. CDCA and UDCA were not metabolized by the liver, suggesting that UDCA is mainly produced by bacterial enzymes as a result of the epimerization of CDCA via the 7-oxoLCA intermediate [9,14,15]. Using human liver preparations Amuro et al. [16] provided evidence that 7-oxoLCA is primarily reduced to CDCA and lower amounts of UDCA by NADPH-dependent microsomal enzyme(s).

In order to identify this missing link, i.e. the source of hepatic reduction of bacterially derived 7-oxoLCA and formation of UDCA, we aimed in the present study to identify the hepatic 7-oxo bile acid reductase. Initially, human liver microsomes were used to characterize the 7-oxo bile acid reductase activity, which provided evidence for an ER (endoplasmic reticulum) luminal localization of the enzyme. Then, using recombinant enzyme, we demonstrated for the first time that 11β-HSD1 (11β-hydroxysteroid dehydrogenase 1) catalyses the irreversible reduction of 7-oxoLCA.

11β-HSD1 functions in intact cells primarily as a reductase and converts inactive 11-oxoglucocorticoids into 11β-hydroxyglucocorticoids using co-substrate NADPH, which is provided by H6PDH (hexose-6-phosphate dehydrogenase) in the ER [17]. Owing to the adverse metabolic effects of elevated 11β-HSD1-dependent glucocorticoid activation in tissues such as liver, skeletal muscle and adipose, 11β-HSD1 has emerged as a promising therapeutic target to treat metabolic diseases, and there is considerable effort to develop therapeutic inhibitors (reviewed in [18–21]). However, regarding safety aspects of such inhibitors, it is necessary to identify other substrates of 11β-HSD1 [22], including bile acids as in the present study, and to understand the role of 11β-HSD1 in their metabolism.

EXPERIMENTAL

Microsomal preparations and activity assays using human liver microsomes

Human liver microsomes (*InVitro* CYP H-class™ microsomes from a male donor, Celsis International) were thawed on ice and used immediately for activity assays. Microsomes, 0.2 mg per reaction, were incubated at 37 °C for 0–40 min in a total volume of 500 μl containing TS2 buffer (100 mM NaCl, 1 mM EGTA, 1 mM EDTA, 1 mM $MgCl_2$, 250 mM sucrose and 20 mM Tris/HCl, pH 7.4), a final concentration of 500 μM NADPH, 1 μM substrate and vehicle or 5 μM 11β-HSD1 inhibitor as indicated. To assess the latency of 7-oxoLCA reduction and dependence on cofactor regeneration, microsomes were incubated in reaction mixture supplemented with the detergent Nonidet P40 (final concentration of 0.5%), G6P (glucose 6-phosphate) or G6S (glucose 6-sulfate) (final concentration of 1 mM), or the glucose-6-phosphate translocase inhibitor S3483 (obtained from Sanofi-Aventis; final concentration of 20 μM). Reactions were started by adding microsomes into freshly prepared reaction mixture and stopped by rapid freezing in solid CO_2.

Rat liver microsomes and microsomes of HEK (human embryonic kidney)-293 cells transfected with human 11β-HSD1 or mock-transfected were prepared as described previously [23]. For immunoblotting, 50 μg of total microsomal proteins was separated by 12% PAGE, followed by transfer of proteins on to PVDF membranes. 11β-HSD1 was detected using primary anti-(human 11β-HSD1) antibody (Cayman Chemical).

Reduction of 7-oxoLCA by recombinant human 11β-HSD1

To assess 7-oxoLCA reductase activity in intact HEK-293 cells stably expressing recombinant human 11β-HSD1 or co-expressing 11β-HSD1 and H6PDH (AT6 and HHH7 clones respectively) [24], 20000 cells per well were distributed in 24-well plates and allowed to adhere for 16 h. Cells were then incubated with doubly charcoal-treated DMEM (Dulbecco's modified Eagle's medium), and the 7-oxidoreduction of 7-oxoLCA was measured at a final concentration of 1 μM after incubation for up to 24 h at 37 °C in a total volume of 1 ml. To determine the apparent K_m of 11β-HSD1, frozen cell lysates were thawed, sonicated and immediately incubated for 10 min at 37 °C in a total volume of 500 μl containing 500 μM NADPH and 7-oxoLCA at concentrations between 62.5 nM and 4 μM. Reactions were terminated by freezing in solid CO_2.

Impact of bile acids on the interconversion of glucocorticoids

The conversion of cortisone into cortisol using cell lysates was measured as described previously [25] (see the Supplementary Online Data at http://www.BiochemJ.org/bj/436/bj4360621add.htm). To assess the effect of 7-oxoLCA on the ratio of active to inactive glucocorticoids in intact cells at steady state, cells (30000 cells per well of a poly-L-lysine-coated 96-well plate, Becton-Dickinson) expressing 11β-HSD1 or co-expressing 11β-HSD1 and H6PDH were incubated for 24 h in a total volume of 40 μl of steroid-free DMEM in the presence of either 200 nM cortisone or cortisol and various concentrations of 7-oxoLCA.

Analysis of non-labelled steroids and bile acids by LC (liquid chromatography)–MS

Frozen samples from reactions using intact cells, cell lysates or microsomes were thawed, and a fixed amount of deuterated

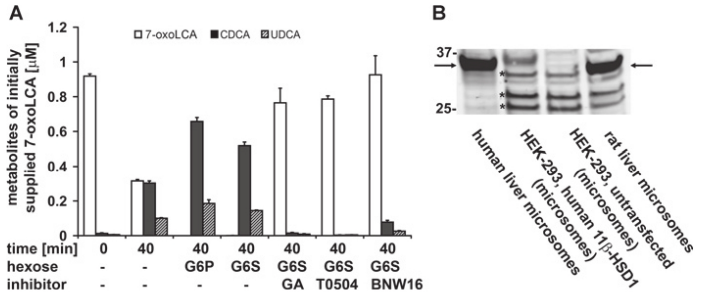

Figure 2 Reduction of 7-oxoLCA by human liver microsomes

(**A**) Human liver microsomes were incubated for 40 min with 7-oxoLCA (1 μM), NADPH (500 μM) and either vehicle or hexose 6-phosphate (1 mM G6P or G6S) and 11β-HSD1 inhibitor [5 μM glycyrrhetinic acid (GA), Merck-544 (T0504) or BNW16] as indicated. Samples were analysed for the amount of unconverted substrate 7-oxoLCA (white bars) and the products CDCA (black bars) and UDCA (hatched bars). Results ($n = 3$) are means $\pm$ S.D. (**B**) Expression of 11β-HSD1 in liver microsomes and in microsomes of transfected HEK-293 cells. A total amount of 50 μg of microsomal proteins was separated by gel electrophoresis, and proteins were blotted on to PVDF membranes and probed with an anti-(human 11β-HSD1) antibody. Asterisks indicate non-specific bands, and arrows indicate 11β-HSD1. Molecular masses are indicated in kDa.

CDCA (0.5 nmol) or corticosterone (0.2 nmol) was added as an internal standard, followed by mixing and centrifugation at 3000 ***g*** for 5 min. Supernatants were loaded on to Oasis HBL SPE cartridges (pre-conditioned with 1 ml of methanol and 1 ml of water), followed by washing with 2 ml of water and elution with 2 ml of methanol. The solvent was evaporated and the residue was reconstituted in 100 μl of methanol.

7-OxoLCA and its metabolites were separated on an Atlantis T3 column (Waters) using an Agilent Technologies model 1200 liquid chromatograph (see the Supplementary Online Data). The liquid chromatograph was interfaced to an Agilent 6410 triple-quad mass spectrometer, operated in atmospheric pressure electrospray positive-ionization mode. Data acquisition was performed using MassHunter workstation software (version B.01.04).

Metabolites were identified by comparing their retention times and mass to charge ratios (m/z) with those of authentic standards. UDCA, 7-oxoLCA and CDCA were detected in the selected positive-ionization MS Scan2 mode (mass range, m/z 300–500). They were typically eluted at 5.2, 6.2 and 7.3 min, and were monitored at m/z 357.3, 373.2 and 357.3 (dehydrated bile acids) respectively. Quantitative determination of bile acids was performed by positive-ionization and MRM (Multiple Reaction Monitoring). Deuterated CDCA was used as internal standard (m/z 361.2).

Quantitative analysis of glucocorticoids was performed similarly by MRM. Cortisone (precursor and product ion at m/z 361 and 163) and cortisol (precursor and product ion at m/z 363 and 121) were eluted at 9.8 and 9.5 min respectively. Corticosterone (m/z 347.2) was used as internal standard and was eluted at 12.1 min.

Metabolites were quantified from calibration curves of the peak area ratio of the authentic standard and internal standard incubated in lysates of untransfected HEK-293 cells at a total protein concentration identical with that of the experimental setting and plotted against the concentration of authentic standards (normalization using internal standard).

Calculation of enzyme kinetic parameters

Enzyme kinetics was analysed by non-linear regression using four-parameter logistic curve fitting. For statistical comparisons, the ratio t-test in GraphPad Prism 5 software was used. Results (means $\pm$ S.D.) were obtained from at least three independent experiments.

Molecular modelling of 11β-HSD1 with bile acids

Mouse 11β-HSD1 (PDB code 1Y5R) [26] was extracted from the PDB for use as a template to investigate the interactions of 7-oxo, 7α-hydroxy and 7β-hydroxy bile acids with 11β-HSD1. We used PDB code 1Y5R because it contains both corticosterone and $NADP^+$, unlike other three-dimensional structures of 11β-HSD1 in the PDB. Human and mouse 11β-HSD1 have 79 % sequence identity, which allows mouse 11β-HSD1 to be a good model for the interaction of bile acids with human 11β-HSD1.

To obtain 11β-HSD1 complexed with 7-oxoLCA, we superimposed the crystal structure of *E. coli* 7α-HSD [27] complexed with 7-oxoLC-Gly (PDB code 1FMC) with PDB code 1Y5R and extracted 7-oxoLC-Gly from PDB code 1FMC. Then we inserted 7-oxoLCA into 11β-HSD1. For conversion of the 7-oxo into either a 7α-hydroxy or a 7β-hydroxy, we used the Biopolymer option in Insight II. The glycine-conjugated bile acids also were constructed with Biopolymer. The final three-dimensional model of 11β-HSD1 with each bile acid was refined using Discover 3, which was run for 10 000 iterations with a distant dependent dielectric constant of 2.

RESULTS

Reduction of 7-oxoLCA by human liver microsomes

Previous studies provided evidence for the existence of one or more hepatic enzymes catalysing the 7-oxo reduction of 7-oxoLCA to CDCA and/or UDCA [12,13,16,28,29]. These earlier studies suggested that the 7-oxo bile acid reductase is a microsomal enzyme preferentially using NADPH [16]. To identify this 7-oxo bile acid reductase, we first incubated human liver microsomes with 7-oxoLCA and studied the properties of the enzymatic reaction. After incubation for 40 min, approximately 70 % of 7-oxoLCA was converted, mainly into CDCA and into approximately three times lower amounts of UDCA (Figure 2A). In addition, some minor products, including muricholic acids, were observed, but were not analysed further. The 7-oxoLCA reduction was approximately ten times more efficient in the

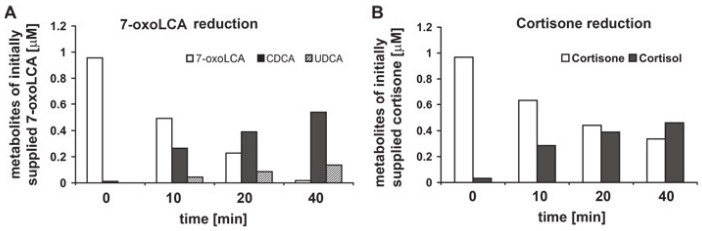

Figure 3 Comparison of the reduction of 7-oxoLCA and cortisone by human liver microsomes

Human liver microsomes were incubated at a final concentration of 1 μM 7-oxoLCA (**A**) or 1 μM cortisone (**B**) for 0–40 min, followed by analysis by LC–MS of the amounts of residual substrate and products formed. One of three representative experiments is shown.

presence of NADPH compared with NADH, and no 7-oxoLCA formation could be detected when microsomes were incubated with CDCA or UDCA and either $NADP^+$ or NAD^+ respectively, suggesting that the enzyme acts exclusively as a reductase.

Ketoconazole (5 μM) had no effect either on the amount of CDCA and UDCA formed or on their ratio, suggesting that CYPs play a minor role in the metabolism of 7-oxoLCA to its 7-hydroxylated forms. Experiments using the detergent Nonidet P40 suggested latency of the 7-oxo bile acid reductase; however, prolonged incubation with the detergent also seemed to inhibit the enzyme activity (results not shown).

In the ER lumen, NADPH is regenerated by H6PDH, which, under physiological conditions, is primarily dependent on G6P [30]. We therefore tested whether the 7-oxo bile acid reductase is stimulated in the presence of the hexose phosphate. In the presence of G6P, the 7-oxoLCA supplied was almost completely metabolized. Comparable stimulation was observed in the presence of G6S (Figure 2A), which is a specific substrate of the luminal H6PDH, but not the cytoplasmic G6PDH [30]. Furthermore, the glucose-6-phosphate translocase inhibitor S3483 abolished the G6P- and G6S-induced stimulation of 7-oxoLCA reduction (results not shown).

To our knowledge, the only currently known luminal oxidoreductase using NADPH is 11β-HSD1, which is a reversible enzyme and catalyses the interconversion of glucocorticoids and some other substrates, including 7-oxycholesterol, 7-oxydehydroepiandrosterone, 11-oxyprogesterone and 11-oxyandrogen metabolites [22,31–33]. An antibody raised against human 11β-HSD1 detected a single band at approximately 35 kDa and confirmed the high expression in human liver microsomes [34–36] (Figure 2B). A band at approximately 33 kDa was detected in rat liver microsomal preparations. The size difference can be explained by the presence of three glycosylation sites in human 11β-HSD1 and two in the rat enzyme [37]. The occurrence of three non-specific bands in rat liver microsomes and in HEK-293 microsomal preparations indicates some cross-reactivity of the antibody. The recombinant enzyme was constructed with a C-terminal FLAG epitope, resulting in a slightly slower migration of the protein in gel electrophoresis. Probing the blot with anti-FLAG antibody resulted in a single band at 35 kDa (results not shown).

To test whether 11β-HSD1 might catalyse the reduction of 7-oxoLCA, we used human liver microsomes and studied the effect of three structurally unrelated 11β-HSD1 inhibitors, i.e. glycyrrhetinic acid, T0504 (also known as Merck-544) and BNW16 [25]. All three inhibitors abolished the conversion of 7-oxoLCA into CDCA and UDCA (Figure 2A). Next, we compared the reduction of 7-oxoLCA and cortisone. The human liver microsomes (0.2 mg in a reaction volume of 500 μl) converted approximately 50 and 80 % of 7-oxoLCA (1 μM) after 10 and 20 min respectively, and 7-oxoLCA was almost completely metabolized after 40 min (Figure 3). In comparison, in analogous experiments, 37, 56 and 67 % of cortisone was converted, indicating a higher capacity to metabolize 7-oxoLCA compared with cortisone.

Reduction of 7-oxoLCA by recombinant 11β-HSD1

To verify that the reduction of 7-oxoLCA indeed is catalysed by 11β-HSD1, experiments in lysates of HEK-293 cells expressing the recombinant enzyme were performed. 11β-HSD1 efficiently catalysed the reduction of 7-oxoLCA with an apparent K_m of 980 ± 210 nM and a V_{max} of 2.8 ± 0.4 $nmol \cdot mg^{-1} \cdot h^{-1}$ as calculated by four-parametric non-linear regression (Figure 4A). Comparable values were obtained using the Hanes–Woolf equation (Figure 4B). No conversion of 7-oxoLCA was observed in untransfected HEK-293 control cells. The taurine- and glycine-conjugated 7-oxo bile acids, 7-oxoLC-Tau and 7-oxoLC-Gly, were similarly converted into the 7α-hydroxylated CDC-Tau (chenodeoxycholyltaurine) and CDC-Gly (chenodeoxycholylglycine) with minor amounts of UDC-Tau (ursodeoxycholyltaurine) and UDC-Gly (ursodeoxycholylglycine) respectively, demonstrating that 11β-HSD1 accepts both unconjugated and conjugated 7-oxoLCA as substrate.

Next, we studied the impact of H6PDH on 11β-HSD1-dependent reduction of 7-oxoLCA in intact HEK-293 cells stably expressing either human 11β-HSD1 alone or co-expressing 11β-HSD1 and H6PDH. Co-expression with H6PDH stimulated the 7-oxo reductase activity of 11β-HSD1 (Figure 5). In cells co-expressing 11β-HSD1 and H6PDH, the reaction was almost completed after 24 h, resulting in the formation of approximately 90 % CDCA and 10 % UDCA. In contrast, only approximately 50 % of 7-oxoLCA was converted in cells expressing solely 11β-HSD1, and it took more than 48 h until the reaction was completed (results not shown). No oxidation of CDCA and UDCA was detected, independent of the cell line used, confirming the observation from human liver microsomes and showing that 11β-HSD1 catalyses the irreversible conversion of 7-oxoLCA into CDCA and lower amounts of UDCA.

Interference of bile acids with the metabolism of glucocorticoids by 11β-HSD1

Several bile acids, including CDCA and LCA, have been found in previous studies to inhibit 11β-HSD1 and 11β-HSD2 respectively

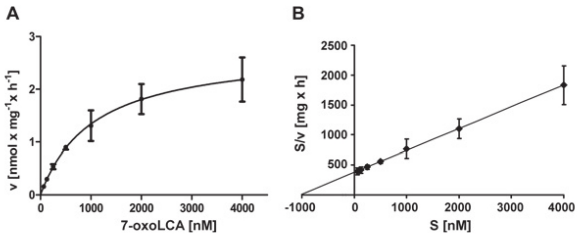

Figure 4 Enzyme kinetic profile of 7-oxo reduction of 7-oxoLCA by recombinant human 11β-HSD1

Enzymatic activity of human 11β-HSD1 was determined in lysates of transfected HEK-293 cells as described in the Experimental section. (**A**) Reaction rate against substrate concentration plot of 10 min incubations with 7-oxoLCA. (**B**) Hanes–Woolf plot of the data shown in (**A**). Results ($n = 3$) are means $\pm$ S.D.

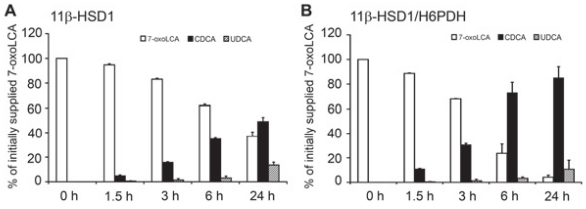

Figure 5 Impact of H6PDH on 11β-HSD1-dependent 7-oxo reduction of 7-oxoLCA in living cells

Intact HEK-293 cells stably expressing human 11β-HSD1 (**A**) or 11β-HSD1 and H6PDH (**B**) were incubated for 0–24 h with 1 μM 7-oxoLCA, followed by quantification of bile acids by LC–MS. Results ($n = 3$) are means $\pm$ S.D.

Table 1 Inhibition by bile acids of the oxidation and reduction of glucocorticoids by 11β-HSD1

11β-HSD activities were measured in lysates of HEK-293 cells expressing the respective human recombinant enzyme as described in the Experimental section. Results are IC_{50} values in μM (means $\pm$ S.D.) from four independent experiments.

Bile acid	11β-HSD1 oxidation IC_{50} (μM)	11β-HSD1 reduction IC_{50} (μM)
7-OxoLCA	2.8 $\pm$ 0.8	1.1 $\pm$ 0.3
LCA	0.21 $\pm$ 0.06	0.36 $\pm$ 0.05
CDCA	0.27 $\pm$ 0.08	4.1 $\pm$ 0.6
UDCA	2.3 $\pm$ 1.0	6.9 $\pm$ 1.2
DCA	7.2 $\pm$ 2.0	8.9 $\pm$ 1.4
CA	>50	50 $\pm$ 13
7-OxoLC-Tau	>50	1.9 $\pm$ 0.3
7-OxoLC-Gly	>50	1.6 $\pm$ 0.2
CDC-Tau	0.61 $\pm$ 0.05	16 $\pm$ 3
CDC-Gly	1.0 $\pm$ 0.2	18 $\pm$ 2
UDC-Tau	23 $\pm$ 6	>50
UDC-Gly	25 $\pm$ 5	>50

[38–40]. We therefore compared the effect on 11β-HSD1 activities of 7-oxoLCA and its taurine- and glycine-conjugated forms with that of other relevant bile acids (Table 1). Whereas the 7α-hydroxylated CDCA and its conjugated derivatives CDC-Tau and CDC-Gly showed a more than 10-fold preference to inhibit the dehydrogenase over the reductase activity of 11β-HSD1, 7-oxoLCA displayed a slight preference to inhibit the reduction of cortisone, an effect that was more pronounced for the conjugated derivatives. The 7β-hydroxylated bile acids UDCA and UDC-Tau preferentially inhibited 11β-HSD1 dehydrogenase activity; however, they were approximately 10-fold less potent than the 7α-hydroxylated forms.

Impact of 7-oxoLCA on the ratio of cortisol to cortisone at steady state

Bile acids can reach high concentrations in the liver and may affect not only initial rates of conversion, but also steady-state ratios of cortisol to cortisone controlled by 11β-HSD1. We therefore determined the effect of 7-oxoLCA on the steady-state ratio of cortisol to cortisone in HEK-293 cells stably expressing 11β-HSD1 or co-expressing 11β-HSD1 and H6PDH. As shown in Figure 6(A), approximately 40% cortisol was produced in 11β-HSD1-expressing cells, whereas over 90% of initially supplied cortisone was converted into cortisol upon co-expression with H6PDH, in line with earlier observations [33]. A mirror image was obtained when cells were incubated initially with cortisol (Figure 6B). Co-incubation of the cells with the respective glucocorticoid and increasing concentrations of 7-oxoLCA resulted in diminished cortisol production when cortisone was supplied and enhanced cortisone formation when cortisol was supplied initially, thus reflecting a shift from the active to the inactive glucocorticoid at steady state in the presence of high concentrations of 7-oxoLCA.

Analysis of binding of bile acids to 11β-HSD1 by three-dimensional modelling

We used the crystal structure of 11β-HSD1 with corticosterone [26] (see Supplementary Figure S1 at http://www.BiochemJ.org/bj/436/bj4360621add.htm) as a benchmark for comparison of the three-dimensional models of 11β-HSD1 with 7-oxoLCA, CDCA and UDCA (Figure 7). In the crystal structure of 11β-HSD1 in complex with corticosterone, the phenolic group of Tyr^{183} on 11β-HSD1 and C4 on $NADP^+$ are 2.8 and 3.9 Å (1 Å = 0.1 nm) respectively from the 11β-hydroxy group on

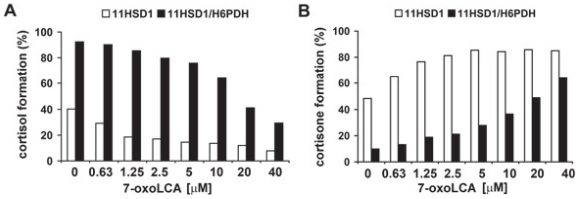

Figure 6 Effect of 7-oxoLCA on the steady-state ratio of cortisol to cortisone

(**A**) Intact HEK-293 cells expressing 11β-HSD1 (white bars) or co-expressing 11β-HSD1 and H6PDH (black bars) were incubated for 24 h with 200 nM radiolabelled cortisone and increasing concentrations of 7-oxoLCA, followed by determination of cortisol formation. (**B**) Similarly, cells were incubated with 200 nM radiolabelled cortisol, followed by measuring cortisone formation. Results representative of three independently performed experiments are shown.

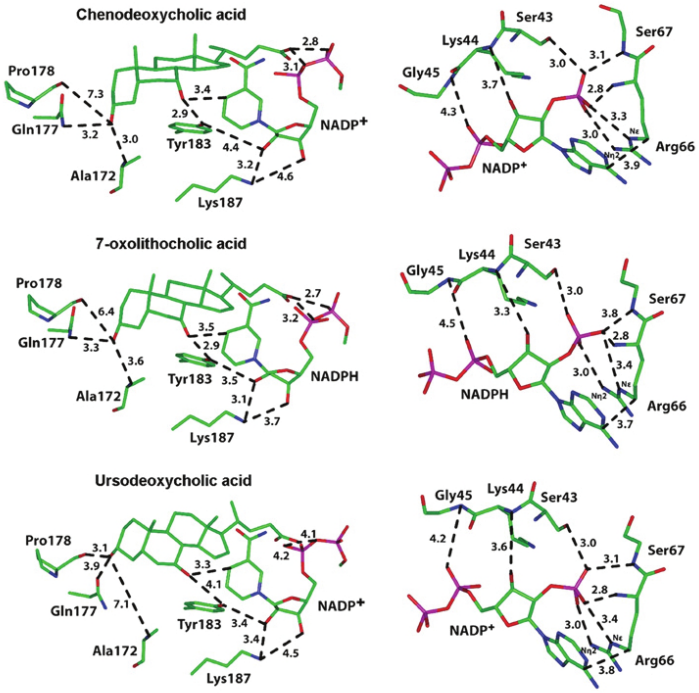

Figure 7 Three-dimensional models of mouse 11β-HSD1 complexed with CDCA, 7-oxoLCA and UDCA

In the complexes of 11β-HSD1 with CDCA and 7-oxoLCA, Tyr^{183} and C-4 on NADP(H) have favourable contacts with the 7α-hydroxy group on CDCA and 7-carbonyl on 7-oxoLCA. The phenolic hydroxy group on Tyr^{183} on 11β-HSD1 is 4.1 Å from the 7β-hydroxy group on UDCA. The ε-amino group on Lys^{187} has stabilizing interactions with the ribose hydroxy groups on NADPH for 11β-HSD1 complexed with 7-oxoLCA. However, this is not the case with NADP$^+$ and 11β-HSD1 complexed with CDCA and UDCA. Arg^{66} has an electrostatic interaction with the 2′-phosphate on NADP(H) in all three complexes.

corticosterone. The hydroxy group on Tyr^{183} is hydrogen-bonded with the 2′-hydroxy group on the nicotinamide ribose. The ε-amino group on Lys^{187} is 3.2 Å from the 2′- and 3′-hydroxy groups on the nicotinamide ribose. This stabilizes the orientation of the nicotinamide ribose [26]. Nε and Nη on the guanidinium group of Arg^{66} have an electrostatic interaction with the 2′-phosphate of NADP$^+$. This electrostatic interaction is characteristic of NADP(H)-dependent SDRs (short-chain dehydrogenase/reductases), including 17β-HSD1 [41–43].

Although all three bile acid substrates have favourable interactions with 11β-HSD1, there are differences in some interactions that can explain differences in the observed binding and catalytic activity. In the three-dimensional model of 11β-HSD1 in complex with 7-oxoLCA, the phenolic group on Tyr^{183} on 11β-HSD1 and C-4 on the nicotinamide ring of NADPH are 2.9 and 3.5 Å respectively from the 7-oxo group on 7-oxoLCA. The ε-amino group on Lys^{187} has two favourable contacts with the 2′- and 3′-ribose hydroxy groups on NADPH, and the hydroxy group

on Tyr^{183} is 3.5 Å from the 2′-hydroxy group of the nicotinamide ribose. Furthermore, Arg^{66} and other residues in the N-terminal end of 11β-HSD1 have favourable contacts with the adenosine on NADPH. Together, this three-dimensional model indicates that 7-oxoLCA fits into 11β-HSD1 in an orientation that favours reduction of the 7-oxo group to an alcohol.

In the three-dimensional model of 11β-HSD1 in complex with CDCA, Tyr^{183} on 11β-HSD1 and C-4 on NADP$^+$ are 2.9 and 3.4 Å respectively from the 7α-hydroxy group on CDCA. However, Lys^{187} has an asymmetric orientation to the ribose hydroxy groups. The ε-amino group on Lys^{187} is 4.6 Å from 3′-hydroxy group, which is too far to form a hydrogen bond. Also, the hydroxy group on Tyr^{183} is 4.4 Å from the 2′-hydroxy group of the nicotinamide ribose. Thus the nicotinamide ribose lacks two stabilizing interactions that are present in 11β-HSD1 in complex with 7-oxoLCA. Arg^{66} and other residues in the N-terminal end of 11β-HSD1 have favourable contacts with the adenosine on NADP$^+$.

In the three-dimensional model of 11β-HSD1 in complex with UDCA, Tyr^{183} on 11β-HSD1 and C-4 on NADP$^+$ are 4.1 and 3.3 Å respectively from the 7β-hydroxy group on UDCA. Lys^{187} has an asymmetric orientation to the ribose hydroxy groups. The ε-amino group on Lys^{187} is 4.5 Å from 3′-hydroxy group, which is too far to form a hydrogen bond. Arg^{66} and other residues in the N-terminal end of 11β-HSD1 have favourable contacts with the adenosine on NADP$^+$ (see also the Supplementary Online Data).

We also constructed three-dimensional models of 11β-HSD1 in complex with the glycine conjugates of 7-oxoLCA, CDCA and UDCA, as shown in Supplementary Figure S2 at http://www.BiochemJ.org/bj/436/bj4360621add.htm. All three glycine–bile acid conjugates have stabilizing contacts with various backbone nitrogens or oxygens in 11β-HSD1. Examination of these three-dimensional models reveals an unexpected coulombic interaction between the glycine carbonyl group and Nη2 on Arg^{66}, which also has a key electrostatic interaction with the 2′-ribose phosphate on NADP$^+$. Thus Arg^{66} has two important stabilizing interactions in the complexes of 11β-HSD1 with glycine conjugates of bile acids.

Thus the three-dimensional models of 11β-HSD1 with bile acids (Figure 7) reveal that 7-oxoLCA has the most favourable interaction with the catalytic site in 11β-HSD1 and that glycine–bile acid conjugates also can fit into 11β-HSD1 in which they have a coulombic interaction with Arg^{66}, a key residue in the stabilization of NADPH binding to 11β-HSD1.

DISCUSSION

By catalysing the biotransformation of gut bacteria-derived secondary bile acids, the liver plays a key role in damage and repair; damage being changes in the steroid nucleus by bacterial enzymes, and repair being rectification of these changes by the hepatocyte. Several bacterial strains express 7α-HSDs to yield 7-oxoLCA from CDCA and 7-oxoDCA from CA [7]. 7-OxoLCA can be metabolized further by reversible bacterial 7β-HSDs, or taken up actively via sodium-dependent transporter [SLC10A2 (solute carrier 10A2)] from the lumen of the ileal segment or passively in the colon. Although 7-oxoLCA is readily detectable in faeces and portal blood, it cannot be detected at substantial levels in bile and plasma [44,45], suggesting efficient hepatic metabolism.

In the present paper, we report the identification of 11β-HSD1 as a hepatic 7-oxoreductase, providing an explanation for the low circulating 7-oxoLCA concentrations. Human and rodent liver expresses high levels of 11β-HSD1 [34,35] (Figure 2B). Previous studies demonstrated that 11β-HSD1 purified from human or rodent liver catalyses the NADPH-dependent conversion of cortisone into cortisol and 11-dehydrocorticosterone to corticosterone respectively [36]. In addition, it was shown that 11β-HSD1 purified from rabbit and hamster liver accepts not only glucocorticoids as substrates, but also 7-oxycholesterol metabolites [46,47]. We now demonstrate that both human liver microsomes and recombinant human 11β-HSD1 expressed in HEK-293 cells catalysed the NADPH-dependent 7-oxo reduction of 7-oxoLCA to form preferentially the 7α-hydroxy bile acid CDCA and to a lesser extent the 7β-hydroxy isomer UDCA (10–20%). The ratio of CDCA to UDCA observed in our experiments with human liver microsomes as well as recombinant human enzyme is in line with earlier observations with human liver preparations and measurements in blood following i.v. administration [13,16]. Importantly, the 7-oxo reduction of 7-oxoLCA in liver microsomes was completely abolished by the 11β-HSD1 inhibitors glycyrrhetinic acid, T0504 and BNW16 (Figure 2A). Although we cannot exclude the existence of another enzyme that catalyses the 7-oxo reduction of 7-oxoLCA in the liver, it is highly unlikely that such an enzyme would be completely inhibited by all of the three structurally unrelated compounds. Thus the results provide strong evidence that 11β-HSD1 is the major enzyme catalysing the 7-oxo reduction of 7-oxoLCA in humans.

Analysis of the kinetic properties revealed that 11β-HSD1 efficiently catalyses 7-oxo reduction of 7-oxoLCA with approximately 2-fold lower affinity, but 2-fold higher V_{max} compared with reduction of cortisone. The conversion of both 7-oxoLCA and cortisone was latent, dependent on H6PDH and stimulated to a similar extent by addition of G6P to the reaction mixture. 11β-HSD1 accepted the taurine- and glycine-conjugated forms as substrates, with catalytic efficiencies comparable with those for the free bile acids. This is consistent with predictions of the three-dimensional models of the three bile acids conjugated to glycine, which uncovered an unexpected interaction between the glycine carbonyl group and Nη2 on Arg^{66} on 11β-HSD1 (see Supplementary Figure S2). Arg^{66} has an important role in neutralizing the negative charge on the 2′-phosphate on NADP(H) in 11β-HSD1 and other SDRs that use NADP(H) as a cofactor [26,41–43]. Thus Arg^{66} has two key coulombic interactions in 11β-HSD1 complexed with the three glycine-conjugated bile acids.

Unlike other steroid and sterol substrates, 11β-HSD1 irreversibly catalyses the 7-oxo reduction of 7-oxoLCA, and the stereoselectivity for the bile acid metabolites formed is just opposite of that observed for the metabolites of 7-oxocholesterol [31,32], 7-oxodehydroepiandrosterone and 7-oxopregnenolone [33]. Neither CDCA nor UDCA, even upon prolonged incubation and at high concentrations, were converted into 7-oxoLCA, and there was also no isomerization of CDCA to UDCA or vice versa, as has been observed for 7α- and 7β-hydroxyepiandrosterone [48] and 7α- and 7β-hydroxydehydroepiandrosterone [33] respectively. Our results are in line with an earlier report on the metabolism of radiolabelled CDCA in rats with bile fistulas [12], where conversion of CDCA into trihydroxylated metabolites and minor amounts of UDCA, but no formation of 7-oxoLCA was observed. Furthermore, in humans, after a single hepatic passage following i.v. administration, neither CDCA nor UDCA was modified on the steroid ring.

The three-dimensional models indicate that only 7-oxoLCA has optimal binding of substrate and cofactor to Tyr^{183} and Lys^{187} (Figure 7), which is necessary for reduction of 7-oxoLCA to CDCA. In contrast, in the three-dimensional models of 11β-HSD1 with CDCA and UDCA, the ε-amino group on the key catalytic

residue Lys^{187} is too far from the 3′-ribose hydroxy group on $NADP^+$ to form a stabilizing hydrogen bond required for catalytic activity. The distance between the 7β-hydroxy group on UDCA and the phenolic group on Tyr^{183} is 4.1 Å, which indicates weaker binding than found for the similar interaction between Tyr^{183} and either CDCA or 7-oxoLCA. This may explain the preference for CDCA as a product in the reduction of 7-oxoLCA by 11β-HSD1. Although only 7-oxoLCA was metabolized by 11β-HSD1, the three-dimensional models predicted binding of all three bile acids and their conjugates, and supported the more potent inhibitory effect of free and conjugated forms of CDCA compared with UDCA on cortisol oxidation (Table 1).

Alterations in the availability of bile acids, which reach high concentrations in the hepatocyte in cholestatic liver disease, may affect the hepatic activation of glucocorticoids. In intact HEK-293 cells expressing 11β-HSD1, but not H6PDH, CDCA and its conjugates preferentially inhibited 11β-HSD1 dehydrogenase activity and stimulated cortisone reduction. However, upon co-expression with H6PDH, which reflects the situation in hepatocytes, CDCA displayed weak inhibitory activity on 11β-HSD1. In contrast, 7-oxoLCA preferentially inhibited 11β-HSD1 reductase activity, and the presence of high concentrations of 7-oxoLCA stimulated cortisol oxidation and shifted the ratio of active to inactive glucocorticoids under steady-state conditions, probably by altering the ratio of NADPH to $NADP^+$ in the ER lumen. It was shown previously that a ratio of NADPH to $NADP^+$ greater than 10 is required for 11β-HSD1 to efficiently reduce cortisone [49]. The presence of high concentrations of 7-oxo bile acids, 7-oxo cholesterols or 7-oxo steroids may thus result in decreased ER luminal NADPH levels and lower concentrations of active glucocorticoids, thereby modulating redox signalling pathways and glucocorticoid-dependent adaptive responses.

Further research is needed to elucidate the physiological role for the rapid hepatic removal of 7-oxoLCA. Distinct effects of 7-oxoLCA, CDCA and UDCA on bile acid sensing receptors may affect the regulation of genes involved in lipid metabolism and inflammation. CDCA has been found to be a potent activator of the FXR (farnesoid X receptor)/RXR (retinoid X receptor) heterodimeric receptor [50,51]. In contrast, UDCA showed no or very little effect and 7-oxoLCA was a modest activator of human FXR, but did not activate mouse FXR. Thus, by converting the weak activator 7-oxoLCA into the more potent CDCA, 11β-HSD1 might play a role in modulating FXR activity. However, the amount of CDCA from *de novo* synthesis in the liver probably exceeds that from conversion of bacterially derived 7-oxoLCA, and the relative contribution remains to be determined. Also, there are currently no data available on potential effects of 7-oxoLCA on other nuclear receptors, including LXR (liver X receptor), VDR (vitamin D receptor) and PXR (pregnane X receptor).

Nevertheless, the results may be relevant regarding the current development of 11β-HSD1 inhibitors for treatment of metabolic diseases [19–21]. Inhibition of 11β-HSD1 is expected to abolish hepatic metabolism of 7-oxoLCA, thereby leading to elevated hepatic and circulating 7-oxoLCA levels, similar to the observed accumulation of 7-oxocholesterol following 11β-HSD1 inhibition in rats [32]. 11β-HSD1 inhibition is not expected to affect bacterially derived production of UDCA and its metabolism in the liver; however, as shown in Figure 5, some UDCA is formed in the 11β-HSD1-dependent reduction of 7-oxoLCA, and inhibition of the enzyme might lower the local availability of UDCA. Clearly, further studies in 11β-HSD1-knockout mice and pre-clinical and clinical studies using selective inhibitors are needed to elucidate the impact of 11β-HSD1 on bile acid composition and function.

AUTHOR CONTRIBUTION

Alex Odermatt had the responsibility for the overall planning and conduct of the work, performed inhibitor experiments, analysed data and wrote the paper. Thierry Da Cunha and Carlos Penno developed the LC–MS protocol, performed enzyme activity experiments and analysed data. Christian Reichert performed activity experiments. Min Dong and Armin Wolf assisted in the design of experiments with human liver microsomes and analysis of protein expression. Charlie Chandsawangbhuwana performed three-dimensional modelling and analysed data, and Michael Baker performed three-dimensional modelling, analysed data and wrote the paper. All authors read and approved the final paper.

ACKNOWLEDGEMENTS

We thank Dr Alan F. Hofmann (University of California, San Diego, San Diego, CA, U.S.A.) for providing some of the bile acids for this study, and also for critical comments on the paper. M. D. and A. W. are employees of Novartis AG, Basel, Switzerland. The employer did not influence the design and interpretation of the data of this study.

FUNDING

This work was supported by the Swiss National Science Foundation [grant number 31003A-124912 to A.O.]. A.O. has a Chair in Molecular and Systems Toxicology by the Novartis Research Foundation.

REFERENCES

1 Hofmann, A. F. and Hagey, L. R. (2008) Bile acids: chemistry, pathochemistry, biology, pathobiology, and therapeutics. Cell. Mol. Life Sci. **65**, 2461–2483
2 Russell, D. W. (2003) The enzymes, regulation, and genetics of bile acid synthesis. Annu. Rev. Biochem. **72**, 137–174
3 Rossi, S. S., Converse, J. L. and Hofmann, A. F. (1987) High pressure liquid chromatographic analysis of conjugated bile acids in human bile: simultaneous resolution of sulfated and unsulfated lithocholyl amidates and the common conjugated bile acids. J. Lipid Res. **28**, 589–595
4 van Berge Henegouwen, G. P., Brandt, K. H., Eyssen, H. and Parmentier, G. (1976) Sulphated and unsulphated bile acids in serum, bile, and urine of patients with cholestasis. Gut **17**, 861–869
5 Ridlon, J. M., Kang, D. J. and Hylemon, P. B. (2006) Bile salt biotransformations by human intestinal bacteria. J. Lipid Res. **47**, 241–259
6 Hofmann, A. F. (1990) Bile acid secretion, bile flow and biliary lipid secretion in humans. Hepatology **12**, 17S–22S
7 Fukiya, S., Arata, M., Kawashima, H., Yoshida, D., Kaneko, M., Minamida, K., Watanabe, J., Ogura, Y., Uchida, K., Itoh, K. et al. (2009) Conversion of cholic acid and chenodeoxycholic acid into their 7-oxo derivatives by *Bacteroides intestinalis* AM-1 isolated from human feces. FEMS Microbiol. Lett. **293**, 263–270
8 Macdonald, I. A., Williams, C. N., Mahony, D. E. and Christie, W. M. (1975) NAD- and NADP-dependent 7α-hydroxysteroid dehydrogenases from *Bacteroides fragilis*. Biochim. Biophys. Acta **384**, 12–24
9 Fedorowski, T., Salen, G., Tint, G. S. and Mosbach, E. (1979) Transformation of chenodeoxycholic acid and ursodeoxycholic acid by human intestinal bacteria. Gastroenterology **77**, 1068–1073
10 MacDonald, I. A., Rochon, Y. P., Hutchison, D. M. and Holdeman, L. V. (1982) Formation of ursodeoxycholic acid from chenodeoxycholic acid by a 7β-hydroxysteroid dehydrogenase-elaborating *Eubacterium aerofaciens* strain cocultured with 7α-hydroxysteroid dehydrogenase-elaborating organisms. Appl. Environ. Microbiol. **44**, 1187–1195
11 Hirano, S. and Masuda, N. (1981) Epimerization of the 7-hydroxy group of bile acids by the combination of two kinds of microorganisms with 7α- and 7β-hydroxysteroid dehydrogenase activity, respectively. J. Lipid Res. **22**, 1060–1068
12 Mahowald, T. A., Yin, M. W., Matschiner, J. T., Hsia, S. L., Doisy, Jr, E. A., Elliott, W. H. and Doisy, E. A. (1958) Bile acids. VIII. Metabolism of 7-ketolithocholic acid-24-C_{14} in the rat. J. Biol. Chem. **230**, 581–588
13 Fromm, H., Carlson, G. L., Hofmann, A. F., Farivar, S. and Amin, P. (1980) Metabolism in man of 7-ketolithocholic acid: precursor of cheno- and ursodeoxycholic acids. Am. J. Physiol. **239**, G161–G166
14 Salen, G., Tint, G. S., Eliav, B., Deering, N. and Mosbach, E. H. (1974) Increased formation of ursodeoxycholic acid in patients treated with chenodeoxycholic acid. J. Clin. Invest. **53**, 612–621

15 Fromm, H., Sarva, R. P. and Bazzoli, F. (1983) Formation of ursodeoxycholic acid from chenodeoxycholic acid in the human colon: studies of the role of 7-ketolithocholic acid as an intermediate. J. Lipid Res. **24**, 841–853

16 Amuro, Y., Yamade, W., Kudo, K., Yamamoto, T., Hada, T. and Higashino, K. (1989) Reduction of 7-ketolithocholic acid by human liver enzyme preparations *in vitro*. Am. J. Physiol **256**, G67–G71

17 Odermatt, A., Atanasov, A. G., Balazs, Z., Schweizer, R. A., Nashev, L. G., Schuster, D. and Langer, T. (2006) Why is 11β-hydroxysteroid dehydrogenase type 1 facing the endoplasmic reticulum lumen? Physiological relevance of the membrane topology of 11β-HSD1. Mol. Cell. Endocrinol. **248**, 15–23

18 Atanasov, A. G. and Odermatt, A. (2007) Readjusting the glucocorticoid balance: an opportunity for modulators of 11β-hydroxysteroid dehydrogenase type 1 activity? Endocr. Metab. Immune Disord. Drug Targets **7**, 125–140

19 Hadoke, P. W., Iqbal, J. and Walker, B. R. (2009) Therapeutic manipulation of glucocorticoid metabolism in cardiovascular disease. Br. J. Pharmacol. **156**, 689–712

20 Boyle, C. D. and Kowalski, T. J. (2009) 11β-Hydroxysteroid dehydrogenase type 1 inhibitors: a review of recent patents. Expert Opin. Ther. Pat. **19**, 801–825

21 Hughes, K. A., Webster, S. P. and Walker, B. R. (2008) 11β-Hydroxysteroid dehydrogenase type 1 (11β-HSD1) inhibitors in type 2 diabetes mellitus and obesity. Expert Opin. Invest. Drugs **17**, 481–496

22 Odermatt, A. and Nashev, L. G. (2010) The glucocorticoid-activating enzyme 11β-hydroxysteroid dehydrogenase type 1 has broad substrate specificity: physiological and toxicological considerations. J. Steroid Biochem. Mol. Biol. **119**, 1–13

23 Senesi, S., Legeza, B., Balazs, Z., Csala, M., Marcolongo, P., Kereszturi, E., Szelenyi, P., Egger, C., Fulceri, R., Mandl, J. et al. (2010) Contribution of fructose 6-phosphate to glucocorticoid activation in the endoplasmic reticulum: possible implication in the metabolic syndrome. Endocrinology **151**, 4830–4839

24 Gumy, C., Thurnbichler, C., Aubry, E. M., Balazs, Z., Pfisterer, P., Baumgartner, L., Stuppner, H., Odermatt, A. and Rollinger, J. M. (2009) Inhibition of 11β-hydroxysteroid dehydrogenase type 1 by plant extracts used as traditional antidiabetic medicines. Fitoterapia **80**, 200–205

25 Schuster, D., Maurer, E. M., Laggner, C., Nashev, L. G., Wilckens, T., Langer, T. and Odermatt, A. (2006) The discovery of new 11β-hydroxysteroid dehydrogenase type 1 inhibitors by common feature pharmacophore modeling and virtual screening. J. Med. Chem. **49**, 3454–3466

26 Zhang, J., Osslund, T. D., Plant, M. H., Clogston, C. L., Nybo, R. E., Xiong, F., Delaney, J. M. and Jordan, S. R. (2005) Crystal structure of murine 11β-hydroxysteroid dehydrogenase 1: an important therapeutic target for diabetes. Biochemistry **44**, 6948–6957

27 Tanaka, N., Nonaka, T., Tanabe, T., Yoshimoto, T., Tsuru, D. and Mitsui, Y. (1996) Crystal structures of the binary and ternary complexes of 7α-hydroxysteroid dehydrogenase from *Escherichia coli*. Biochemistry **35**, 7715–7730

28 Kanai, S., Sato, Y., Nokubo, M. and Kitani, K. (1989) Hepatic biotransformation and choleretic effect of 7-ketolithocholic acid in the rat. Lipids **24**, 859–865

29 Amuro, Y., Yamade, W., Nakano, T., Hayashi, E., Hada, T. and Higashino, K. (1985) Reduction of 7-ketolithocholic acid to chenodeoxycholic acid by rat liver preparations *in vitro*. Biochim. Biophys. Acta **841**, 229–231

30 Clarke, J. L. and Mason, P. J. (2003) Murine hexose-6-phosphate dehydrogenase: a bifunctional enzyme with broad substrate specificity and 6-phosphogluconolactonase activity. Arch. Biochem. Biophys. **415**, 229–234

31 Hult, M., Elleby, B., Shafqat, N., Svensson, S., Rane, A., Jornvall, H., Abrahmsen, L. and Oppermann, U. (2004) Human and rodent type 1 11β-hydroxysteroid dehydrogenases are 7β-hydroxycholesterol dehydrogenases involved in oxysterol metabolism. Cell. Mol. Life Sci. **61**, 992–999

32 Schweizer, R. A., Zurcher, M., Balazs, Z., Dick, B. and Odermatt, A. (2004) Rapid hepatic metabolism of 7-ketocholesterol by 11β-hydroxysteroid dehydrogenase type 1: species-specific differences between the rat, human, and hamster enzyme. J. Biol. Chem. **279**, 18415–18424

33 Nashev, L. G., Chandsawangbhuwana, C., Balazs, Z., Atanasov, A. G., Dick, B., Frey, F. J., Baker, M. E. and Odermatt, A. (2007) Hexose-6-phosphate dehydrogenase modulates 11β-hydroxysteroid dehydrogenase type 1-dependent metabolism of 7-keto- and 7β-hydroxy-neurosteroids. PLoS ONE **2**, e561

34 Gomez-Sanchez, E. P., Romero, D. G., de Rodriguez, A. F., Warden, M. P., Krozowski, Z. and Gomez-Sanchez, C. E. (2008) Hexose-6-phosphate dehydrogenase and 11β-hydroxysteroid dehydrogenase-1 tissue distribution in the rat. Endocrinology **149**, 525–533

35 Maser, E., Volker, B. and Friebertshauser, J. (2002) 11β-Hydroxysteroid dehydrogenase type 1 from human liver: dimerization and enzyme cooperativity support its postulated role as glucocorticoid reductase. Biochemistry **41**, 2459–2465

36 Ozols, J. (1995) Lumenal orientation and post-translational modifications of the liver microsomal 11β-hydroxysteroid dehydrogenase. J. Biol. Chem. **270**, 2305–2312

37 Arampatzis, S., Kadereit, B., Schuster, D., Balazs, Z., Schweizer, R. A., Frey, F. J., Langer, T. and Odermatt, A. (2005) Comparative enzymology of 11β-hydroxysteroid dehydrogenase type 1 from six species. J. Mol. Endocrinol. **35**, 89–101

38 Buhler, H., Perschel, F. H., Fitzner, R. and Hierholzer, K. (1994) Endogenous inhibitors of 11β-OHSD: existence and possible significance. Steroids **59**, 131–135

39 Ackermann, D., Vogt, B., Escher, G., Dick, B., Reichen, J., Frey, B. M. and Frey, F. J. (1999) Inhibition of 11β-hydroxysteroid dehydrogenase by bile acids in rats with cirrhosis. Hepatology **30**, 623–629

40 Stauffer, A. T., Rochat, M. K., Dick, B., Frey, F. J. and Odermatt, A. (2002) Chenodeoxycholic acid and deoxycholic acid inhibit 11β-hydroxysteroid dehydrogenase type 2 and cause cortisol-induced transcriptional activation of the mineralocorticoid receptor. J. Biol. Chem. **277**, 26286–26292

41 Mazza, C., Breton, R., Housset, D. and Fontecilla-Camps, J. C. (1998) Unusual charge stabilization of $NADP^+$ in 17β-hydroxysteroid dehydrogenase. J. Biol. Chem. **273**, 8145–8152

42 Jornvall, H., Persson, B., Krook, M., Atrian, S., Gonzalez-Duarte, R., Jeffery, J. and Ghosh, D. (1995) Short-chain dehydrogenases/reductases (SDR). Biochemistry **34**, 6003–6013

43 Tanaka, N., Nonaka, T., Nakanishi, M., Deyashiki, Y., Hara, A. and Mitsui, Y. (1996) Crystal structure of the ternary complex of mouse lung carbonyl reductase at 1.8 Å resolution: the structural origin of coenzyme specificity in the short-chain dehydrogenase/reductase family. Structure **4**, 33–45

44 Amuro, Y., Endo, T., Higashino, K., Uchida, K. and Yamamura, Y. (1981) Urinary and fecal keto bile acids in liver cirrhosis. Clin. Chim. Acta **114**, 137–147

45 Bjorkhem, I., Angelin, B., Einarsson, K. and Ewerth, S. (1982) Fasting levels of monoketonic bile acids in human peripheral and portal circulation. J. Lipid Res. **23**, 1020–1025

46 Shiotsuki, H., Maeda, Y. and Chijiiwa, K. (2004) Purification and characterization of 7β-hydroxysteroid dehydrogenase from rabbit liver microsomes. J. Steroid Biochem. Mol. Biol. **91**, 185–190

47 Song, W., Chen, J., Dean, W. L., Redinger, R. N. and Prough, R. A. (1998) Purification and characterization of hamster liver microsomal 7α-hydroxycholesterol dehydrogenase: similarity to type I 11β-hydroxysteroid dehydrogenase. J. Biol. Chem. **273**, 16223–16228

48 Hennebert, O., Pernelle, C., Ferroud, C. and Morfin, R. (2007) 7α- and 7β-hydroxy-epiandrosterone as substrates and inhibitors for the human 11β-hydroxysteroid dehydrogenase type 1. J. Steroid Biochem. Mol. Biol. **105**, 159–165

49 Dzyakanchuk, A. A., Balazs, Z., Nashev, L. G., Amrein, K. E. and Odermatt, A. (2009) 11α-Hydroxysteroid dehydrogenase 1 reductase activity is dependent on a high ratio of NADPH/$NADP^+$ and is stimulated by extracellular glucose. Mol. Cell. Endocrinol. **301**, 137–141

50 Makishima, M., Okamoto, A. Y., Repa, J. J., Tu, H., Learned, R. M., Luk, A., Hull, M. V., Lustig, K. D., Mangelsdorf, D. J. and Shan, B. (1999) Identification of a nuclear receptor for bile acids. Science **284**, 1362–1365

51 Wang, H., Chen, J., Hollister, K., Sowers, L. C. and Forman, B. M. (1999) Endogenous bile acids are ligands for the nuclear receptor FXR/BAR. Mol. Cell **3**, 543–553

Received 4 January 2011/1 April 2011; accepted 1 April 2011
Published as BJ Immediate Publication 1 April 2011, doi:10.1042/BJ20110022

Biochem. J. (2011) **436**, 621–629 (Printed in Great Britain) doi:10.1042/BJ20110022

SUPPLEMENTARY ONLINE DATA

Hepatic reduction of the secondary bile acid 7-oxolithocholic acid is mediated by 11β-hydroxysteroid dehydrogenase 1

Alex ODERMATT*[1], Thierry DA CUNHA*, Carlos A. PENNO*†, Charlie CHANDSAWANGBHUWANA‡, Christian REICHERT*, Armin WOLF†, Min DONG† and Michael E. BAKER‡

*Division of Molecular and Systems Toxicology, Department of Pharmaceutical Sciences, University of Basel, Klingelbergstrasse 50, CH-4056 Basel, Switzerland, †Preclinical Safety, Novartis Institute for Biomedical Research, CH-4009 Basel, Switzerland, and ‡Department of Medicine, 0693 University of California, San Diego, 9500 Gilman Drive, La Jolla, CA 92093-0693, U.S.A.

EXPERIMENTAL

Materials

Human liver microsomes (*InVitro* CYP H-class microsomes from a male donor) were obtained from Celsis International, [1,2,6,7–^{3}H]cortisone was from American Radiolabeled Chemicals, [1,2,6,7–^{3}H]cortisol was from GE Healthcare, 5*H*-1,2,4-triazolo(4,3-a)azepine,6,7,8,9-tetrahydro-3-tricyclo(3 · 3 · 1 · 13 · 7)dec-1-yl (T0504) was from Enamine, steroids and bile acids were from Steraloids, and [2,2,4,4–^{2}H$_4$]CDCA (>98 % isotopic purity) was from Isotec, Sigma–Aldrich. Cell culture media were purchased from Invitrogen and Sigma. All other chemicals were from Fluka AG of the highest grade available. The conjugated bile acids 7-oxoLC-Tau and 7-oxoLC-Gly were a gift from Dr Alan F. Hofmann (University of California, San Diego, San Diego, CA, U.S.A.) [1]. BNW16 was provided by Dr Thomas Wilckens (BioNetWorks, Munich, Germany) [2], and S3483 was obtained from Sanofi-Aventis. Chemicals were diluted from 10 mM stock solutions in DMSO or methanol using TS2 buffer (final solvent concentrations were kept below 0.2 %).

Measurement of the interconversion of glucocorticoids in cell lysates

HEK-293 cells stably expressing recombinant human 11β-HSD1 alone or co-expressing 11β-HSD1 and H6PDH (AT6 and HHH7 clones respectively [3]) were cultured in DMEM supplemented with 10 % fetal bovine serum, 50 units/ml penicillin, 50 μg/ml streptomycin and 2 mM glutamine. For measurements with cell lysates, cells were detached and centrifuged, and pellets were stored at − 80 °C. Cell pellets were resuspended in TS2 buffer (100 mM NaCl, 1 mM EGTA, 1 mM EDTA, 1 mM $MgCl_2$, 250 mM sucrose and 20 mM Tris/HCl, pH 7.4), sonicated and used immediately to measure enzyme activity. Lysates of HEK-293 cells expressing human 11β-HSD1 were incubated for 10 min at 37 °C in a total volume of 22 μl containing 200 nM and 10 nCi of [1,2–^{3}H]cortisone or [1,2,6,7–^{3}H]cortisol and 500 μM cofactor NADPH or $NADP^+$ respectively and vehicle or various concentrations of bile acids.

Following conversion of radiolabelled glucocorticoids and termination of reactions by adding methanol containing 2 mM unlabelled cortisone and cortisol, 15 μl was spotted on Polygram SIL G-25 UV254 silica plates (Macherey-Nagel), plates were dried, and cortisone and cortisol were separated using a solvent system of 9:1 (v/v) chloroform/methanol. The separated steroids were analysed by scintillation counting.

Results (means ± S.D.) were obtained from at least three independent experiments. Enzyme kinetics was analysed by non-linear regression using four-parameter logistic curve fitting. For statistical comparisons, the ratio *t*-test in GraphPad Prism 5 software was used.

Analysis of non-labelled steroids and bile acids by LC–MS/MS

Frozen samples from reactions using intact cells, cell lysates or microsomes were thawed, and a fixed amount of deuterated CDCA (0.5 nmol) or corticosterone (0.2 nmol) was added as an internal standard, followed by mixing and centrifugation at 3000 ***g*** for 5 min. Supernatants were loaded on to Oasis HBL SPE cartridges (pre-conditioned with 1 ml of methanol and 1 ml of water), followed by washing with 2 ml of water and elution with 2 ml of methanol. The solvent was evaporated and the residue reconstituted in 100 μl of methanol.

7-OxoLCA and its metabolites were separated on an Atlantis T3 (3 μm, 2.1 mm×150 mm) column (Waters) at 30 °C using an Agilent Technologies model 1200 liquid chromatograph. The mobile phase consisted of solvent A (0.1 % formic acid in water) and solvent B (0.1 % formic acid in acetonitrile). A linear gradient was used starting from 65 % solvent A and 35 % solvent B to 5 % solvent A and 95 % solvent B from 0 to 10 min, then 5 % solvent A and 95 % solvent B from 10 to 12 min, 5 % solvent A and 95 % solvent B to 65 % solvent A and 35 % solvent B from 12 to 13 min, and finally re-equilibration with 65 % solvent A and 35 % solvent B from 13 to 18 min. The flow rate was maintained at 0.4 ml/min. The LC was interfaced to an Agilent 6410 triple quad mass spectrometer. The injection volume of each sample was 5 μl. The mass spectrometer was operated in atmospheric pressure electrospray positive-ionization mode, with a source temperature of 350 °C, a gas flow of 10 l/min and nebulizer gas pressure of 45 psi (1 psi = 6.9 kPa) at capillary and cone voltages of 4 kV and 190 V respectively. Data acquisition was performed using MassHunter workstation software (version B.01.04).

For the separation of cortisone and cortisol, a linear gradient was used starting from 70 % solvent A and 30 % solvent B to 5 % solvent A and 95 % solvent B from 0 to 13 min, then 5 % solvent A from 13 to 15 min, 5 % solvent A and 95 % solvent B to 70 % solvent A and 30 % solvent B from 15 to 18 min and finally re-equilibration with 70 % solvent A and 30 % solvent B for 5 min. The flow rate was maintained at 0.3 ml/min using the same MS conditions as for bile acids.

Bile acid and glucocorticoid metabolites were identified and quantified as outlined in the main text.

[1] To whom correspondence should be addressed (email alex.odermatt@unibas.ch).

RESULTS

Analysis of binding of bile acids to 11β-HSD1 by three-dimensional modelling

Figure S1 shows a three-dimensional model based on the crystal structure of 11β-HSD1 with corticosterone. In addition to the main stabilizing interactions described in the main text, the three-dimensional models also reveal differences in the stabilization of the A-ring on the three bile acids and corticosterone by 11β-HSD1 (compare Figure S1 with Figure 7 of the main text). All three bile acids have different interactions compared with corticosterone. Gln^{177} on 11β-HSD1 has a stabilizing contact with the C-3 hydroxy group on each bile acid. Ala^{172} also stabilizes the C-3 hydroxy group on CDCA and 7-oxoLCA. Pro^{178} has a contact with the C-3 hydroxy group on UDCA that is not found in CDCA and 7-oxoLCA. None of these residues has a stabilizing contact with C-3 ketone on corticosterone, which has a van der Waals contact with the backbone nitrogen on Leu^{217} [4].

Interestingly, the crystal structure of human 11β-HSD1 complexed with CHAPS as determined by Hosfield et al. [5] has the 7α-hydroxy group on CHAPS approximately 2.93 Å from Tyr^{183}, which could mean that 11β-HSD1 metabolizes this bile acid. However, regarding turnover of CHAPS or its core CA by 11β-HSD1, our analysis indicates that 11β-HSD1 does not oxidize 7α-hydroxy bile acids. Indeed, 11β-HSD1 preferentially metabolizes 7-oxoLCA.

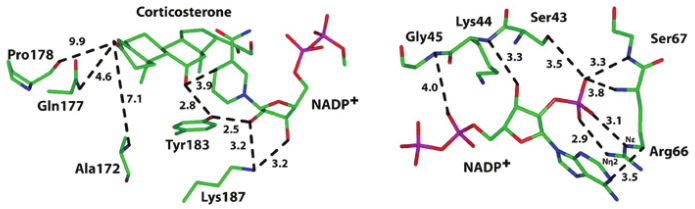

Figure S1 Binding of corticosterone to mouse 11β-HSD1

Tyr^{183} and Lys^{187} have critical stabilizing contacts respectively with the 11β-hydroxy group on corticosterone and ribose hydroxy groups on NADP$^+$. The guanidinium group on Arg^{66} forms a salt bridge with the 2′-phosphate on NADP$^+$.

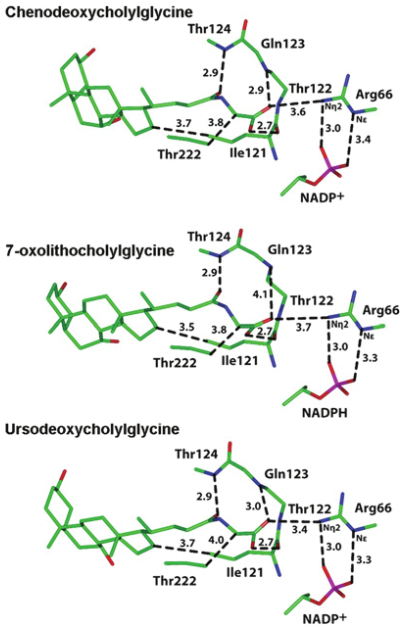

Figure S2 Three-dimensional models of mouse 11β-HSD1 complexed with glycine conjugates of CDCA, 7-oxoLCA and UDCA

In all three three-dimensional models, the carbonyl group on each glycine–bile acid conjugate has a stabilizing interaction with the guanidinium group of Arg^{56}. Backbone interactions also stabilize the glycine substituent.

REFERENCES

1 Nakagaki, M., Danzinger, R. G., Hofmann, A. F. and DiPietro, R. A. (1984) Biliary secretion and hepatic metabolism of taurine-conjugated 7α-hydroxy and 7β-hydroxy bile acids in the dog: defective hepatic transport and bile hyposecretion. Gastroenterology **87**, 647–659

2 Schuster, D., Maurer, E. M., Laggner, C., Nashev, L. G., Wilckens, T., Langer, T. and Odermatt, A. (2006) The discovery of new 11β-hydroxysteroid dehydrogenase type 1 inhibitors by common feature pharmacophore modeling and virtual screening. J. Med. Chem. **49**, 3454–3466

3 Gumy, C., Thurnbichler, C., Aubry, E. M., Balazs, Z., Pfisterer, P., Baumgartner, L., Stuppner, H., Odermatt, A. and Rollinger, J. M. (2009) Inhibition of 11β-hydroxysteroid dehydrogenase type 1 by plant extracts used as traditional antidiabetic medicines. Fitoterapia **80**, 200–205

4 Zhang, J., Osslund, T. D., Plant, M. H., Clogston, C. L., Nybo, R. E., Xiong, F., Delaney, J. M. and Jordan, S. R. (2005) Crystal structure of murine 11β-hydroxysteroid dehydrogenase 1: an important therapeutic target for diabetes. Biochemistry **44**, 6948–6957

5 Hosfield, D. J., Wu, Y., Skene, R. J., Hilgers, M., Jennings, A., Snell, G. P. and Aertgeerts, K. (2005) Conformational flexibility in crystal structures of human 11β-hydroxysteroid dehydrogenase type I provide insights into glucocorticoid interconversion and enzyme regulation. J. Biol. Chem. **280**, 4639–4648

Received 4 January 2011/1 April 2011; accepted 1 April 2011
Published as BJ Immediate Publication 1 April 2011, doi:10.1042/BJ20110022

5. QUANTIFICATION OF MULTIPLE BILE ACIDS IN UNINEPHRECTOMIZED RATS USING ULTRA-PERFORMANCE CHROMATOGRAPHY-TANDEM MASS SPECTROMETRY.

Carlos A Penno[1,2,5], Denis Arsenijevic[3,5], Thierry Da Cunha[1,5], Gerd A. Kullak-Ublick[4,5], Jean-Pierre Montani[3,5], Alex Odermatt[1,5.]

[1] Division of Molecular and Systems Toxicology, Department of Pharmaceutical Sciences, University of Basel, Basel, Switzerland

[2] Novartis Institute for Biomedical Research, Novartis, Basel, Switzerland

[3] Department of Medicine/Physiology, University of Fribourg, Fribourg, Switzerland

[4] Department of Clinical Pharmacology and Toxicology, University Hospital 10 Zurich, Zurich, Switzerland

[5] The Swiss National Center of Competence in Research (NCCR) Kidney Control of Homeostasis (Kidney.CH)

In this study, we reported the development, validation and application of a method using UPLC-MS/MS for quantification of concentrations of multiple BAs in biological samples.

Analytical Methods

RSC Publishing

PAPER

View Article Online
View Journal

Quantification of multiple bile acids in uninephrectomized rats using ultra-performance liquid chromatography-tandem mass spectrometry†

Cite this: DOI: 10.1039/c3ay26520j

Carlos A. Penno,*[abe] Denis Arsenijevic,[ce] Thierry Da Cunha,[ae] Gerd A. Kullak-Ublick,[de] Jean-Pierre Montani[ce] and Alex Odermatt*[ae]

Received 8th November 2012
Accepted 11th January 2013

DOI: 10.1039/c3ay26520j

www.rsc.org/methods

In order to study the roles of individual BAs and due to limited blood sample volumes available from experimental animals, improved methods for the simultaneous quantification of multiple BAs are needed. We developed and validated an ultra-performance liquid chromatography tandem mass spectrometry (UPLC-MS/MS) method for the quantification of 24 BAs, including 11 unconjugated, 6 glycine-conjugated and 7 taurine-conjugated BAs, in 50 μL of rat serum or plasma. The UPLC-MS/MS method, operated in negative and positive ion mode, allows quantification of BAs using multiple-reaction monitoring (MRM), with specific fragmentation of BAs. The method showed acceptable intra- and inter-day accuracy, precision, extraction recovery and high sensitivity, with a lower limit of quantification (LLOQ) in the pM range for several taurine-conjugated BAs. We applied the established method to investigate potential time-dependent changes of BAs in plasma from sham-operated and uninephrectomized male Sprague-Dawley rats. The levels of several primary and secondary BAs were transiently elevated one week after uninephrectomy, followed by normalization thereafter. In contrast, several conjugated BAs were slightly increased after the second week post-surgery. The established UPLC-MS/MS method, employing specific fragmentation of free and conjugated BAs by MRM, allows the simultaneous quantification of multiple BAs in 50 μL serum or plasma samples, and can be used to assess BA profiles in patho-physiological situations.

Introduction

The importance of bile acids (BAs) as end products of cholesterol catabolism and as emulsifiers for the absorption of dietary lipids and lipid soluble vitamins (A and D) has long been known.[1–3] More recently, their ability to activate nuclear receptors such as the farnesoid-X-receptor (FXR-α), pregnane-X-receptor (PXR), constitutive androstane receptor (CAR), vitamin D receptor (VDR) and G-protein coupled bile acid receptor (TGR5), as well as their role in liver regeneration have been identified.[4–7] Through the modulation of the activities of these various receptors, BAs regulate their own homeostasis as well as that of lipids and glucose, thereby controlling energy metabolism and thus opening new opportunities for therapeutic interventions to combat metabolic diseases.[3,8,9] Besides, BAs are involved in the solubilization and excretion of xenobiotics and are thus of toxicological relevance. Therefore, establishing novel, highly sensitive and accurate methods enabling the simultaneous quantification of a larger number of BAs in biofluids from normal and pathological conditions is expected to broaden our understanding of their functions.

Liquid chromatography tandem mass spectrometry (LC-MS/MS) has been considered the gold standard for quantification of BAs in biological fluids and tissues, due to several advantages over traditional techniques such as gas chromatography (GC)-MS, including ease of sample preparation and no need for hydrolysis of conjugated BAs or complex derivatization reactions.[10] However, despite the technological advance in MS to increase sensitivity, several problems still remain to be overcome such as the requirement of large sample volumes depending on the analyte to be quantified,[11] the need for derivatization depending on the availability of sample amount,[12] interference with contaminating endogenous BAs in biological matrices,[11] and limited specificity when using selective ion monitoring (SIM) for quantification.[10] Although there is a consensus in the literature regarding the use of multiple

[a]Division of Molecular and Systems Toxicology, Department of Pharmaceutical Sciences, University of Basel, Klingelbergstrasse 50, CH-4056 Basel, Switzerland. E-mail: alex.odermatt@unibas.ch; Fax: +41 61 267 1515; Tel: +41 61 267 1530
[b]Novartis Institute for Biomedical Research, Novartis, CH-4009 Basel, Switzerland. E-mail: carlos.penno@unibas.ch; Fax: +41 61 267 1515; Tel: +41 61 267 1484
[c]Department of Medicine/Physiology, University of Fribourg, Fribourg, Switzerland
[d]Department of Clinical Pharmacology and Toxicology, University Hospital Zurich, Zurich, Switzerland
[e]The Swiss National Center of Competence in Research (NCCR) Kidney Control of Homeostasis (Kidney.CH); Web: http://www.nccr-kidney.ch/

† Electronic supplementary information (ESI) available. See DOI: 10.1039/c3ay26520j

reaction monitoring (MRM) for the quantification of taurine- and glycine-conjugated BAs, MRM has not yet been widely used for quantification of unconjugated BAs.[11,13–25] In the present study, we applied specific fragmentation using MRM for both conjugated and unconjugated BAs in order to increase the specificity of detection and sensitivity for quantification of BAs in complex biological matrices such as serum and plasma.

Primary BAs are synthesized and conjugated in hepatocytes, followed by excretion into bile and the intestinal tract. Gut microorganisms generate secondary BAs by deconjugation and dehydroxylation. Upon reuptake by intestinal transporters, BAs are reconjugated in the liver to complete the enterohepatic cycle. BAs can also be filtered in the kidney through the glomerulus, followed by urinary excretion. Most BAs undergo reuptake by renal tubular transporters and, under normal conditions, the amount of excreted BAs is low. However, impaired hepatorenal function can lead to increased urinary BA excretion.

The kidney has a key role in the control of whole body homeostasis, including electrolyte balance and blood pressure, production and utilization of systemic glucose, degradation of hormones and excretion of waste metabolites.[26] Recent observations unraveled the importance of the kidney in the regulation of lipid metabolism, fat distribution and adipocyte differentiation.[27] In rats reduced renal function upon uninephrectomy has been linked with several aspects of the metabolic syndrome such as lipodystrophy of subcutaneous and visceral adipose depots, with lipid depletion, adipocyte dedifferentiation, lipid peroxidation, hypercholesterolemia and hypertriglyceridemia.[28] Similarly, nondiabetic patients on hemodialysis manifested fat redistribution with increasing visceral fat and altered serum lipid profiles.[29] These findings indicate that reduced renal function can cause disturbances of lipid homeostasis. Due to the close association between BA signaling and metabolic homeostasis[30–33] and the observed impact of reduced kidney function on lipid homeostasis, we investigated the impact of uninephrectomy in rats on plasma BA profiles by applying the validated UPLC-MS/MS method.

Materials and methods

Ethics statement

The animal experimental protocol was approved by the Ethical Committee of the Veterinary Office of Fribourg, Switzerland.

Chemicals and reagents

Cholic acid (CA), chenodeoxycholic acid (CDCA), deoxycholic acid (DCA), lithocholic acid (LCA), ursodeoxycholic acid (UDCA), glyco-deoxycholic acid (G-DCA), glyco-chenodeoxycholic acid (G-CDCA), tauro-chenodeoxycholic acid (T-CDCA), [2,2,4,4-2H4]-CA (98% isotopic purity), [2,2,4,4-2H4]-CDCA (>98% isotopic purity) and [2,2,4,4-2H4]-LCA (98% isotopic purity) were purchased from Sigma-Aldrich (St. Louis, MO). 7-Oxodeoxycholic acid (7-oxoDCA), 7-oxolithocholic acid (7-oxoLCA), hydeoxycholic acid (HDCA), α-muricholic acid (α-MCA), β-muricholic acid (β-MCA), ω-muricholic acid (ω-MCA), glyco-lithocholic acid (G-LCA), glyco-ursodeoxycholic acid (G-UDCA), tauro-lithocholic acid (T-LCA), tauro-α-muricholic acid (T-α-MCA), tauro-β-muricholic acid (T-β-MCA) and [2,2,4,4-2H4]-DCA (98% isotopic purity) were obtained from Steraloids (Newport, RI). Glyco-cholic acid (G-CA), tauro-cholic acid (T-CA), tauro-deoxycholic acid (T-DCA) and tauro-ursodeoxycholic acid (T-UDCA) were purchased from Calbiochem (Läufelfingen, Switzerland), and [2,2,4,4-2H4]-UDCA (>98% isotopic purity), [2,2,4,4-2H4]-G-CA (>98% isotopic purity), [2,2,4,4-2H4]-G-CDCA (>98% isotopic purity) and [2,2,4,4-2H4]-G-UDCA (>98% isotopic purity) from C/D/N Isotopes Inc. (Pointe-Claire, Canada). The conjugated bile acids tauro-7-oxoLCA (T-7-oxoLCA) and glyco-7-oxoLCA (G-7-oxoLCA) were a gift from Dr Alan F. Hofmann (University of California at San Diego, San Diego, CA, USA). All other chemicals were from Fluka AG (Buchs, Switzerland) of the highest grade available.

Preparation of stock solutions, calibrators and quality control (QC) samples

Stock solutions were prepared in methanol for each standard and deuterium-labeled internal standards (IS) at a concentration of 10 mM. Thereafter, working solutions containing standards and deuterium-labeled IS (100 μM each) were prepared. All stock solutions of standards and deuterium-labeled IS were stored at −20 °C. Unspiked charcoal-treated rat serum represented the zero calibration point. Calibration curves were prepared by serial dilution of the working solutions of standards in charcoal-treated pooled male rat serum (Dunn Labortechnik GmbH, Asbach, Germany). For that purpose, 100 mg mL^{-1} of activated charcoal was stirred overnight at 4 °C, and centrifuged thereafter for 20 min at 13 000 × *g* to remove endogenous BAs. Following three centrifugation cycles, the supernatant was filtered through a 0.20 μm membrane and stored in aliquots at −20 °C until further use. The absence of remaining endogenous BAs from the matrix was verified by UPLC-MS/MS.

Animal preparation and experimental protocol

Male Sprague Dawley rats (Elevage Janvier, France) of ~5 weeks of age were caged singly in a temperature-controlled room (22 ± 1 °C) with a 12 h light/dark cycle. After one week of acclimation, the rats (eight animals per group) underwent surgery under general anesthesia with ketamine/xylazine (150 mg kg^{-1} and 2 mg kg^{-1}, respectively) and sterile conditions for uninephrectomy or sham-surgery. Briefly, an incision was made on the left flank to access the kidney retroperitoneally. In half of the rats, renal blood vessels and the urethra were ligated with a surgical thread, the connection to the kidney was cut and the kidney was removed. Tissues were sutured and the wound was closed with metal clips. In sham-operated rats, the surgery was identical except that the kidney was left intact in place. For the whole experiment, rats were fed an isocaloric diet 90 kcal per day (low fat diet Nr 2125 from Kliba, Kaiseraugst, Switzerland). Eight rats per group were sacrificed by decapitation 1 week, 2 weeks and 4 weeks after surgery, and blood was collected from the neck immediately after decapitation in EDTA tubes under

ice and cold-centrifuged. The plasma was separated and stored at −20 °C for later analysis.

Sample preparation

Plasma samples (total volume of 50 μL) and calibrators were subjected to protein precipitation by adding 500 μL of ice-cold acetonitrile containing deuterium-labeled internal standards (IS), at a final concentration of 100 nM each of CA-d4, CDCA-d4, DCA-d4, UDCA-d4, G-CA-d4, G-CDCA-d4 and G-UDCA-d4. The final concentration of LCA-d4 was adjusted to 1000 nM due to its low ionization efficiency. The concentrations of IS used are similar to those used by other investigators and did not interfere with the concentrations of endogenous BAs found in samples.[23] Extraction was performed for 30 min at 4 °C with continuous shaking. Samples were centrifuged at 14 000 × *g* for 15 min at 4 °C, and the supernatants were transferred to new tubes, followed by evaporation and reconstitution in 50 μL of methanol/water of 50/50 (v/v). The injection volume was 5 μL.

Separation, ionization and detection conditions

The UPLC-MS/MS consisted of an Agilent 1290 UPLC coupled to an Agilent 6490 triple quadrupole mass spectrometer equipped with an electrospray ionization (ESI) source (Agilent Technologies, Basel, Switzerland). Separation of analytes was achieved using reversed-phase column (ACQUITY UPLC BEH C18, 1.7 μm, 2.1 × 150 mm, Waters, Wexford, Ireland) heated to 65 °C. Data acquisition and analysis was performed using Mass Hunter software (Agilent Technologies).

The mobile phase consisted of water–acetonitrile–formic acid (A) (95/5/0.1; v/v/v) and (B) (5/95/0.1; v/v/v). The eluent gradients were set from 25%–35% of B during 0–8 min, 35%–70% eluent B during 8–18 min and 95% of B at 18.1 min onwards. The run was stopped at 20 min, followed by re-equilibration of the column. The flow rate was set to 0.75 mL min^{-1}. Ionization was performed using an ESI source operated in the positive and negative ion modes. Fragmentation was tuned for each compound using Optimizer software (Agilent Technologies). Optimized conditions are shown in Table 1. The source parameters were set to gas temperature 350 °C, gas flow 15 L min^{-1}, nebulizer pressure 20 psi, sheath gas temperature 250 °C, sheath gas flow 11 L min^{-1}, capillary voltage 3000 V (positive and negative), nozzle voltage 2000 V and cell accelerator voltage 5 V.

Method validation

Method validation was performed according to the FDA guidelines for Bioanalytical Method Validation.[34] The linearity of each BA calibration curve was determined by analyzing charcoal treated rat serum prepared to contain standards at the concentration ranges of 0.12 nM, 0.98 nM, 7.8 nM, 62.5 nM, 500 nM and 4 μM. Calibration curve linearity was evaluated by assessing the correlation coefficient (R^2) of three freshly prepared calibration curves. Standard curves were constructed by least-squares linear regression analysis using the peak area ratio of a given BA over its reference IS against the nominal concentration of the calibrator. Quantification of samples was performed identically. Due to the unavailability of reference IS, 7-oxoDCA, HDCA, 7-oxoLCA, α-MCA, β-MCA, ω-MCA, G-DCA, G-LCA, G-7-oxoLCA, T-CA, T-CDCA, T-DCA, T-LCA, T-7-oxoLCA, T-β-MCA and T-UDCA were semi-quantified by referring to a surrogate deuterium-labeled IS (Table 1).

Values of the lower limit of quantification (LLOQ) were calculated by assessing the signal to noise ratio (SNR) (baseline noise determined on an interval before and after the peak of interest and using the peak height as signal definition). Five replicates were extracted and analyzed for each concentration. A signal equal or higher than ten times that of the baseline was considered the LLOQ, with accuracy between 80 and 120% of the true value and coefficient of variation (CV) of 15%. Due to the persistence of trace amounts of G-CA, G-CDCA and G-DCA after charcoal treatment, their LLOQs were determined as being the lowest concentration at which these analytes could be quantified with sufficient precision (CV of 15%) and accuracy (between 85% and 115%).

In order to assess intra- and inter-day precision and accuracy, five replicates of five different quality control (QC) samples with concentrations ranging from 0.002 μM to 2 μM were extracted and quantified using freshly prepared calibrators in charcoal treated rat serum. Replicates of each QC sample were analyzed in a given day in order to determine intra-day accuracy and precision as well as over a period of three days (inter-day) using freshly prepared calibration curves.

Recovery experiments were performed using untreated and charcoal-treated serum samples in order to mimic extraction conditions similar to those of real samples and to assess the impact of matrix components on extraction recoveries. In order to assess extraction recovery, twelve untreated and charcoal-treated serum samples were taken for each of the concentration levels (2000 nM, 200 nM and 20 nM). From these twelve samples, six were spiked with the appropriate amount of standard stock solution and IS prior to extraction, and the remaining six samples were extracted as blanks and reconstituted with the same amount of standard stock solution and IS after extraction. Six additional unspiked serum samples were extracted in order to determine endogenous concentrations of BAs. Thereafter, samples were evaporated, reconstituted and injected. Correction of the spiked serum samples was performed by subtracting the endogenous amounts of the respective BAs. Recovery results were obtained by expressing the average of the mean peak area of samples spiked prior to extraction as a percentage of that of samples spiked after extraction.

Matrix effects were assessed by using untreated pooled rat serum in order to mimic chemical conditions of those of real samples. For that purpose, six samples were spiked with defined amounts of standard stock solutions (2000 nM, 200 nM and 20 nM) and IS after extraction. Six additional unspiked serum samples were extracted in order to determine the endogenous concentration of BAs. Thereafter, all samples were evaporated and reconstituted in the mobile phase. Correction of the spiked serum samples was performed by subtracting the endogenous amounts of the respective BAs, and matrix effects were calculated by expressing the peak area of spiked serum samples after extraction as a percentage of the peak area of that of net solutions containing only the pure standard in methanol.

Table 1 Precursor and product ions of BAs with optimized fragmentation parameters (collision energy) as well as the corresponding deuterium-labeled internal standard used for quantitative analysis

BA	Precursor Ion (*m*/*z*)	Product ion (*m*/*z*)	Collision energy (V)	Polarity	Internal Standard
CA	373.3	355.2	48	Positive	CA-d4
CDCA	357.2	95.1	40	Positive	CDCA-d4
DCA	357.2	95.1	40	Positive	DCA-d4
7-oxoDCA	371.3	353.2	8	Positive	DCA-d4
HDCA	357.2	95.1	40	Positive	UDCA-d4
LCA	359.3	135.1	24	Positive	LCA-d4
7-oxoLCA	373.3	355.2	8	Positive	UDCA-d4
α-MCA	373.3	355.2	8	Positive	UDCA-d4
β-MCA	373.3	355.2	8	Positive	UDCA-d4
ω-MCA	373.3	355.2	8	Positive	UDCA-d4
UDCA	357.2	95.1	40	Positive	UDCA-d4
G-CA	464.2	74	37	Negative	G-CA-d4
G-CDCA	448.2	74	41	Negative	G-CDCA-d4
G-DCA	448.2	74	41	Negative	G-CA-d4
G-LCA	432.2	74	41	Negative	G-UDCA-d4
G-7-oxoLCA	446.2	74	37	Negative	G-UDCA-d4
G-UDCA	448.2	74	37	Negative	G-UDCA-d4
T-CA	480.3	126	24	Positive	G-UDCA-d4
T-CDCA	464.2	126	28	Positive	G-CDCA-d4
T-DCA	464.2	126	28	Positive	DCA-d4
T-LCA	466.2	126	28	Positive	G-UDCA-d4
T-7-oxoLCA	480.3	126	20	Positive	G-UDCA-d4
T-β-MCA	480.3	126	24	Positive	G-DCA-d4
T-UDCA	464.2	126	28	Positive	G-UDCA-d4
CA-d4	377.3	359.2	48	Positive	—
CDCA-d4	361.2	95.1	40	Positive	—
DCA-d4	361.3	95.1	40	Positive	—
LCA-d4	363.3	135.1	24	Positive	—
UDCA-d4	361.2	95.1	40	Positive	—
G-CA-d4	468.2	74	37	Negative	—
G-CDCA-d4	452.2	74	41	Negative	—
G-UDCA-d4	452.2	74	41	Negative	—

Statistical analysis

Data are presented as mean ± SD. Statistical significance was assessed by Student's *t*-test.

Results and discussion

In the present study, a sensitive and specific UPLC-MS/MS method for the quantification of 24 BAs, including 11 unconjugated, 6 glycine- and 6 taurine-conjugated BAs was developed. Additionally, T-α-MCA was included in the analytical method after validation. The method was validated according to the Food and Drug Administration (FDA) guidelines,[34] using 50 μL of rat serum. In the validation procedure we included the following parameters: linearity of calibration curves, inter- and intra-day accuracy and precision, extraction recoveries and matrix effects. Following validation, the method was applied to determine BA profiles in the plasma of sham-operated and uninephrectomized male Sprague-Dawley rats.

Chromatography and ionization conditions

Due to the fact that it is impossible to differentiate isobaric BA species by MS, a prior chromatographic step is needed (see Fig. 1 for structures). Our chromatography conditions allowed the separation of the 24 BAs in a 20 min run using a reversed-phase column heated to 65 °C (Fig. 2). T-α-MCA and T-β-MCA

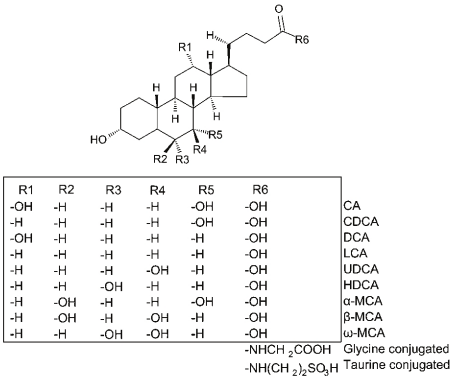

Fig. 1 Structure of BAs.

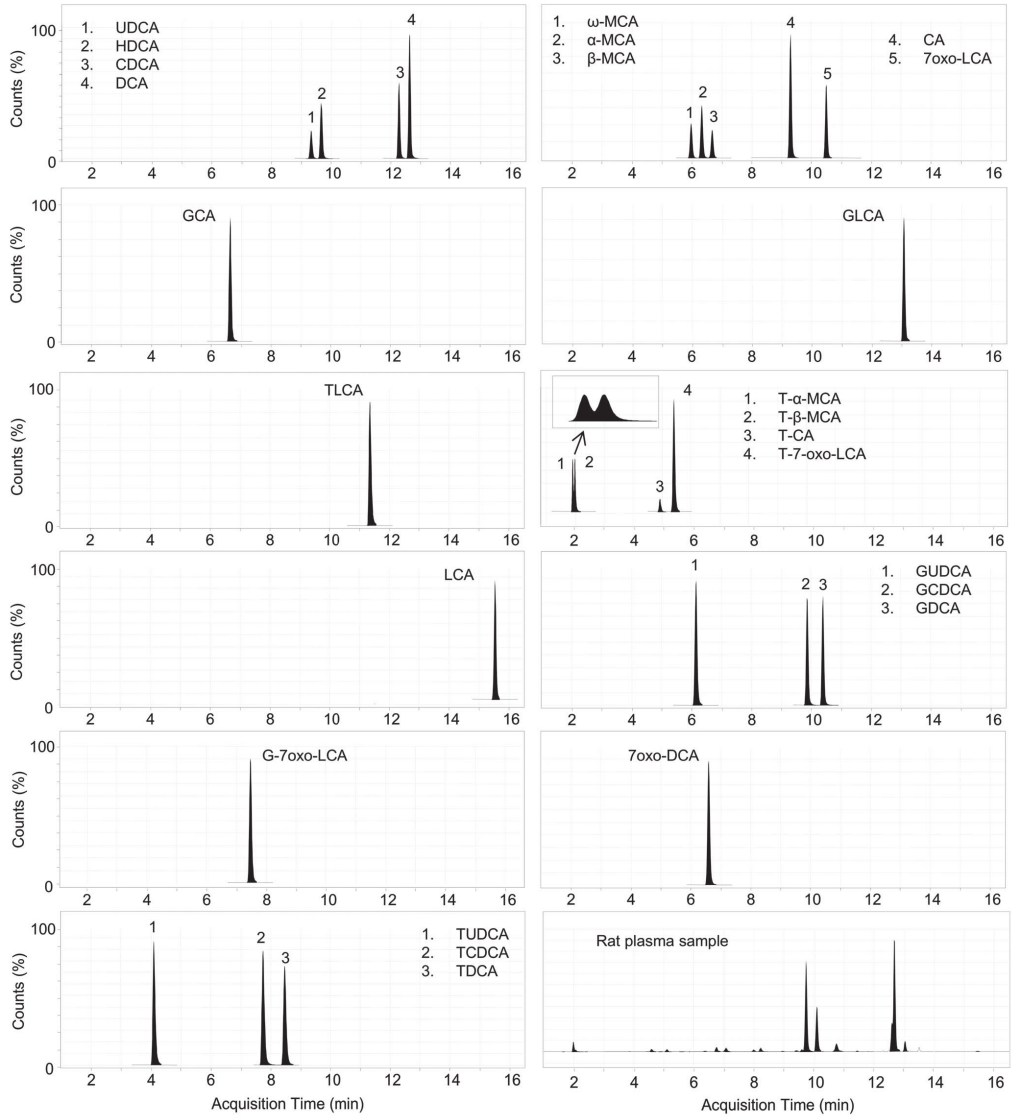

Fig. 2 Representative chromatogram of bile acids extracted from a plasma sample and charcoal-treated rat serum spiked with 24 bile acids standard.

peaks were resolved with a resolution of approximately 1.0 (Fig. 2, insert). In order to gain sensitivity, the MS program was divided in segments in which defined transitions were monitored according to the retention time of the metabolites. An electrospray ionization (ESI) source operating in the negative ion mode was used for glycine-conjugated BAs and in the positive ion mode for unconjugated and taurine-conjugated BAs (Table 1). Most studies so far reported the use of negative ion mode for the quantification of BAs in biological matrices.[11,13,15–25,35–37] In spite of this, we found that ESI-positive ion mode provided higher ionization efficiency for unconjugated and taurine-conjugated BAs, regardless of whether formic acid or ammonium formate was used as the ionizing agent. Moreover, we obtained more stable and abundant fragments for

MRM transitions of unconjugated BAs in positive but not in negative ion mode. Superior signal-to-noise ratios (SNRs) and LOD values (SNR∼3) have been obtained with positive ion mode. LCA, for example, could not be quantified in negative ion mode using transitions reported in the literature (Fig. S1 and S2†).[23] This may be explained by the solvent system employed in the present study. Supporting this idea, Qiao *et al.* reported more efficient ionization of DCA in ESI-negative mode using a solvent system consisting of water-methanol compared with acetonitrile, while maintaining reasonable signal intensity in

Table 2 Intra- and inter-day accuracy, precision of BA samples in serum[a]

	QC 2 nM		QC 4 nM		QC 100 nM		QC 1000 nM		QC 2000 nM	
	CV (%)	Accuracy (%)	CV (%)	Accuracy (%)	CV (%)	Accuracy (%)	CV (%)	Accuracy (%)	CV (%)	Accuracy (%)
Intra-day										
CA	N.D.		N.D.		6.4	100.0	2.5	111.1	1.5	93.0
CDCA	N.D.		N.D.		2.1	88.0	2.2	99.3	1.9	102.7
DCA	N.D.		N.D.		3.1	90.6	2.6	101.0	4.8	103.3
7-oxoDCA	N.D.		N.D.		8.3	104.6	3.2	101.0	2.7	98.3
HDCA	N.D.		N.D.		10.2	88.7	9.6	110.4	11.1	103.4
LCA	N.D.		N.D.		6.2	94.2	3.8	95.0	6.4	98.5
7-oxoLCA	N.D.		N.D.		5.1	109.9	3.2	102.4	6.3	102.7
α-MCA	N.D.		N.D.		2.4	106.8	1.4	98.6	5.1	105.9
β-MCA	N.D.		N.D.		6.5	103.7	4.3	108.0	2.4	101.7
ω-MCA	N.D.		N.D.		5.9	95.8	2.2	108.7	9.5	98.6
UDCA	N.D.		N.D.		8.6	96.3	3.5	106.0	3.9	102.3
G-CA	N.D.		12.9	95.2	2.9	87.5	4.2	105.8	4.5	96.5
G-CDCA	N.D.		N.D.		2.4	91.2	2.3	104.2	1.8	90.6
G-DCA	8.9	102.0	8.3	92.5	2.0	90.1	3.6	104.8	1.9	103.1
G-LCA	10.4	111.1	7.4	102.6	2.7	90.1	6.4	100.2	1.9	99.5
G-7-oxo-LCA	5.4	113.8	3.3	88.5	1.5	86.8	3.2	108.0	3.6	94.6
G-UDCA	7.7	106.8	11.7	102.6	3.2	95.4	6.8	112.5	1.7	94.7
T-CA	9.3	96.2	8.8	105.3	4.7	94.3	1.9	101.9	3.2	96.3
T-CDCA	10.6	88.4	8.2	91.7	3.8	93.8	2.6	105.0	3.2	104.5
T-DCA	9.4	103.3	3.0	87.7	4.8	98.0	2.4	96.6	3.3	99.4
T-LCA	8.6	108.2	12.6	101.0	4.2	99.4	4.6	100.0	4.0	96.7
T-7-oxo-LCA	14.8	92.6	6.4	97.6	3.4	92.9	4.2	93.5	3.2	98.6
T-β-MCA	7.2	114.9	12.6	101.0	4.1	100.6	6.9	97.7	4.2	99.4
T-UDCA	12.2	92.3	5.2	97.1	3.9	96.5	3.0	104.7	4.5	97.6
Inter-day										
CA	N.D.		5.5	96.8	5.2	99.4	4.4	97.0	3.8	93.8
CDCA	N.D.		6.0	93.4	2.2	97.4	1.9	95.1	3.8	97.1
DCA	N.D.		3.5	93.8	4.0	93.0	1.7	96.4	2.0	100.0
7-oxoDCA	N.D.		N.D.		5.1	106.6	1.9	100.2	1.2	104.0
HDCA	N.D.		N.D.		4.6	92.0	3.0	94.8	3.7	96.1
LCA	N.D.		N.D.		4.3	97.8	1.8	93.3	2.9	99.8
7-oxoLCA	N.D.		N.D.		4.4	104.0	5.9	92.3	4.4	99.1
α-MCA	N.D.		N.D.		3.8	99.4	3.5	92.4	5.4	98.1
β-MCA	N.D.		N.D.		5.5	96.5	4.3	94.9	5.3	99.2
ω-MCA	N.D.		N.D.		3.7	95.0	2.1	97.5	6.7	95.6
UDCA	N.D.		N.D.		7.1	97.2	4.8	93.7	1.8	98.3
G-CA	N.D.		4.8	102.9	1.8	91.8	2.4	99.5	3.4	101.7
G-CDCA	N.D.		N.D.		2.3	92.9	1.8	97.9	1.9	93.2
G-DCA	12.3	90.1	7.2	96.0	2.4	93.3	2.3	98.7	4.9	101.4
G-LCA	9.2	105.6	4.8	94.9	1.3	88.9	1.3	98.0	1.4	99.8
G-7-oxo-LCA	9.3	109.5	2.1	90.6	2.2	90.7	1.7	99.0	1.8	98.3
G-UDCA	9.5	102.7	7.8	100.8	2.9	96.1	2.4	98.2	1.5	94.7
T-CA	8.5	96.8	4.7	90.9	2.8	95.1	1.8	99.3	1.4	101.4
T-CDCA	12.0	90.6	4.6	91.5	3.3	96.4	2.9	104.4	4.0	96.8
T-DCA	14.2	102.1	2.5	86.8	2.1	96.2	5.0	99.9	1.1	104.2
T-LCA	8.2	111.4	4.2	98.0	2.2	98.1	3.2	101.4	1.7	102.7
T-7-oxo-LCA	15.0	95.2	2.2	93.9	3.2	94.9	1.3	95.6	1.4	102.1
T-β-MCA	11.7	109.5	5.5	92.4	2.1	95.1	4.3	99.9	2.8	104.3
T-UDCA	12.3	95.4	2.5	87.2	3.1	94.3	3.7	104.7	3.1	105.5

[a] CV: coefficient of variation. N.D.: not determined owing to concentration below lower limit of quantification.

positive ion mode.[38] Controversially, García-Canãveras *et al.* used acetonitrile as a solvent and negative ion mode for quantification of DCA and LCA, with LLOQ of 5 and 10 nM, respectively.[23] The discrepancy between results obtained in positive and negative ion mode may be dependent, at least in part, on the different instruments used.

Fragmentation of BAs

To achieve higher specificity and sensitivity in the quantitative analysis of BAs in biological samples, we aimed at defining MRM transitions for each metabolite, including unconjugated BAs (Table 1). Several earlier studies reported stable fragments for conjugated BAs; however, identical precursors and product ions were employed for the quantification of free BAs.[11,13–23] This approach is called selective ion monitoring (SIM) and, although useful, it has limited specificity.[10] There are only a few studies on the fragmentation of unconjugated BAs,[24,25] and it is important to identify and validate novel fragments that may enhance sensitivity and specificity for the quantification of BAs in biological matrices. Fragmentation of BAs was defined by direct injection of each individual standard into the MS, and identification of the most abundant fragments was performed using Optimizer software (Agilent technologies). Glycine- and taurine-conjugated BAs were efficiently fragmented, yielding the product ions *m*/*z* 74 and 126, respectively. This fragmentation pattern is derived from the elimination of glycine and taurine, respectively.[38] The unconjugated BAs 7-oxoLCA, 7-oxoDCA, α-MCA, β-MCA, ω-MCA and CA yielded product ions by the consecutive neutral loss of water molecules, so-called dehydrated BAs. HDCA, UDCA, CDCA and DCA were fragmented to generate the ion *m*/*z* 95.1, whereas LCA was monitored with *m*/*z* 135.1. Deuterium-labeled IS yielded fragmentation patterns similar to those of their corresponding non-deuterated forms (Table 1). In a recent study Qiao, *et al.* characterized the fragmentation behavior of BAs.[38] They found similar fragmentation patterns for taurine- and glycine-conjugated BAs and also observed the neutral loss of water for CA and the ion *m*/*z* 135.1 for LCA. However, the ion *m*/*z* 95.1 for CDCA, UDCA, HDCA and DCA detected in the present study has not yet been described or validated.[38] The differences in fragmentation behavior and peak abundances are probably due to limitations in low mass measurements by the different instruments used. Although Qiao *et al.* reported on the fragmentation patterns of several BAs, they did not investigate the applicability, reproducibly and robustness of BA fragments for MRM quantification. Here, we report the identification and applicability of novel fragments for the quantification of free BAs using UPLC-MS/MS. The use of fragmentation conditions not only for conjugated, but also for unconjugated BAs is expected to enhance specificity and sensitivity of measurements.

Table 3 Lower limit of quantification (LLOQ), retention time, linearity and recovery of BAs in rat serum

						Extraction recoveries[a] (%)		
Bile acids	LLOQ (nM)	SNR	RT (min)	Linearity (R^2)	Calibration range (nM)	20 nM	200 nM	2 μM
CA	3	11 ± 4	9.3	0.9921	4000–0.98	78 ± 30	97 ± 14	70 ± 11
CDCA	3	13 ± 4	12.3	0.9914	4000–0.98	76 ± 3	94 ± 12	83 ± 8
DCA	3	10 ± 1	12.6	0.9985	4000–0.98	75 ± 12	86 ± 26	63 ± 7
7-oxoDCA	25	11 ± 1	6.6	0.9955	4000–7.8	78 ± 9	71 ± 16	73 ± 5
HDCA	8	11 ± 2	9.6	0.9957	4000–7.8	43 ± 8	33 ± 6	39 ± 9
LCA	13	10 ± 2	15.5	0.9963	4000–7.8	95 ± 13	60 ± 4	68 ± 4
7-oxoLCA	8	10 ± 2	10.5	0.9902	4000–7.8	76 ± 22	68 ± 5	79 ± 3
α-MCA	13	17 ± 3	6.3	0.9952	4000–7.8	77 ± 6	64 ± 12	60 ± 9
β-MCA	13	11 ± 2	6.7	0.9922	4000–7.8	77 ± 11	66 ± 13	61 ± 8
ω-MCA	13	16 ± 4	5.9	0.9954	4000–7.8	76 ± 7	59 ± 7	54 ± 2
UDCA	13	11 ± 2	9.3	0.9962	4000–7.8	62 ± 15	68 ± 6	74 ± 4
G-CA	3	N.A.[b]	6.6	0.9926	4000–0.98	79 ± 13	71 ± 15	52 ± 12
G-CDCA	6	N.A.[b]	9.8	0.9970	4000–0.98	61 ± 6	58 ± 12	61 ± 8
G-DCA	1	N.A.[b]	10.4	0.9978	4000–0.98	57 ± 24	62 ± 3	58 ± 5
G-LCA	1	17 ± 4	13.1	0.9936	4000–0.98	53 ± 1	56 ± 5	69 ± 4
G-7-oxoLCA	1	18 ± 4	7.5	0.9910	4000–0.98	55 ± 1	64 ± 3	77 ± 6
G-UDCA	1	12 ± 3	6.1	0.9951	4000–0.98	60 ± 12	60 ± 6	73 ± 5
T-CA	1	14 ± 3	4.5	0.9955	4000–0.98	67 ± 18	92 ± 10	80 ± 4
T-CDCA	0.2	10 ± 4	7.7	0.9900	4000–0.1221	65 ± 17	87 ± 9	89 ± 6
T-DCA	0.2	10 ± 3	8.3	0.9947	4000–0.1221	78 ± 12	73 ± 6	83 ± 5
T-LCA	0.4	12 ± 1	11.4	0.9910	4000–0.1221	62 ± 2	79 ± 5	93 ± 4
T-7-oxoLCA	1	14 ± 3	5.2	0.9963	4000–0.98	60 ± 4	81 ± 3	96 ± 4
T-β-MCA	0.2	10 ± 3	1.9	0.9945	4000–0.1221	71 ± 10	110 ± 3	80 ± 6
T-UDCA	0.2	11 ± 1.5	4.1	0.9967	4000–0.1221	73 ± 3	78 ± 4	93 ± 3

[a] Data are presented as the average ± %R.S.D of three levels of QC concentrations (20 nM, 200 nM and 2 μM), six samples per concentration. [b] N.A. not applicable: LLOQs were determined as the lowest concentration in which these analytes were quantified with sufficient precision (CV of 15%) and accuracy (between 85% and 115%).

Inter- and intra-day accuracy, precision, linearity and lower limits of quantification (LLOQ)

Overall accuracy and precision were appropriate for all measurements (Table 2). Intra- and inter-day accuracy ranged from 85% to 115%. Intra- and inter-day precision measured as coefficient of variation (CV) (%) ranged from 1.1% to 15.0% (Table 2). Accuracy and precision were also evaluated for selected bile acids (TCA, GCDCA, GUDCA, DCA, CA, LCA, CDCA and α-MCA) in a fortification assay by adding 3 increasing concentrations (+25%, +50% and +100% of endogenous) to samples, and acceptable accuracy and precision intervals were obtained (data not shown). Linearity of calibration curves was acceptable with a correlation coefficient after linear regression of ≥ 0.99 (Table 3). The LLOQ was defined as the lowest concentration of a given analyte with a signal-to-noise ratio (SNR) ≥ 10. The LLOQs for BAs obtained in the present study ranged from 200 pM to 25 nM. Surprisingly, T-CDCA, T-DCA, T-LCA, T-β-MCA and T-UDCA reached LLOQs at the pM range and are remarkably lower than those of previous studies (Table 3).[18,23] This can be explained by employing MRM and using specific fragments for quantification of BAs, thereby reducing the SNR in the second mass filter and improving sensitivity. Recently, García-Cañaveras *et al.* reported comparable LLOQs for a number of unconjugated BAs in 25 μL of sample volume using SIM operated in negative ion mode, differences that are likely to be caused by different sensitivities of the instruments used.[23] Nevertheless, MRM is generally accepted as the superior approach for the specific determination of chemicals, and therefore its usage is likely to improve the quality of data generated.

Extraction recovery and matrix effects

Since it was reported that solid phase extraction (SPE) is not optimal for BA extraction owing to low recovery for some analytes,[23] and to avoid excessive sample handling, a single extraction step using acetonitrile was performed in the present method. The deuterium-labeled IS UDCA-d4, CDCA-d4, LCA-d4, G-UDCA-d4, G-CA-d4, CA-d4 and DCA-d4 were included to minimize possible bias during extraction.

Low extraction recoveries were observed for a few BAs (HDCA, G-DCA, G-LCA and G-UDCA), in contrast to a previous study using a similar extraction procedure.[14] A possible explanation for these discrepancies may be the presence of matrix components interfering with the extraction of the aforementioned BAs, because identical experiments using charcoal-treated instead of untreated rat serum provided superior extraction recoveries (Table S1†). Overall, extraction recoveries using acetonitrile were reproducible across the concentration studied and ranged from 33% to 110% in untreated serum and from 70% to 88% in charcoal-treated serum. According to the FDA guidelines for validation of analytical methods, the recovery of a given analyte does not need to be 100%, but the amount of recovery must be consistent, precise and reproducible.[34] Due to the fact that HDCA extraction recovery was discrepant between untreated and charcoal-treated samples, its value may not reflect the absolute concentration. Regarding matrix effects, the ionization of BAs studied was not affected by the matrix components at the three concentrations studied (Table 4). Overall, our findings are in line with that of other investigators.[18]

Profiling of circulating BAs in sham-operated and uninephrectomized rats

We hypothesized that reduced renal function might affect BA homeostasis due to reduced filtration capacity and/or proximal tubular reuptake. Therefore, we applied the established UPLC-MS/MS method to determine BA profiles in sham-operated and uninephrectomized male Sprague-Dawley rats following one, two and four weeks after the surgical intervention (Table 5). A 2-fold increase in circulating total primary BAs was observed one week after uninephrectomy, which was fully reversed after the second week. The two most abundant primary BAs, CA and CDCA, were increased by 2.3- and 2.2-fold at one week post-surgery. The amount of total secondary BAs was also slightly elevated one week after uninephrectomy, followed by reversal to normal levels at the second week. In contrast to primary BAs, total taurine-conjugated BAs remained unchanged at one week post-surgery, but they were increased by 40% after the second week and tended to be higher by 20% after the fourth week, suggesting a delayed response. Thus, the established method allowed the detection of transient changes in the levels of circulating BAs following uninephrectomy in rats.

Table 4 Quantitative assessment of matrix effects for BAs. The analytical response in the presence of a matrix was expressed as a percentage of the analytical response in the absence of a matrix[a]

	Relative response (%)		
	20 nM	200 nM	2000 nM
CA	108 ± 6	99 ± 14	114 ± 5
CDCA	91 ± 3	110 ± 6	115 ± 1
DCA	90 ± 15	114 ± 1	114 ± 3
7-oxoDCA	87 ± 10	104 ± 10	110 ± 2
HDCA	100 ± 10	111 ± 5	111 ± 1
LCA	77 ± 9	105 ± 1	106 ± 3
7-oxoLCA	87 ± 10	115 ± 7	114 ± 5
α-MCA	103 ± 15	103 ± 8	109 ± 1
β-MCA	95 ± 13	104 ± 10	115 ± 3
ω-MCA	92 ± 13	99 ± 6	112 ± 2
UDCA	97 ± 7	105 ± 9	113 ± 2
G-CA	89 ± 15	102 ± 8	113 ± 2
G-CDCA	92 ± 12	102 ± 7	114 ± 1
G-DCA	96 ± 15	114 ± 2	111 ± 4
G-LCA	107 ± 2	113 ± 2	115 ± 2
G-7-oxo-LCA	112 ± 3	113 ± 1	111 ± 2
G-UDCA	105 ± 4	120 ± 1	115 ± 3
T-CA	98 ± 3	96 ± 6	115 ± 2
T-CDCA	114 ± 6	107 ± 3	114 ± 2
T-DCA	111 ± 10	113 ± 1	118 ± 1
T-LCA	106 ± 7	114 ± 1	112 ± 3
T-7-oxo-LCA	99 ± 2	112 ± 2	111 ± 2
T-β-MCA	84 ± 12	99 ± 6	97 ± 4
T-UDCA	98 ± 4	115 ± 4	115 ± 2

[a] Data is presented as the average ± CV (%).

Table 5 BA profiling in rat plasma followed by uninephrectomy[a]

	1 Week sham	1 Week UNX	Fold increase	1 Week sham	2 Weeks UNX	Fold increase	4 Weeks sham	4 Weeks UNX	Fold increase
Primary BAs									
α-MCA	381 ± 332	642 ± 326	1.7	616 ± 486	481 ± 391	0.8	256 ± 187	328 ± 2000	1.3
β-MCA	357 ± 335	428 ± 166	1.2	346 ± 256	429 ± 384	1.2	252 ± 201	338 ± 235	1.3
CDCA	483 ± 420	1052 ± 436*	2.2	801 ± 576	794 ± 577	1	644 ± 602	380 ± 310	0.6
CA	795 ± 653	1860 ± 1515	2.3	1037 ± 881	1192 ± 1094	1.1	884 ± 576	830 ± 669	0.9
Total	2016 ± 202	3983 ± 632*	2	2800 ± 292	2896 ± 351	1	2035 ± 310	1878 ± 242	0.9
Secondary BAs									
LCA	14 ± 7	17 ± 9	1.3	9 ± 6	14 ± 4	1.6	5 ± 1	6 ± 2	1.2
DCA	22 ± 15	46 ± 34	2.1	38 ± 27	58 ± 48	1.5	40 ± 25	55 ± 24	1.4
UDCA	176 ± 161	300 ± 137	1.7	243 ± 162	230 ± 168	0.9	131 ± 62	160 ± 93	1.2
HDCA	199 ± 119	214 ± 158	1.1	372 ± 371	398 ± 419	1.1	209 ± 247	213 ± 248	1
7-oxoLCA	23 ± 25	38 ± 23	1.6	35 ± 30	55 ± 52	1.6	22 ± 16	23 ± 14	1.1
7-oxoDCA	482 ± 590	479 ± 222	1	716 ± 779	645 ± 745	0.9	249 ± 254	323 ± 184	1.3
ω-MCA	69 ± 36	111 ± 61	1.6	107 ± 79	163 ± 155	1.5	90 ± 64	121 ± 67	1.4
Total	986 ± 169	1204 ± 170*	1.2	1519 ± 256	1563 ± 228	1.0	746 ± 94	901 ± 114	1.2
Taurine-conjugated BAs									
T-UDCA	3 ± 1	4 ± 1*	1.2	3 ± 1	5 ± 4*	1.9	2 ± 1	4 ± 3	1.5
T-CDCA	52 ± 22	59 ± 16	1.1	33 ± 19	31 ± 13	0.9	25 ± 10	34 ± 21	1.3
T-CA	150 ± 38	189 ± 79	1.3	134 ± 73	213 ± 85*	1.6	123 ± 60	190 ± 124	1.5
T-DCA	6 ± 4	8 ± 6	1.3	7 ± 3	12 ± 9	1.8	7 ± 5	12 ± 9	1.8
T-LCA	N.D.	1 ± 0.7*		N.D.	2 ± 4		N.D.	1 ± 0.6*	
T-α-MCA	320 ± 100	300 ± 88	0.9	279 ± 99	348 ± 159	1.2	269 ± 92	286 ± 168	1.1
T-β-MCA	56 ± 31	47 ± 7	0.8	48 ± 29	85 ± 64	1.8	62 ± 26	67 ± 48	1.1
T-7oxo-LCA	3 ± 1	3 ± 1	1.3	2 ± 1	5 ± 3*	2	3 ± 1	3 ± 2	1.2
Total	591 ± 112	612 ± 110	1	506 ± 98	700 ± 127	1.4	490 ± 94	597 ± 107	1.2
Glycine-conjugated BAs									
G-CA	29 ± 13	27 ± 15	0.9	51 ± 58	93 ± 95	1.8	79 ± 84	84 ± 76	1.1
G-UDCA	N.D.	N.D.		N.D.	N.D.		N.D.	N.D.	
G-CDCA	3 ± 1	3 ± 2	0.9	5 ± 2	8 ± 8	1.6	7 ± 6	7 ± 6	1
G-DCA	0.4 ± 0.4	1 ± 0.9	1.2	1.5 ± 1.6	4 ± 6	2.9	3 ± 4	4 ± 3	1.2
G-LCA	N.D.	N.D.		N.D.	N.D.		N.D.	N.D.	
G-7oxo-LCA	N.D.	N.D.		N.D.	N.D.		N.D.	N.D.	
Total	33 ± 14	31 ± 13	0.9	57 ± 24	106 ± 44	1.8	90 ± 38	95 ± 40	1.1

[a] The results are expressed in nM as mean ± standard deviation ($n = 8$). N.D.: not detected. Underlined values represent below lower limit of quantification. Sham, sham-operated control rats; UNX, uninephrectomized rats. Statistics: * for $p \leq 0.05$.

Conclusions

We established a method for the quantification of BAs in serum and plasma by employing specific fragmentation of BAs, which has demonstrated to be robust, reproducible and accurate, thus enhancing the specificity of the quantitative analysis of BAs in biological samples. We applied the method to study the impact of uninephrectomy in healthy rats on BA homeostasis and observed that impaired kidney function indeed alters BA homeostasis by transiently increasing their circulating concentrations. The mechanisms and physiological significance of these findings remain to be further investigated.

Acknowledgements

We thank Jean-François Cajot, University of Fribourg, for support in animal experimentation and Dr Alan F. Hofmann, University of California at San Diego, for providing some of the bile acid standards. This work was supported by the NCCR Kidney.CH, funded by the Swiss National Science Foundation.

Notes and references

1 A. F. Hofmann, *Hepatology*, 2009, **49**, 1403–1418.
2 M. J. Monte, J. J. G. Marin, A. Antelo and J. Vazquez-Tato, *World J. Gastroenterol.*, 2009, **15**, 804–816.
3 C. Thomas, R. Pellicciari, M. Pruzanski, J. Auwerx and K. Schoonjans, *Nat. Rev. Drug Discovery*, 2008, **7**, 678–693.
4 W. Huang, K. Ma, J. Zhang, M. Qatanani, J. Cuvillier, J. Liu, B. Dong, X. Huang and D. D. Moore, *Science*, 2006, **312**, 233–236.
5 C. Thomas, A. Gioiello, L. Noriega, A. Strehle, J. Oury, G. Rizzo, A. Macchiarulo, H. Yamamoto, C. Mataki, M. Pruzanski, R. Pellicciari, J. Auwerx and K. Schoonjans, *Cell Metab.*, 2009, **10**, 167–177.
6 P. B. Hylemon, H. Zhou, W. M. Pandak, S. Ren, G. Gil and P. Dent, *J. Lipid Res.*, 2009, **50**, 1509–1520.
7 A. A. Khan, E. C. Chow, R. J. Porte, K. S. Pang and G. M. Groothuis, *Toxicol. in Vitro*, 2011, **25**, 80–90.
8 J. Prawitt, S. Caron and B. Staels, *Curr. Diabetes Rep.*, 2011, **11**, 160–166.

9 T. W. Pols, L. G. Noriega, M. Nomura, J. Auwerx and K. Schoonjans, *J. Hepatol.*, 2011, **54**, 1263–1272.
10 W. J. Griffiths and J. Sjovall, *J. Lipid Res.*, 2009, **51**, 23–41.
11 X. Xiang, Y. Han, M. Neuvonen, J. Laitila, P. J. Neuvonen and M. Niemi, *J. Chromatogr., B: Anal. Technol. Biomed. Life Sci.*, 2010, **878**, 51–60.
12 T. Higashi, Y. Shibayama, T. Ichikawa, K. Ito, T. Toyo'oka, K. Shimada, K. Mitamura, S. Ikegawa and H. Chiba, *Steroids*, 2010, **75**, 338–345.
13 L. Yang, A. Xiong, Y. He, Z. Wang, C. Wang, Z. Wang, W. Li, L. Yang and Z. Hu, *Chem. Res. Toxicol.*, 2008, **21**, 2280–2288.
14 Y. Alnouti, I. L. Csanaky and C. D. Klaassen, *J. Chromatogr., B: Anal. Technol. Biomed. Life Sci.*, 2008, **873**, 209–217.
15 J. Huang, S. P. R. Bathena, I. L. Csanaky and Y. Alnouti, *J. Pharm. Biomed. Anal.*, 2011, **55**, 1111–1119.
16 M. Scherer, C. Gnewuch, G. Schmitz and G. Liebisch, *J. Chromatogr., B: Anal. Technol. Biomed. Life Sci.*, 2009, **877**, 3920–3925.
17 M. Hagio, M. Matsumoto, M. Fukushima, H. Hara and S. Ishizuka, *J. Lipid Res.*, 2009, **50**, 173–180.
18 C. Steiner, A. von Eckardstein and K. M. Rentsch, *J. Chromatogr., B: Anal. Technol. Biomed. Life Sci.*, 2010, **878**, 2870–2880.
19 X. Qiao, M. Ye, C. Xiang, T. Bo, W.-z. Yang, C.-f. Liu, W.-j. Miao and D.-a. Guo, *Steroids*, 2012, **77**, 745–755.
20 M. Ando, T. Kaneko, R. Watanabe, S. Kikuchi, T. Goto, T. Iida, T. Hishinuma, N. Mano and J. Goto, *J. Pharm. Biomed. Anal.*, 2006, **40**, 1179–1186.
21 I. Burkard, A. von Eckardstein and K. M. Rentsch, *J. Chromatogr., B: Anal. Technol. Biomed. Life Sci.*, 2005, **826**, 147–159.
22 E. J. Want, M. Coen, P. Masson, H. C. Keun, J. T. M. Pearce, M. D. Reily, D. G. Robertson, C. M. Rohde, E. Holmes, J. C. Lindon, R. S. Plumb and J. K. Nicholson, *Anal. Chem.*, 2010, **82**, 5282–5289.
23 J. C. García-Canãveras, M. T. Donato, J. V. Castell and A. Lahoz, *J. Lipid Res.*, 2012, **53**, 2231–2241.
24 N. Janzen, S. Sander, M. Terhardt, A. M. Das, J. O. Sass, R. Kraetzner, H. Rosewich, M. Peter and J. Sander, *J. Lipid Res.*, 2010, **51**, 1591–1598.
25 X. Qiao, M. Ye, D.-l. Pan, W.-j. Miao, C. Xiang, J. Han and D.-a. Guo, *J. Chromatogr., A*, 2011, **1218**, 107–117.
26 A. Odermatt, *Am. J. Physiol.: Renal Physiol.*, 2011, **301**, F919–F931.
27 H.-L. Zhao, Y. Sui, L. He, J. Guan, S.-J. Xiao, D.-R. Zhong, Q. Xu and S.-E. Zeng, *Acta Diabetol. Lat.*, 2011, **48**, 317–328.
28 H.-L. Zhao, Y. Sui, J. Guan, L. He, X. Zhu, R.-R. Fan, G. Xu, A. P. S. Kong, C. S. Ho, F. M. M. Lai, D. K. Rowlands, J. C. N. Chan and P. C. Y. Tong, *Kidney Int.*, 2008, **74**, 467–477.
29 M. Odamaki, R. Furuya, S. Ohkawa, T. Yoneyama, M. Nishikino, A. Hishida and H. Kumagai, *Nephrol., Dial., Transplant.*, 1999, **14**, 2427–2432.
30 T. Li, E. Owsley, M. Matozel, P. Hsu, C. M. Novak and J. Y. L. Chiang, *Hepatology*, 2010, **52**, 678–690.
31 K. Ma, P. K. Saha, L. Chan and D. D. Moore, *J. Clin. Invest.*, 2006, **116**, 1102–1109.
32 Y. Zhang, F. Y. Lee, G. Barrera, H. Lee, C. Vales, F. J. Gonzalez, T. M. Willson and P. A. Edwards, *Proc. Natl. Acad. Sci. U. S. A.*, 2006, **103**, 1006–1011.
33 T. Li, M. Matozel, S. Boehme, B. Kong, L.-M. Nilsson, G. Guo, E. Ellis and J. Y. L. Chiang, *Hepatology*, 2011, **53**, 996–1006.
34 FDA. http://www.fda.gov/downloads/Drugs/GuidanceComplianceRegulatoryInformation/Guidances/UCM070107.pdf.
35 L. Humbert, M. A. Maubert, C. Wolf, H. Duboc, M. Mahé, D. Farabos, P. Seksik, J. M. Mallet, G. Trugnan, J. Masliah and D. Rainteau, *J. Chromatogr., B: Anal. Technol. Biomed. Life Sci.*, 2012, **899**, 135–145.
36 I. Bobeldijk, M. Hekman, J. de Vries-van der Weij, L. Coulier, R. Ramaker, R. Kleemann, T. Kooistra, C. Rubingh, A. Freidig and E. Verheij, *J. Chromatogr., B: Anal. Technol. Biomed. Life Sci.*, 2008, **871**, 306–313.
37 S. Perwaiz, B. Tuchweber, D. Mignault, T. Gilat and I. M. Yousef, *J. Lipid Res.*, 2001, **42**, 114–119.
38 X. Qiao, M. Ye, C.-f. Liu, W.-z. Yang, W.-j. Miao, J. Dong and D.-a. Guo, *Steroids*, 2012, **77**, 204–211.

Electronic Supplementary Material (ESI) for Analytical Methods

Electronic supplementary information

Figure S1

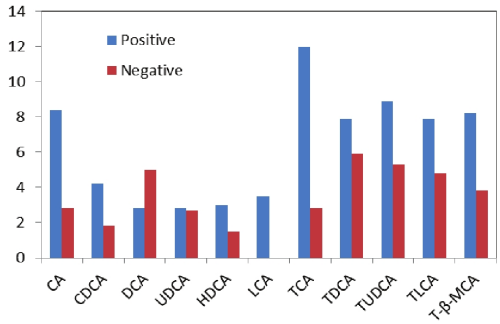

Fig. S1. Comparison of signal to noise ratios (SNRs) of several BAs at the lower limit of detection (LOD) in positive and negative ion modes.

Figure 2S

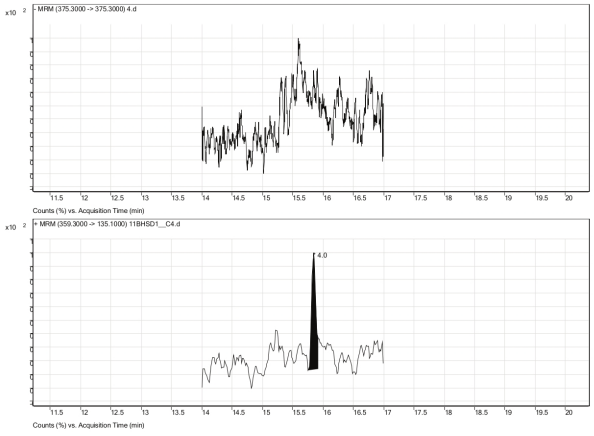

Fig. S2. Comparison of molecular ion intensity of LCA in negative ion mode (375.3 → 375.3; *upper panel*) and positive ion mode (359.3→ 135.1; *lower panel*) using MRM. The signal to noise ratio (SNR) of the latter was 4.0, thus above the lower limit of detection.

Electronic Supplementary Material (ESI) for Analytical Methods

Table S1. Extraction recovery of BAs in charcoal-treated serum.

Bile acids	Extract recovery (%)
CA	84 ± 12
CDCA	79 ± 20
DCA	67 ± 19
7-oxoDCA	71 ± 23
HDCA	80 ±6
LCA	74 ± 17
7-oxoLCA	76 ± 13
α-MCA	72 ± 15
β-MCA	70 ± 11
ω-MCA	73 ± 12
UDCA	79 ± 11
G-CA	68 ± 19
G-CDCA	69 ± 17
G-DCA	76 ± 24
G-LCA	75 ± 11
G-7-oxoLCA	76 ± 15
G-UDCA	76 ± 16
T-CA	86 ± 17
T-CDCA	80 ± 17
T-DCA	88 ± 10
T-LCA	82 ± 9
T-7-oxoLCA	77 ± 19
T-β-MCA	81 ± 15
T-UDCA	74 ± 23

Data are presented as the average ± % R.S.D of two levels of QC concentrations (200 nM and 2000 nM), six samples per concentration.

LACK OF 7-OXOLITHOCHOLIC ACID REDUCTION BY 11B-HSD1 LEADS TO ITS ACCUMULATION: A POTENTIAL BIOMARKER OF IMPAIRED GLUCOCORTICOID ACTIVATION.

Carlos A Penno[1], Agnieszka E. Zielisnka[2], Gareth Lavery[2], Alex Odermatt[1]

[1] Division of Molecular and Systems Toxicology, Department of Pharmaceutical Sciences, University of Basel, Basel, Switzerland.

[2] Centre for Endocrinology Diabetes and Metabolism (CEDAM), Institute of Biomedical Research, Medical School Building, School of Clinical and Experimental Medicine, College of Medical and Dental Sciences, University of Birmingham, Edgbaston, Birmingham B15 2TT, UK.

C**orrespondence to**:
Dr. Alex Odermatt, Division of Molecular and Systems Toxicology, Department of Pharmaceutical Sciences, University of Basel, Klingelbergstrasse 50, 4056 Basel, Switzerland, Phone: +41 61 267 1530, Fax: +41 61 267 1515, E-mail: alex.odermatt@unibas.ch.

ABSTRACT

11β-hydroxysteroid dehydrogenase type 1 (11β-HSD1) has emerged as a promising therapeutic target to treat metabolic diseases; however, suitable biomarkers to assess its activity *in vivo* are still lacking. Recently, we characterized the *in vitro* metabolism of a novel substrate of 11β-HSD1 – the secondary bile acid 7-oxolithocholic acid (7-oxoLCA). Here, we provide further *in vitro* and *in vivo* evidence for an exclusive role of 11β-HSD1 in the oxoreduction of 7-oxoLCA. Hepatic microsomes of liver-specific 11β-HSD1 deficient mice were devoid of 7-oxoLCA oxoreductase activity. In addition, 7-oxoLCA and its taurine and glycine conjugates were 18- , 47- and 7-fold elevated in serum and 2- and 6- in liver from liver-specific 11β-HSD1 deficient mice, respectively. Since glucocorticoids can regulate the expression of genes involved in bile acid (BA) homeostasis, we assessed the impact of 11β-HSD1 deficiency on circulating and hepatic BA profiles in mice. We observed an accumulation of unconjugated BAs in the liver and serum from liver-specific 11β-HSD1 deficient mice, an effect attributable to a down-regulation of BA coenzyme A conjugating enzymes (*VLCS* and *VLCSH2*) and the reduced expression of *OATP4*. In conclusion, the results suggest a role of 11β-HSD1 in the regulation of BA homeostasis, whereby 7-oxoLCA and its taurine conjugate may serve as biomarkers for impaired 11β-HSD1 activity. Importantly, we found that guinea-pig cannot reduce 7-oxoLCA, providing explanation why 7-oxoLCA is a major BA in this species.

INTRODUCTION

11β-Hydroxysteroid dehydrogenase type 1 (11β-HSD1) is a NADPH-dependent enzyme facing the endoplasmic reticulum lumen and responsible for cortisol (corticosterone in rodents) regeneration from inactive cortisone (11-dehydrocorticosterone in rodents), thus mediating tissue specific exposure to active glucocorticoids (Odermatt, Arnold et al. 1999; Odermatt, Atanasov et al. 2006). Glucocorticoid excess is implicated in the pathogenesis of the metabolic syndrome characterized by glucose intolerance, insulin resistance, dyslipidaemia and hypertension (Tomlinson and Stewart 2007). Evidences from transgenic mice (knockout or overexpression of 11β-HSD1) revealed potential benefits of 11β-HSD1 inhibition to ameliorate obesity and the metabolic syndrome (Kotelevtsev, Holmes et al. 1997; Masuzaki, Paterson et al. 2001; Morton, Holmes et al. 2001; Masuzaki, Yamamoto et al. 2003; Morton, Paterson et al. 2004; Paterson, Morton et al. 2004; Hughes, Webster et al. 2008; Boyle and Kowalski 2009; Hadoke, Iqbal et al. 2009; Wamil, Battle et al. 2011). More recently, data from human phase II clinical trials are supporting results from animal studies, and currently several companies are developing selective inhibitors (Rosenstock, Banarer et al. 2010; Thomas and Potter 2011). However, validated biomarkers of 11β-HSD1 inhibition in preclinical and clinical studies are still unavailable and are of great interest in order to assess the *in vivo* efficacy of therapeutic inhibitors. In this regard, circulating concentrations of glucocorticoids are not suitable biomarkers because they are not significantly altered in plasma of liver-specific 11β-HSD1 deficient and 11β-HSD1-null mice (Carter, Paterson et al. 2009; Lavery, Zielinska et al. 2012). Similarly, urinary 11-dehydrocorticosterone (11-DHC) levels are unchanged in heterozygous 11β-HSD1 deficient compared with wild-type mice, suggesting that 11β-HSD1 does not significantly alter systemic glucocorticoid levels (Abrahams, Semjonous et al. 2012). An ideal biomarker should be independent of mechanisms of negative feedback regulation such as control by the HPA axis of circulating glucocorticoids, and stress-induced fluctuations (Harno and White 2010; Odermatt and Nashev 2010). 11β-HSD1 has a broad substrate specificity and metabolizes endogenous and exogenous compounds such as 7-hydroxy- and 7-keto-DHEA, 7-oxygenated pregnenolone, 7-ketocholesterol, 7-ketoepiandrosterone, 7-

keto-5-androstane-3,17-diol, metyrapone, p-nitroacetophenone, p-nitrobenzaldehyde, ketoprofen, oracin, triadimefon and the tobacco carcinogen nicotine-derived nitrosamine ketone (NNK). (Maser and Bannenberg 1994; Hult, Nobel et al. 2001; Wsól, Szotáková et al. 2003; Hult, Elleby et al. 2004; Schweizer, Zürcher et al. 2004; Martin, Breyer-Pfaff et al. 2006; Muller, Pompon et al. 2006; Hennebert, Le Mée et al. 2007; Hennebert, Pernelle et al. 2007; Nashev, Chandsawangbhuwana et al. 2007; Kenneke, Mazur et al. 2008). We recently identified a novel role of 11β-HSD1 in the metabolism of the secondary BA 7-oxoLCA (Odermatt, Da Cunha et al. 2011). 11β-HSD1 reduced 7-oxoLCA preferentially to the 7α-hydroxylated chenodeoxycholic (CDCA) and to a lesser extent to the 7β-hydroxylated ursodeoxycholic acid (UDCA) (Odermatt, Da Cunha et al. 2011). 7-oxoLCA is formed in the colon by 7α-hydroxysteroid dehydrogenation of CDCA and UDCA by microorganism such as *Eschericha coli, Bacteroides fragilis and Bacteroides intestinalis* (Macdonald, Williams et al. 1975; Fukiya, Arata et al. 2009). Thereafter, 7-oxoLCA is reabsorbed in the intestine and reaches the liver through the enterohepatic cycle. In this work, we provide further evidences for an exclusive role of 11β-HSD1 in the oxoreduction of 7-oxoLCA both *in vitro* and *in vivo.* Furthermore, we suggest that its accumulation may serve as a potential readout of 11β-HSD1 inhibition *in vivo*. Moreover, we revealed the impact of hepatic 11β-HSD1 deficiency on BA homeostasis. Liver-specific disruption of 11β-HSD1 altered BA homeostasis, resulting in the accumulation of unconjugated BAs in the liver and serum of liver-specific 11β-HSD1 deficient mice, a phenomenon likely mediated by the glucocorticoid receptor (GR) and an altered intrahepatic concentration of active glucocorticoids.

MATERIALS AND METHODS

CHEMICALS AND REAGENTS

Chenodeoxycholic acid (CDCA), ursodeoxycholic acid (UDCA), [2,2,4,4-2H4]-CDCA (>98% isotopic purity) and [9,11,12,12-2H4]-cortisol (>98% isotopic purity) were purchased from Sigma-Aldrich (St. Louis, MO). 7-oxolithocholic acid (7-oxoLCA) was purchased from Steraloids (Newport, RI). Cell culture media were purchased from Invitrogen (Carlsbad, CA) and Sigma (Buchs, Switzerland). [1,2,6,7-3H]-cortisone were obtained from American Radiolabeled Chemicals (St. Louis, MO), [1,2,6,7-3H]-cortisol from Amersham Pharmacia (Piscataway, NJ) and 5H-1,2,4-triazolo(4,3-a)azepine,6,7,8,9-tetrahydro-3- tricyclo(3·3·1·13·7)dec-1-yl (T0504) from Enamine (Kiev, Ukraine). Male guinea-pig liver microsomes were obtained from Celsis International and serum of 12-16 h fasted mice (balb/c and C57bL/6), rats (Han Wistar and Sprague-Dawley), canine (*Canis familiaris*, beagle bred), guinea-pigs (dunkin-hartley) and hamsters (golden syrian) were obtained from Harlan (Gannat, France).

REDUCTION OF 7-OXOLCA BY RECOMBINANT HUMAN 11B-HSD1 OF VARIOUS SPECIES

In order to access species-dependent differences of 7-oxoLCA metabolism by 11β-HSD1, HEK-293 cells cultured in Dulbecco's Modified Eagle's Medium (DMEM) supplemented with 10% fetal bovine serum (FBS), 50 units/ml penicillin, 50 µg/ml streptomycin and 2 mM glutamine were transiently transfected with recombinant 11β-HSD1 from rat, mouse, human, hamster, canine and guinea-pig as described previously (Odermatt, Arnold et al. 1999; Schweizer, Zürcher et al. 2004; Arampatzis, Kadereit et al. 2005). Thereafter, cells were detached, centrifuged and pellets stored at -80°C. Cell pellets were resuspended in TS2 buffer (100 mM NaCl, 1 mM EGTA, 1 mM EDTA, 1 mM $MgCl_2$, 250 mM sucrose and 20 mM Tris/HCl, pH 7.4), sonicated and used immediately to measure enzyme activity.

To determine the apparent Km and apparent Vmax of 11β-HSD1, lysates were incubated for 10 min at 37ºC in a total volume of 500 µl containing 500 µM NADPH and

7-oxoLCA at concentrations between 62.5 nM and 4 µM. Reactions were terminated by freezing samples in dry ice. Concomitantly, lysates were used in parallel experiments to assess the conversion of radiolabeled glucocorticoids. Briefly, lysates were incubated for 10 min at 37ºC in a total volume of 22 µl containing 200 nM and 10 nCi of [1,2–3H]cortisone and 500 µM cofactor NADPH. Following conversion of radiolabeled glucocorticoids and termination of reactions by adding methanol containing 2 mM unlabeled cortisone and cortisol, 15 µl were spotted on Polygram SIL G-25 UV254 silica plates (Macherey-Nagel), plates were dried, and cortisone and cortisol were resolved using a solvent system of 9:1 (v/v) chloroform/methanol. The separated steroids were analysed by scintillation counting. The expression level in different transfection experiments was determined semiquantitatively by immunoblotting. Protein concentrations were determined by bicinchoninic acid (BCA) method. An amount of 25 µg of total protein was resolved on 12% Bis-Tris gels (NuPage®, Invitrogen) using 1 × MES as buffer (Invitrogen, NuPAGE® MES SDS Running Buffer) and transferred to nitrocellulose membranes (iBlot®, Invitrogen). Thereafter, membranes were blocked with Odyssey® blocking buffer (LI-COR, Biosciences, Lincoln, NE, USA) overnight at 4ºC. Immunoreaction was carried out with primary antibody anti-FLAG M2 (Invitrogen) or anti-human 11β-HSD1 antibody (Cayman Chemical, Ann Arbor) and secondary goat anti-mouse Alexa Fluor® 790, respectively (Invitrogen). After immunoreaction of FLAG-enzymes the membranes were stripped, and the expression of β-actin was determined. All detection and quantification reactions were performed using a LI-COR Odyssey Infrared Imaging system (LI-COR, Biosciences, Lincoln, NE).

CALCULATION OF ENZYME KINETIC PARAMETERS

Enzyme kinetics were analysed by non-linear regression using four-parameter logistic curve fitting. For statistical comparisons, the ratio t-test in GraphPad Prism 5 software was used. Results (mean ± S.D.) were obtained from at least three independent experiments. For calculation of Vmax, the expression level of the FLAG-tagged enzyme was compared with the expression signal from β-actin as an internal control.

MICROSOMAL PREPARATIONS AND ACTIVITY ASSAYS USING WILD-TYPE AND LIVER-SPECIFIC 11B-HSD1 KNOCKOUT LIVER MICROSOMES

Mouse wild-type and liver-specific 11β-HSD1 dificient liver microsomes were prepared as previously described (Senesi, Legeza et al. 2010). Thereafter, the quality of microsomal preparations was validated by measuring NADPH-Cytochrome c reductase activity (Sigma, Saint Louis, MO). To assess 11β-HSD1 reductase activity microsomes (0.05 mg/mL) were incubated for 60 min at 37°C in a total volume of 25 µL containing TS2 buffer, 500 µM NADPH or 1 mM G6P, 1 µM of 7-oxoLCA or 1 of µM cortisone, and vehicle or 5 µM of the 11β-HSD1 inhibitor as indicated. Substrates and inhibitors were diluted from 10 mM stock solutions in DMSO or in methanol. The final solvent concentration in all reactions was kept below 0.2%. Reactions were started by adding microsomes into freshly prepared reaction mixture and stopped by adding 500 µL of acetonitrile containing CDCA-d4 and cortisol-d4 at the concentration of 100 nM as internal standards for UPLC-MS/MS analysis. Thereafter, the organic phase was evaporated to dryness, samples were reconstituted in 50% methanol/water solution and injected in the UPLC-MS/MS.

ANIMAL EXPERIMENTATION

In order to assess the impact of 11β-HSD1 on BA homeostasis and to determine the circulating levels of 7-oxoLCA and conjugated metabolites, 16 adult wild-type male C57BL/6 mice and 16 liver-specific 11β-HSD1 deficient mice (previously described by (Lavery, Zielinska et al. 2012), were fasted overnight and blood collected by intra-cardiac puncture. Serum was prepared and samples were stored at -80 ºC until further processing.

ANALYSIS OF BILE ACID PROFILES BY UPLC-MS/MS

Extraction and quantification of BAs were done as previously described, with the exception that T-ω-MCA was included in the method (Penno, Arsenijevic et al. 2013). The extraction of BAs and glucocorticoids from liver tissue was performed using 100 mg

of tissue homogenized in 200 µL 50% methanol. Samples were spiked with 300 µL of deuterium labeled BAs (UDCA-d4, CDCA-d4, LCA-d4, G-UDCA-d4, G-CA-d4, CA-d4 and DCA-d4) at the final concentration of 1000 nM in acetonitrile followed by protein precipitation with 1.5 mL of alkaline ice-cold acetonitrile (5% NH4OH). Thereafter, samples were shaked continuously for 1 h and centrifugated at 11,000×g for 10 min. The supernatant was transferred to a new tube, evaporated and reconstituted in 100 µL of 50% methanol and further centrifugated to remove insoluble particles. The method was qualified on the basis of extraction efficiency, intra-day accuracy and precision for representative BAs including CA, CDCA, DCA. LCA, α-MCA, G-CDCA, G-UDCA, T-CA, T-α-MCA. The method presented acceptable extraction efficiency, accuracy and precision for the BAs studied (Supplemental Table 1, 2, and 3).

GENE EXPRESSION

Total mRNA was extracted from liver tissue using Trizol (Invitrogen, Carlsbad CA) according to the manufacturer´s instruction. RNA concentration and purity was determined spectrophotometrically (NanoDrop™ 1000 Spectrophotometer, Thermo Scientific) by measuring fluorescence at 260 nm, 230 nm and 280 nm. 2 µg of total mRNA was reverse transcribed to cDNA using the Superscript III First-Strand Synthesis System and oligo dT following the manufacturer´s instruction (Invitrogen). Relative quantification of genes involved in BA homeostasis was performed by RT-PCR (RotorGene 6000; Corbett) and using SYBR Green (KAPA SYBR® FAST qPCR Kit). The relative expression of each gene compared with the internal control cyclophiline was determined using the delta-delta-CT method. Primers were either obtained from Sigma or synthesized from validated sequences obtained at Primerbank (Wang, Spandidos et al. 2012). Quality of primers was evaluated by determination of their melting curves. Samples were evaluated in triplicates (supplemental Table 5).

TRANSIENT TRANSFECTION AND REPORTER ASSAYS

In FXR transactivation assays, Huh7 cells were seeded at 1×10^5 cells per well in 24-well plates and transfected using JetPEI (Polyplus) with 375 ng of hOATP1b3 luciferase reporter construct (Jung, Podvinec et al. 2002) and 175 ng of plasmids for FXR, RXRα

and human 11β-HSD1. To normalize the amount of CMV promoter-containing expression constructs, an appropriate amount of the pcDNA3.1 (+) vector (Invitrogen) was included in transfection mixtures. To control for variations in transfection efficiency 125 ng of the phRG-TK *Renilla reniformis* luciferase reporter plasmid (Promega) was cotransfected in each well. Twelve hours after transfection cells were treated with vehicle, ligands and inhibitors as indicated. Twenty-four hours after adding the ligands, cells were harvested in 1 × Passive Lysis Buffer (Promega), and luciferase activities were measured with luminometer (SpectraMax). Relative promoter activities were obtained by normalizing firefly luciferase activities to *R. reniformis* luciferase activities. VDR transactivation assays were performed similarly in Caco-2 cells, using a luciferase reporter construct based on the human PCFT promoter (Proton-coupled Folate Tranporter) (Eloranta, Zaïr et al. 2009).

STATISTICAL ANALYSIS

Data are presented as mean ± SD. Statistical significance was assessed by Student´s t test. A p-value ≤ 0.05 was considered to be significant.

RESULTS

COMPARISON OF 11B-HSD1-MEDIATED 7-OXOLCA OXOREDUCTION BY SIX SPECIES

We have previously shown that human 11β-HSD1 preferentially converts 7-oxoLCA to CDCA. Evidence from studies using rat liver microsomes indicated the formation of both CDCA and UDCA from 7-oxoLCA. In the present study, we investigated whether these differences are due to species-specific differences in the stereoselective product formation by 11β-HSD1 or whether additional enzymes might be relevant to 7-oxoLCA reduction in rodents. Recombinant 11β-HSD1 from six species were expressed in HEK-293 cells and the oxoreduction of 7-oxoLCA was determined. We observed that canine and hamster 11β-HSD1 presented stereoselectivity similar to that of human 11β-HSD1, thus producing higher levels of the 7α-hydroxyl chenodeoxycholic acid (CDCA) and minor amounts of the 7β-hydroxyl ursodeoxycholic acid (UDCA). Interestingly, rat and mouse 11β-HSD1 reduced 7-oxoLCA to equivalent amounts of CDCA and UDCA (Figure 1A). Surprisingly, we did not observe 7-oxoLCA oxoreduction using HEK-293 cell lysates expressing recombinant guinea-pig 11β-HSD1 nor when using guinea-pig liver microsomes (Figure 1A and 1B), in spite of the fact that cortisone was efficiently reduced by recombinant guinea-pig 11β-HSD1 with a Vmax of 8 $nmol \times h^{-1} \times mg^{-1}$, similar to an earlier report (Arampatzis, Kadereit et al. 2005) (Figure 1 C, Table 1). On the other hand, 11β-HSD1 from human, mouse, rat, hamster and dog efficiently converted 7-oxoLCA (Table 1).

PROFILING OF CIRCULATING BILE ACIDS IN VARIOUS SPECIES

Owing to the fact that 7-oxoLCA oxoreduction activity was absent in guinea-pig liver microsomes and in lysates of HEK-293 expressing recombinant guinea-pig 11β-HSD1, we hypothesized that 7-oxoLCA and its conjugated metabolites would accumulate in the serum of guinea-pigs. To assess this hypothesis, we compared BA profiles in serum of various species including humans, mice (balb/c and C57bL/6), rats (Han Wistar and Sprague-Dawley), canine (*Canis familiaris*, beagle bred), guinea-pig (dunkin-hartley)

and hamster (golden syrian). As expected, we observed elevated levels of 7-oxoLCA and its glycine conjugate in serum of guinea-pigs in contrast to other species studied (Table 2), whereas T-7-oxoLCA levels were negligible. In addition, the comparison of BA profiles among species revealed species-dependent differences with regard to circulating BAs composition (supplemental Table 4)

RELATIVE CONTRIBUTION OF 11B-HSD1 TO THE OXOREDUCTION OF 7-OXOLCA.

In order to clarify whether 7-oxoLCA oxoreduction is mainly due to 11β-HSD1 activity or whether other enzymes may be also relevant, we performed experiments with liver microsomes derived from liver-specific 11β-HSD1 deficient mice (Lavery, Zielinska et al. 2012). We supplied NADPH or glucose-6-phosphate (G6P) in order to distinguish between NADPH-dependent enzymes that are oriented to the cytosol (e.g. cytochrome P450 and aldoketoreductases) and enzymes that are facing the endoplasmic reticulum (ER), such as 11β-HSD1. In the ER lumen, NADPH is regenerated by H6PDH, which is primarily dependent on G6P under physiological conditions (Clarke and Mason 2003). After 60 min of incubation with G6P approximately 60% of initially supplied 7-oxoLCA was converted to approximately 40% CDCA and 20% UDCA. The reaction was inhibited by the 11β-HSD1 specific inhibitor T0504 (also known as Merck-544). When NAPDH was supplied, we observed only traces formation of CDCA and UDCA, which were abolished by T0504, suggesting that either a small amount of NAPDH can penetrate into the microsomes or, more likely, that a small fraction of microsomes have inverted orientation. Importantly, in identical experiments using liver-specific 11β-HSD1 deficient liver microsomes we did not detect 7-oxoLCA reduction, regardless of whether G6P or NADPH was supplied to the reaction mixture (Figure 2). On the other hand, wild-type and liver-specific 11β-HSD1 deficient liver microsomes showed comparable cytochrome c reductase activity (data not shown).

IMPACT OF LIVER-SPECIFIC 11B-HSD1 DISRUPTION ON CIRCULATING LEVELS OF 7-OXOLCA AND ITS CONJUGATED FORMS

We hypothesized that in a scenario of hepatic 11β-HSD1 disruption, circulating levels of 7-oxoLCA and its conjugated metabolites would elevate as observed in guinea-pigs, who are devoid of 7-oxoLCA oxoreductase activity. Therefore, we assessed the concentrations of 7-oxoLCA and its tauro- and glyco-conjugates in serum and liver tissue of liver-specific 11β-HSD1 deficient mice (Figure 3). As expected, circulating and hepatic 7-oxoLCA, T-7-oxoLCA and G-7-oxoLCA levels were 18, 47 and 7-fold elevated in serum of liver-specific 11β-HSD1 deficient compared with wild-type mice, respectively. Similarly, in liver, 7-oxoLCA and T-7-oxoLCA were 2- and 6-fold elevated, whereas G-7-oxoLCA levels were unchanged (Figure 3).

BAS PROFILE IN SERUM AND LIVER OF LIVER-SPECIFIC 11B-HSD1 DEFICIENT MICE

The glucocorticoid receptor (GR) is an important modulator of BA homeostasis (Eloranta, Jung et al. 2006; Rose, Díaz et al. 2011; Lu, Zhang et al. 2012). In order to assess the impact of liver-specific 11β-HSD1 disruption on BA homeostasis, we assessed the circulating and hepatic BA levels in liver-specific 11β-HSD1 deficient mice by UPLC-MS/MS (Penno, Arsenijevic et al. 2013). As expected, liver-specific 11β-HSD1 disruption caused disturbances in BA homeostasis. Circulating unconjugated BAs such as CA, CDCA, 7-oxoDCA and α-MCA were 4- to 16-fold significantly elevated, whereas DCA, HDCA, UDCA, β-MCA and ω-MCA trended to increase, but did not reach statistical significance. Circulating taurine-conjugated species trended to increase up to 8-fold (Table 3); however, statistical significance was not reached for any taurine-BA studied. Intrahepatic BA profiling has revealed a significant increase of several unconjugated BAs in liver-specific 11β-HSD1 deficient compared with wild-type mice (Table 4). BA metabolites such as CA, 7-oxoDCA, HDCA, UDCA, α-MCA, and ω-MCA were up to 8-fold significantly elevated. On the other hand, several taurine- and glycine-

conjugated BA such as T-DCA, T-LCA, T-β-MCA, T-ω-MCA, G-CA, G-DCA, G-LCA and G-UDCA levels trended to decrease in liver from liver-specific 11β-HSD1 deficient mice when compared with wild-type controls, whereas T-UDCA levels reached statistical significance. Of note, T-α-MCA levels were 3-fold significantly increased in liver from liver-specific 11β-HSD1 deficient mice. Nevertheless, total taurine- and glycine-conjugated BA levels suggest a rather decrease of their concentrations upon liver-specific 11β-HSD1 disruption in mice (Table 4).

GENE EXPRESSION

To understand the changes in BA homeostasis observed in liver-specific 11β-HSD1 deficient mice, we analysed the expression of genes involved in BAs homeostasis. We observed reduced expression levels of *VLCS* and *VLCSH2*, enzymes which possess BA coenzyme A synthetase activity. In addition, we found that the expression levels of *CYP7A1* and *OATP4* were reduced, while *SHP-1* was up-regulated. All the other genes studied presented unchanged expression levels compared with wild-type mice (Figure 4).

DISCUSSION

Biomarkers for impaired 11β-HSD1 activity are of great interest for clinical researchers as well as for pharmaceutical industry in order to assess the *in vivo* efficacy of therapeutic inhibitors. Despite the fact that their efficiency can also be assessed through traditional and indirect clinical markers such as fasting plasma glucose and lipid profiles, biomarkers to assess direct 11β-HSD1 inhibition in preclinical and clinical trials are still unavailable. In this regard, although it has been demonstrated that 11β-HSD1 deficient mice have slightly elevated plasma levels of corticosterone and adrenocorticotropic hormone (ACTH), strain-dependent differences have been a major problem (Harris, Kotelevtsev et al. 2001; Carter, Paterson et al. 2009). Interestingly, neither 11β-HSD1 full knockout, liver-specific 11β-HSD1 knockout, H6PDH knockout nor 11β-HSD1/H6PDH double knockout developed on a C57BL/6J/129SvJ background presented elevated levels of circulating corticosterone when compared with wild-type mice (Semjonous, Sherlock et al. 2011; Abrahams, Semjonous et al. 2012; Lavery, Zielinska et al. 2012). Therefore, it is reasonable to assume that its levels are unlikely to be affected upon therapeutic intervention, thus excluding the applicability of glucocorticoids levels as a biomarker of 11β-HSD1 inhibition. Likewise, urinary levels of 11-dehydrocorticosterone (11-DHC) are also of limited application owing to the fact that in heterozygous 11β-HSD1 knockout, H6PDH knockout, 11β-HSD1/H6PDH double knockout as well as in liver-specific 11β-HSD1 knockout mice levels are essentially similar to wild-type controls (Abrahams, Semjonous et al. 2012; Lavery, Zielinska et al. 2012). Therefore, the loss of one *HSD11B1* allele, a scenario similar to 50% enzymatic inhibition, is insufficient to elicit a significant change in urinary 11-DHC metabolites (Abrahams, Semjonous et al. 2012). Recently, we have identified a novel substrate of human 11β-HSD1, the secondary bile acid 7-oxoLCA, which is efficiently metabolized to the 7α-hydroxyl CDCA and to a lesser extent to 7β-hydroxyl UDCA in vitro (Odermatt, Da Cunha et al. 2011). 11β-HSD1-dependent metabolism of 7-oxoLCA was irreversible, unlike the metabolism of glucocorticoids, and its taurine and glycine conjugates were also efficiently metabolized (Odermatt, Da Cunha et al. 2011). The stereo specificity of the reaction is opposite to that observed for other alternative 11β-HSD1 substrates such

7-oxodehydroepiandrosterone, 7-oxopregnenolone and 7-ketocholesterol which are preferentially converted to their 7β-hydroxyl metabolites (Schweizer, Zürcher et al. 2004; Nashev, Chandsawangbhuwana et al. 2007). Using recombinant enzymes expressed in HEK-293 cells we found remarkably species differences. Surprisingly, rodents produced equivalent amounts of 7α- and 7β- isomers, whereas hamster and canine 11β-HSD1 are catalytically similar to human 11β-HSD1, thus becoming the preferred animal models to extrapolate the potential physiological and toxicological effects of 11β-HSD1 inhibition and 7-oxoLCA accumulation to humans (Figure 1 A). It has been suggested that canine and hamster might have limited utility for the assessment of the potential toxicological consequences of 11β-HSD1 inhibition with regard to the accumulation of the toxic oxysterol 7-ketocholesterol, owing to their low catalytic efficiency and different stereospecificity to that of humans (Arampatzis, Kadereit et al. 2005). Overall, these results highlight that the selection of the most suitable animal model to assess safety of 11β-HSD1 inhibitors is complex and must take into account the large species-dependent differences of endogenous and xenobiotics metabolism (Odermatt and Nashev 2010). In this study, human, canine and rat 11β-HSD1 displayed the highest catalytic efficiency of 7-oxoLCA oxoreduction while mouse and hamster enzymes showed lower activities (Table 1). Surprisingly, guinea-pig 11β-HSD1 is unable to reduce 7-oxoLCA in cell lysates and guinea-pig liver microsomes do not convert 7-oxoLCA, hence likely to be the underlying cause of 7-oxoLCA and G-7-oxoLCA accumulation in the circulation of fasted guinea-pigs in comparison to other species (Table 2). This finding is also in line with an earlier study pointing out 7-oxoLCA as a primary BA in guinea-pigs, accounting for 30% of gallbladder BAs (Tint, Xu et al. 1990). Owing to the fact that 7-oxoLCA and its glycine-conjugate accumulated in the circulation of guinea-pigs due to an apparent impaired 7-oxoLCA reductase activity and because 11β-HSD1 seems to be the exclusive microsomal enzyme responsible for its reduction, we speculated that 7-oxoLCA and conjugates would also accumulate in liver-specific 11β-HSD1 deficient mice. We have observed a trend increase of hepatic and a significant elevation of circulating 7-oxoLCA (2- and 18-fold, respectively). Importantly, a significant increase of hepatic and

circulating T-7-oxoLCA (6- and 47-fold, respectively) was observed, suggesting that taurine conjugation of 7-oxoLCA is the main route for its elimination in mice. Based on these findings, we hypothesized that 7-oxoLCA and particularly T-7-oxoLCA accumulation may serve as a superior readout of 11β-HSD1 inhibition in mice. In addition, 7-oxoLCA is independent of the HPA axis feedback regulation, it is not involved in adaptive metabolic changes, it lacks overt toxicity, yet it has been shown to reduce the biliary lithogenic index (Salen, Verga et al. 1982), and as revealed in the present study, it is an exclusive substrate of 11β-HSD1. Moreover, 7-oxoLCA is not a ligand for the VDR (Makishima, Lu et al. 2002) and does not activate FXR to the same extent as CDCA and UDCA (Supplemental Figure 1), thus it unlikely influences the activity of these nuclear receptors. Due to the fact that in humans circulating glycine-conjugated BAs are more abundant than taurine-conjugated metabolites, in this species G-7-oxoLCA levels might correlate with 11β-HSD1 inhibition (Supplemental Table 4) (Garcia-Canaveras, Donato et al. 2012). In guinea-pigs, like in humans, circulating glycine-conjugated BAs are more abundant than taurine-conjugated metabolites and only traces of T-7-oxoLCA were detected in this species, whereas the concentration of G-7-oxoLCA was approximately 13 μM (Table 2). These findings are in line with observation of other investigators (Guertin, Loranger et al. 1995). Similar to humans and guinea-pigs, glycine conjugation seems to prevail in hamsters (Supplemental Table 4), as also observed by others (Cowles, Lee et al. 2002). Conversely, in rodents and canine taurine-conjugation prevails and only minor amounts of glycine-conjugated BAs were found (Supplemental Table 4), results which are in line with other investigators (Washizu 1991; Garcia-Canaveras, Donato et al. 2012). Nevertheless, the applicability of 7-oxoLCA and T-7-oxoLCA as potential biomarkers has to the further investigated *in vivo* with specific 11β-HSD1 inhibitors in cortisone reductase deficiency patients.

Owing to the fact that glucocorticoids are modulators of BA homeostasis, we assessed the influence of liver-specific 11β-HSD1 disruption on BAs handling. In order to dissect the effects of glucocorticoids on BA homeostasis, administration of synthetic glucocorticoids (e.g., dexamethasone, prednisone, budesonide) in rodents is a common approach; however, the fact that they may modulate the activity of other nuclear

receptors, including CAR and PXR (Pascussi, Drocourt et al. 2000; Pascussi, Gerbal-Chaloin et al. 2000), and that dose selection, treatment duration, animal strains/species and compound specific properties make it particularly challenging to compare data from different studies (Cheng, Buckley et al. 2007; Lu, Zhang et al. 2012; Rosales, Romero et al.). In order to overcome those obstacles, we hypothesized that liver-specific 11β-HSD1 deficient mice would represent a more physiologically relevant model to study the effects of glucocorticoids and GR on BAs since these mice are still able to regenerate 35-40% of glucocorticoids, present no major gene expression changes in the gluconeogenic pathway, and the levels of circulating and hepatic glucocorticoids were unaltered (Supplemental Figure 2) (Lavery, Zielinska et al. 2012). Given that 11β-HSD1 immunostaining in hepatocytes is prominent at adjacent sites of the central vein and decreases toward the portal vein, we assumed that a heterogeneous intrahepatic distribution of active glucocorticoids in liver-specific 11β-HSD1 deficient mice may elicit the observation of glucocorticoids and GR-dependent changes on BAs homeostasis at physiological concentrations (Ricketts, Verhaeg et al. 1998; Brereton, van Driel et al. 2001). In fact, the profile of BAs has revealed disturbances in BA homeostasis caused by liver-specific 11β-HSD1 disruption, which included a significant accumulation of several unconjugated BAs in liver, while conjugated BA levels were rather decreased, suggesting a reduction of the BA conjugating machinery, an observation which is in line with the decreased expression levels of very long-chain coenzyme A synthetase (*VLCS*) and very long-chain acyl-coenzyme A synthetase homolog 2 (*VLCSH2*) in liver of liver-specific 11β-HSD1 deficient compared to wild-type mice. Gene expression profiles also revealed reduced expression levels of *CYP7A1*, an effect likely to be mediated by the small heterodimer partner (SHP-1), suggesting an enhanced FXR transcriptional activity. SHP-1 is a known common negative regulator of *CYP7A1*, and orchestrates a compensatory genetic program to counteract intrahepatic BA accumulation in cholestatic situations by interfering with the activity of liver X receptor-α (LXR-α) and liver receptor homologue 1 (LRH-1) (Goodwin, Jones et al. 2000; Zhang and Chiang 2001; Brendel, Schoonjans et al. 2002; Båvner, Sanyal et al. 2005). Surprisingly, BACS is also a FXR positively regulated gene; however, the expression levels of two enzymes

presenting BA-CoA synthase activity were found to be reduced (Pircher, Kitto et al. 2003). The reasons for these are unclear; it might be a direct and FXR-independent effect of the GR since in silico analysis of 6 KB of the promoter/enhancer sequence of VLCS and VLCSH2 indicated the existence of a putative DNA binding site of GR (Supplemental Figure 3). Lu et. al. showed in a recent study that the direct interaction between the GR and the FXR reduced FXR transcriptional activity through the recruitment of CtBP co-repressor complexes, consequently stimulated BA synthesis in mice and promote BA accumulation in the liver and serum upon dexamethasone (DEX) treatment in mice (Lu, Zhang et al. 2012). Interestingly, DEX effects on BA accumulation were blunted in FXR-null mice, suggesting that GR-mediated FXR reduced transcriptional activity is the main pathway leading to the disturbed BAs homeostasis seen in DEX-treated mice. Nevertheless, DEX-mediated BSEP gene up-regulation was not blunted in FXR-null mice, which suggests the existence of GC-mediated and FXR-independent gene expression changes (Lu, Zhang et al. 2012). Therefore, it is plausible that similar mechanisms are involved in the down-regulation of *VLCS* and *VLCSH2* genes down-regulation in liver-specific 11β-HSD1 deficient mice. We have not observed changes in the expression level of the Na+-taurocholate transporting polypetide (NTCP) (Rose, Díaz et al. 2011; Rosales, Romero et al. 2013), the chief transporter of conjugated BAs on the basolateral membrane, in spite the fact that NTCP transcription levels are also modulated by FXR and glucocorticoids (Denson, Sturm et al. 2001; Eloranta, Jung et al. 2006; Rose, Díaz et al. 2011). Supporting our findings is the fact that liver-specific 11β-HSD1 deficient mice presented only a trend to accumulate taurine-BAs in the circulation. On the other hand, OATP4 (also known as OATP1b2) expression was significantly reduced. It has been shown that OATP4 mediates the hepatic uptake of unconjugated BAs (Csanaky, Lu et al. 2011). It remains to be further investigated whether the reduced expression of OATP4 in the liver of liver-specific 11β-HSD1 deficient mice represents an alternative mechanism to prevent a further uptake of unconjugated BAs into hepatocytes and thus responsible for the accumulation of unconjugated BAs in serum from liver-specific 11β-HSD1 mice. In silico analysis of the promoter/enhancer sequence of OATP4 revealed putative GR binding

sites; hence glucocorticoids may modulate its expression as well. In contrast to other studies using pharmacological intervention with synthetic glucocorticoids to understand the role of glucocorticoids and GR in BAs homeostasis, we assumed that liver-specific 11β-HSD1 deficient mice represents a more physiological relevant model, given the lack of major metabolic abnormalities in these mice (Cheng, Buckley et al. 2007; Lavery, Zielinska et al. 2012; Rosales, Romero et al.). Moreover, the impact of liver-specific 11β-HSD1 disruption on classic gluconeogenic target genes, including genes such as phosphoenolpyruvate carboxykinase (PEPCK), glucose-6-phosphatese catalytic subunit (G6Pase), glucokinase, and peroxisome proliferator-activated receptor gamma coactivator 1α expression levels, was minimal (Lavery, Zielinska et al. 2012). In this context, our results might shed light on the initial mechanism involved in the dysregulation of GR-mediated BAs homeostasis, given that the distribution of glucocorticoids, rather than its systemic concentrations across the liver of liver-specific 11β-HSD1 deficient mice might explain the altered BA homeostasis.

CONCLUSIONS

In this study, we provide further evidences for an exclusive role of 11β-HSD1 in the metabolism of 7-oxoLCA. 7-oxoLCA and particularly its taurine-conjugate were markedly elevated in the serum of liver-specific 11β-HSD1 deficient mice and therefore may be potentially used as a biomarker to identify impaired 11β-HSD1 activity in clinically relevant situation and to assess the efficacy of 11β-HSD1 inhibitors. Moreover, we observed that liver-specific 11β-HSD1 disruption disturbs BA homeostasis and promoted intrahepatic accumulation of BAs, particularly by reducing *VLCS* and *VLCSH2* gene expression. Furthermore, the expression levels of the BA transport *OATP4* were reduced. This might represent the initial mechanism of GR-modulation of BAs homeostasis. The potential physiological consequences of a disturbed BA homeostasis upon a therapeutic intervention with 11β-HSD1 inhibitors and the possible combination with known cholestatic drugs warrant further investigation.

ACKNOWLEDGEMENTS

We acknowledge Dr. Heiko Schadt, Dr. Francois Pognan and Dr. Armin Wolf for experimental and critical comments. We thank Gerd A. Kullak-Ublick for kindly providing luciferase reporter plasmids and expression constructs for transactivation assays.

REFERENCES

1. Odermatt, A., P. Arnold, A. Stauffer, B. M. Frey, and F. J. Frey. 1999. The N-terminal Anchor Sequences of 11β-Hydroxysteroid Dehydrogenases Determine Their Orientation in the Endoplasmic Reticulum Membrane. Journal of Biological Chemistry 274: 28762-28770.
2. Odermatt, A., A. G. Atanasov, Z. Balazs, R. A. S. Schweizer, L. G. Nashev, D. Schuster, and T. Langer. 2006. Why is 11β-hydroxysteroid dehydrogenase type 1 facing the endoplasmic reticulum lumen?: Physiological relevance of the membrane topology of 11β-HSD1. Molecular and Cellular Endocrinology 248: 15-23.
3. Tomlinson, J. W., and P. M. Stewart. 2007. Modulation of glucocorticoid action and the treatment of type-2 diabetes. Best Practice & Research Clinical Endocrinology & Metabolism 21: 607-619.
4. Kotelevtsev, Y., M. C. Holmes, A. Burchell, P. M. Houston, D. Schmoll, P. Jamieson, R. Best, R. Brown, C. R. W. Edwards, J. R. Seckl, and J. J. Mullins. 1997. 11β-Hydroxysteroid dehydrogenase type 1 knockout mice show attenuated glucocorticoid-inducible responses and resist hyperglycemia on obesity or stress. Proceedings of the National Academy of Sciences 94: 14924-14929.
5. Morton, N. M., M. C. Holmes, C. Fiévet, B. Staels, A. Tailleux, J. J. Mullins, and J. R. Seckl. 2001. Improved Lipid and Lipoprotein Profile, Hepatic Insulin Sensitivity, and Glucose Tolerance in 11β-Hydroxysteroid Dehydrogenase Type 1 Null Mice. Journal of Biological Chemistry 276: 41293-41300.
6. Morton, N. M., J. M. Paterson, H. Masuzaki, M. C. Holmes, B. Staels, C. Fievet, B. R. Walker, J. S. Flier, J. J. Mullins, and J. R. Seckl. 2004. Novel Adipose Tissue–Mediated Resistance to Diet-Induced Visceral Obesity in 11β-Hydroxysteroid Dehydrogenase Type 1–Deficient Mice. Diabetes 53: 931-938.
7. Wamil, M., J. H. Battle, S. Turban, T. Kipari, D. Seguret, R. de Sousa Peixoto, Y. B. Nelson, D. Nowakowska, D. Ferenbach, L. Ramage, K. E. Chapman, J. Hughes, D. R. Dunbar, J. R. Seckl, and N. M. Morton. 2011. Novel Fat Depot–Specific Mechanisms Underlie Resistance to Visceral Obesity and Inflammation

in 11β-Hydroxysteroid Dehydrogenase Type 1–Deficient Mice. Diabetes 60: 1158-1167.

8. Masuzaki, H., J. Paterson, H. Shinyama, N. M. Morton, J. J. Mullins, J. R. Seckl, and J. S. Flier. 2001. A Transgenic Model of Visceral Obesity and the Metabolic Syndrome. Science 294: 2166-2170.
9. Masuzaki, H., H. Yamamoto, C. J. Kenyon, J. K. Elmquist, N. M. Morton, J. M. Paterson, H. Shinyama, M. G. F. Sharp, S. Fleming, J. J. Mullins, J. R. Seckl, and J. S. Flier. 2003. Transgenic amplification of glucocorticoid action in adipose tissue causes high blood pressure in mice. The Journal of Clinical Investigation 112: 83-90.
10. Paterson, J. M., N. M. Morton, C. Fievet, C. J. Kenyon, M. C. Holmes, B. Staels, J. R. Seckl, and J. J. Mullins. 2004. Metabolic syndrome without obesity: Hepatic overexpression of 11β-hydroxysteroid dehydrogenase type 1 in transgenic mice. Proceedings of the National Academy of Sciences of the United States of America 101: 7088-7093.
11. Boyle, C. D., and T. J. Kowalski. 2009. 11β-hydroxysteroid dehydrogenase type 1 inhibitors: a review of recent patents. Expert Opinion on Therapeutic Patents 19: 801-825.
12. Hughes, K. A., S. P. Webster, and B. R. Walker. 2008. 11-Beta-hydroxysteroid dehydrogenase type 1 (11β-HSD1) inhibitors in Type 2 diabetes mellitus and obesity. Expert Opinion on Investigational Drugs 17: 481-496.
13. Hadoke, P. W. F., J. Iqbal, and B. R. Walker. 2009. Therapeutic manipulation of glucocorticoid metabolism in cardiovascular disease. British Journal of Pharmacology 156: 689-712.
14. Rosenstock, J., S. Banarer, V. A. Fonseca, S. E. Inzucchi, W. Sun, W. Yao, G. Hollis, R. Flores, R. Levy, W. V. Williams, J. R. Seckl, R. Huber, and f. t. I.-P. Investigators. 2010. The 11-β-Hydroxysteroid Dehydrogenase Type 1 Inhibitor INCB13739 Improves Hyperglycemia in Patients With Type 2 Diabetes Inadequately Controlled by Metformin Monotherapy. Diabetes Care 33: 1516-1522.

15. Thomas, M. P., and B. V. L. Potter. 2011. Crystal structures of 11β-hydroxysteroid dehydrogenase type 1 and their use in drug discovery. Future Medicinal Chemistry 3: 367-390.
16. Lavery, G. G., A. E. Zielinska, L. L. Gathercole, B. Hughes, N. Semjonous, P. Guest, K. Saqib, M. Sherlock, G. Reynolds, S. A. Morgan, J. W. Tomlinson, E. A. Walker, E. H. Rabbitt, and P. M. Stewart. 2012. Lack of Significant Metabolic Abnormalities in Mice with Liver-Specific Disruption of 11β-Hydroxysteroid Dehydrogenase Type 1. Endocrinology 153: 3236-3248.
17. Carter, R. N., J. M. Paterson, U. Tworowska, D. J. Stenvers, J. J. Mullins, J. R. Seckl, and M. C. Holmes. 2009. Hypothalamic-Pituitary-Adrenal Axis Abnormalities in Response to Deletion of 11β-HSD1 is Strain-Dependent. Journal of Neuroendocrinology 21: 879-887.
18. Abrahams, L., N. M. Semjonous, P. Guest, A. Zielinska, B. Hughes, G. G. Lavery, and P. M. Stewart. 2012. Biomarkers of hypothalamic–pituitary–adrenal axis activity in mice lacking 11β-HSD1 and H6PDH. Journal of Endocrinology 214: 367-372.
19. Harno, E., and A. White. 2010. Will treating diabetes with 11β-HSD1 inhibitors affect the HPA axis? Trends in Endocrinology & Metabolism 21: 619-627.
20. Odermatt, A., and L. G. Nashev. 2010. The glucocorticoid-activating enzyme 11β-hydroxysteroid dehydrogenase type 1 has broad substrate specificity: Physiological and toxicological considerations. The Journal of Steroid Biochemistry and Molecular Biology 119: 1-13.
21. Muller, C., D. Pompon, P. Urban, and R. Morfin. 2006. Inter-conversion of 7α- and 7β-hydroxy-dehydroepiandrosterone by the human 11β-hydroxysteroid dehydrogenase type 1. The Journal of Steroid Biochemistry and Molecular Biology 99: 215-222.
22. Nashev, L. G., C. Chandsawangbhuwana, Z. Balazs, A. G. Atanasov, B. Dick, F. J. Frey, M. E. Baker, and A. Odermatt. 2007. Hexose-6-phosphate Dehydrogenase Modulates 11β-Hydroxysteroid Dehydrogenase Type 1-

Dependent Metabolism of 7-keto- and 7β-hydroxy-neurosteroids. PLoS ONE 2: e561.

23. Hult, M., B. Elleby, N. Shafqat, S. Svensson, A. Rane, H. Jörnvall, L. Abrahmsen, and U. Oppermann. 2004. Human and rodent type 1 11ß-hydroxysteroid dehydrogenases are 7ß-hydroxycholesterol dehydrogenases involved in oxysterol metabolism. Cellular and Molecular Life Sciences 61: 992-999.
24. Schweizer, R. A. S., M. Zürcher, Z. Balazs, B. Dick, and A. Odermatt. 2004. Rapid Hepatic Metabolism of 7-Ketocholesterol by 11β-Hydroxysteroid Dehydrogenase Type 1. Journal of Biological Chemistry 279: 18415-18424.
25. Hennebert, O., C. Pernelle, C. Ferroud, and R. Morfin. 2007. 7α- and 7β-hydroxy-epiandrosterone as substrates and inhibitors for the human 11β-hydroxysteroid dehydrogenase type 1. The Journal of Steroid Biochemistry and Molecular Biology 105: 159-165.
26. Hennebert, O., S. Le Mée, C. Pernelle, and R. Morfin. 2007. 5α-Androstane-3β,7α,17β-triol and 5α-androstane-3β,7β,17β-triol as substrates for the human 11β-hydroxysteroid dehydrogenase type 1. Steroids 72: 855-864.
27. Maser, E., and G. Bannenberg. 1994. 11β-hydroxysteroid dehydrogenase mediates reductive metabolism of xenobiotic carbonyl compounds. Biochemical Pharmacology 47: 1805-1812.
28. Hult, M., C. S. I. Nobel, L. Abrahmsen, D. A. Nicoll-Griffith, H. Jörnvall, and U. C. T. Oppermann. 2001. Novel enzymological profiles of human 11β-hydroxysteroid dehydrogenase type 1. Chemico-Biological Interactions 130–132: 805-814.
29. Wsól, V. r., B. Szotáková, L. Skálová, and E. Maser. 2003. Stereochemical aspects of carbonyl reduction of the original anticancer drug oracin by mouse liver microsomes and purified 11β-hydroxysteroid dehydrogenase type 1. Chemico-Biological Interactions 143–144: 459-468.
30. Kenneke, J. F., C. S. Mazur, S. E. Ritger, and T. J. Sack. 2008. Mechanistic Investigation of the Noncytochrome P450-Mediated Metabolism of Triadimefon to Triadimenol in Hepatic Microsomes. Chemical Research in Toxicology 21: 1997-2004.

31. Martin, H.-J., U. Breyer-Pfaff, V. Wsol, S. Venz, S. Block, and E. Maser. 2006. PURIFICATION AND CHARACTERIZATION OF AKR1B10 FROM HUMAN LIVER: ROLE IN CARBONYL REDUCTION OF XENOBIOTICS. Drug Metabolism and Disposition 34: 464-470.
32. Odermatt, A., T. Da Cunha, C. A. Penno, C. Chandsawangbhuwana, C. Reichert, A. Wolf, M. Dong, and M. E. Baker. 2011. Hepatic reduction of the secondary bile acid 7-oxolithocholic acid is mediated by 11beta-hydroxysteroid dehydrogenase 1. The Biochemical journal 436: 621-629.
33. Fukiya, S., M. Arata, H. Kawashima, D. Yoshida, M. Kaneko, K. Minamida, J. Watanabe, Y. Ogura, K. Uchida, K. Itoh, M. Wada, S. Ito, and A. Yokota. 2009. Conversion of cholic acid and chenodeoxycholic acid into their 7-oxo derivatives by Bacteroides intestinalis AM-1 isolated from human feces. FEMS Microbiology Letters 293: 263-270.
34. Macdonald, I., C. Williams, D. Mahony, and W. Christie. 1975. NAD- and NADP-dependent 7alpha-hydroxysteroid dehydrogenases from bacteroides fragilis. Biochimica et Biophysica Acta (BBA) - Molecular Basis of Disease 384: 12-24.
35. Arampatzis, S., B. Kadereit, D. Schuster, Z. Balazs, R. A. S. Schweizer, F. J. Frey, T. Langer, and A. Odermatt. 2005. Comparative enzymology of 11β-hydroxysteroid dehydrogenase type 1 from six species. Journal of Molecular Endocrinology 35: 89-101.
36. Senesi, S., B. Legeza, Z. Balázs, M. Csala, P. Marcolongo, É. Kereszturi, P. Szelényi, C. Egger, R. Fulceri, J. Mandl, R. Giunti, A. Odermatt, G. Bánhegyi, and A. Benedetti. 2010. Contribution of Fructose-6-Phosphate to Glucocorticoid Activation in the Endoplasmic Reticulum: Possible Implication in the Metabolic Syndrome. Endocrinology 151: 4830-4839.
37. Penno, C. A., D. Arsenijevic, T. Da Cunha, G. A. Kullak-Ublick, J.-P. Montani, and A. Odermatt. 2013. Quantification of Multiple Bile Acids in Uninephrectomized Rats Using Ultra-Performance Liquid Chromatography-Tandem Mass Spectrometry. Analytical Methods.

38. Clarke, J. L., and P. J. Mason. 2003. Murine hexose-6-phosphate dehydrogenase: a bifunctional enzyme with broad substrate specificity and 6-phosphogluconolactonase activity. Archives of Biochemistry and Biophysics 415: 229-234.

39. Eloranta, J. J., D. Jung, and G. A. Kullak-Ublick. 2006. The Human Na+-Taurocholate Cotransporting Polypeptide Gene Is Activated by Glucocorticoid Receptor and Peroxisome Proliferator-Activated Receptor-γ Coactivator-1α, and Suppressed by Bile Acids via a Small Heterodimer Partner-Dependent Mechanism. Molecular Endocrinology 20: 65-79.

40. Rose, Adam J., Mauricio B. Díaz, A. Reimann, J. Klement, T. Walcher, A. Krones-Herzig, O. Strobel, J. Werner, A. Peters, A. Kleyman, Jan P. Tuckermann, A. Vegiopoulos, and S. Herzig. 2011. Molecular Control of Systemic Bile Acid Homeostasis by the Liver Glucocorticoid Receptor. Cell metabolism 14: 123-130.

41. Lu, Y., Z. Zhang, X. Xiong, X. Wang, J. Li, G. Shi, J. Yang, X. Zhang, H. Zhang, J. Hong, X. Xia, G. Ning, and X. Li. 2012. Glucocorticoids Promote Hepatic Cholestasis in Mice by Inhibiting the Transcriptional Activity of the Farnesoid X Receptor. Gastroenterology 143: 1630-1640.e1638.

42. Harris, H. J., Y. Kotelevtsev, J. J. Mullins, J. R. Seckl, and M. C. Holmes. 2001. Intracellular Regeneration of Glucocorticoids by 11β-Hydroxysteroid Dehydrogenase (11β-HSD)-1 Plays a Key Role in Regulation of the Hypothalamic-Pituitary-Adrenal Axis: Analysis of 11β-HSD-1-Deficient Mice. Endocrinology 142: 114-120.

43. Semjonous, N. M., M. Sherlock, P. Jeyasuria, K. L. Parker, E. A. Walker, P. M. Stewart, and G. G. Lavery. 2011. Hexose-6-Phosphate Dehydrogenase Contributes to Skeletal Muscle Homeostasis Independent of 11β-Hydroxysteroid Dehydrogenase Type 1. Endocrinology 152: 93-102.

44. Tint, G. S., G. R. Xu, A. K. Batta, S. Shefer, W. Niemann, and G. Salen. 1990. Ursodeoxycholic acid, chenodeoxycholic acid, and 7-ketolithocholic acid are primary bile acids of the guinea-pig. Journal of Lipid Research 31: 1301-1306.

45. Salen, G., D. Verga, A. Batta, G. Tint, and S. Shefer. 1982. Effect of 7-ketolithocholic acid on bile acid metabolism in humans. Gastroenterology 83: 341-347.
46. Garcia-Canaveras, J. C., M. T. Donato, J. V. Castell, and A. Lahoz. 2012. Targeted profiling of circulating and hepatic bile acids in human, mouse and rat using an UPLC-MRM-MS-validated method. Journal of Lipid Research.
47. Guertin, F., A. Loranger, G. Lepage, C. C. Roy, I. M. Yousef, N. Domingo, F. Chanussot, H. Lafont, and B. Tuchweber. 1995. Bile formation and hepatic plasma membrane composition in guinea-pigs and rats. Comparative Biochemistry and Physiology Part B: Biochemistry and Molecular Biology 111: 523-531.
48. Cowles, R. L., J.-Y. Lee, D. D. Gallaher, C. L. Stuefer-Powell, and T. P. Carr. 2002. Dietary Stearic Acid Alters Gallbladder Bile Acid Composition in Hamsters Fed Cereal-Based Diets. The Journal of Nutrition 132: 3119-3122.
49. Washizu, T., Tomoda, I., Kaneko, JJ. 1991. Serum bile acid composition of the dog, cow, horse and human. The Journal of Veterinary Medical Science 53: 81-86.
50. Hadoke, P. W. F., R. S. Lindsay, J. R. Seckl, B. R. Walker, and C. J. Kenyon. 2006. Altered vascular contractility in adult female rats with hypertension programmed by prenatal glucocorticoid exposure. Journal of Endocrinology 188: 435-442.
51. Chapman, K. E., A. E. Coutinho, M. Gray, J. S. Gilmour, J. S. Savill, and J. R. Seckl. 2009. The role and regulation of 11β-hydroxysteroid dehydrogenase type 1 in the inflammatory response. Molecular and Cellular Endocrinology 301: 123-131.
52. Gilmour, J. S., A. E. Coutinho, J.-F. Cailhier, T. Y. Man, M. Clay, G. Thomas, H. J. Harris, J. J. Mullins, J. R. Seckl, J. S. Savill, and K. E. Chapman. 2006. Local Amplification of Glucocorticoids by 11β-Hydroxysteroid Dehydrogenase Type 1 Promotes Macrophage Phagocytosis of Apoptotic Leukocytes. The Journal of Immunology 176: 7605-7611.

53. Goodwin, B., S. A. Jones, R. R. Price, M. A. Watson, D. D. McKee, L. B. Moore, C. Galardi, J. G. Wilson, M. C. Lewis, M. E. Roth, P. R. Maloney, T. M. Willson, and S. A. Kliewer. 2000. A Regulatory Cascade of the Nuclear Receptors FXR, SHP-1-1, and LRH-1 Represses Bile Acid Biosynthesis. Molecular Cell 6: 517-526.

54. Zhang, M., and J. Y. L. Chiang. 2001. Transcriptional Regulation of the Human Sterol 12α-Hydroxylase Gene (CYP8B1): ROLES OF HEPATOCYTE NUCLEAR FACTOR 4α IN MEDIATING BILE ACID REPRESSION. Journal of Biological Chemistry 276: 41690-41699.

55. Brendel, C., K. Schoonjans, O. A. Botrugno, E. Treuter, and J. Auwerx. 2002. The Small Heterodimer Partner Interacts with the Liver X Receptor α and Represses Its Transcriptional Activity. Molecular Endocrinology 16: 2065-2076.

56. Båvner, A., S. Sanyal, J.-Å. Gustafsson, and E. Treuter. 2005. Transcriptional corepression by SHP-1: molecular mechanisms and physiological consequences. Trends in Endocrinology & Metabolism 16: 478-488.

57. Pircher, P. C., J. L. Kitto, M. L. Petrowski, R. K. Tangirala, E. D. Bischoff, I. G. Schulman, and S. K. Westin. 2003. Farnesoid X Receptor Regulates Bile Acid-Amino Acid Conjugation. Journal of Biological Chemistry 278: 27703-27711.

58. Michalopoulos, G. K., W. C. Bowen, K. Mulè, and J. Luo. 2003. HGF-, EGF-, and dexamethasone-induced gene expression patterns during formation of tissue in hepatic organoid cultures. Gene expression 11: 55-75.

59. Inoue, Y., A.-M. Yu, J. Inoue, and F. J. Gonzalez. 2004. Hepatocyte Nuclear Factor 4α Is a Central Regulator of Bile Acid Conjugation. Journal of Biological Chemistry 279: 2480-2489.

60. Warskulat, U., Kubitz, R., Wettstein, M., Stieger, B., Meier, P.J., Häussinger, D. 2005. Regulation of Bile Salt Export Pump mRNA Levels by Dexamethasone and Osmolarity in Cultured Rat Hepatocytes. Biological Chemistry 380: 1273-1279.

61. Rosales, R., M. R. Romero, J. Vaquero, M. J. Monte, P. Requena, O. Martinez-Augustin, F. S. d. Medina, and J. J. G. Marin. FXR-dependent and -independent

interaction of glucocorticoids with the regulatory pathways involved in the control of bile acid handling by the liver. Biochemical Pharmacology.

62. Wang, R., H.-L. Chen, L. Liu, J. A. Sheps, M. J. Phillips, and V. Ling. 2009. Compensatory role of P-glycoproteins in knockout mice lacking the bile salt export pump. Hepatology 50: 948-956.
63. Denson, L. A., E. Sturm, W. Echevarria, T. L. Zimmerman, M. Makishima, D. J. Mangelsdorf, and S. J. Karpen. 2001. The Orphan Nuclear Receptor, SHP-1, Mediates Bile Acid-Induced Inhibition of the Rat Bile Acid Transporter, NTCP. Gastroenterology 121: 140-147.
64. Cattori, V., B. Hagenbuch, N. Hagenbuch, B. Stieger, R. Ha, K. E. Winterhalter, and P. J. Meier. 2000. Identification of organic anion transporting polypeptide 4 (Oatp4) as a major full-length isoform of the liver-specific transporter-1 (rlst-1) in rat liver. FEBS Letters 474: 242-245.
65. Csanaky, I. L., H. Lu, Y. Zhang, K. Ogura, S. Choudhuri, and C. D. Klaassen. 2011. Organic anion–transporting polypeptide 1b2 (OATP1b2) is important for the hepatic uptake of unconjugated bile acids: Studies in OATP1b2-null mice. Hepatology 53: 272-281.

FIGURES

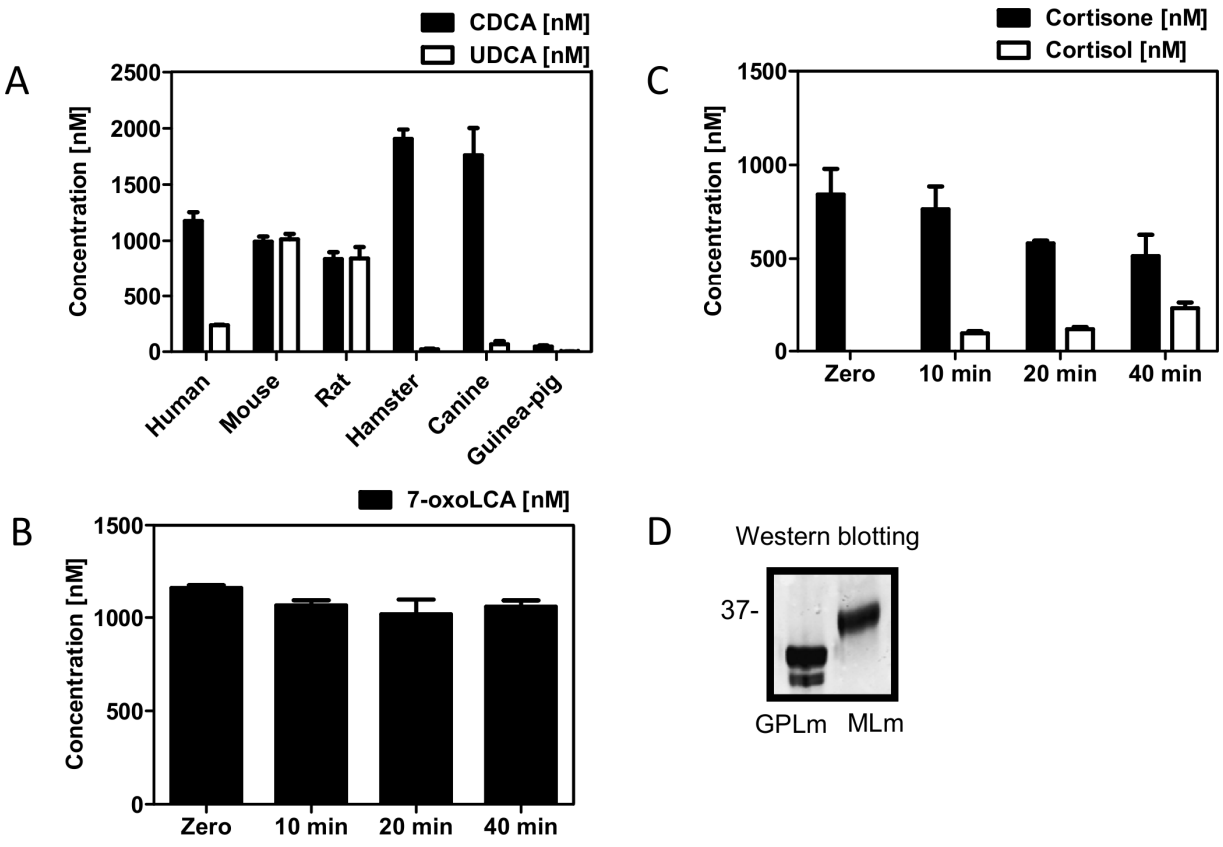

Figure 1. Enzymatic activity of recombinant 11β-HSD1 from various species was determined in lysates of transfected HEK-293 cells as described in "Materials and Methods." *A*, Stereoselectivity of 7-oxoLCA (2 μM) oxoreduction to CDCA (black bars) and UDCA (white bars) formed by 11β-HSD1 from various species after 10 min incubation at 37ºC. *B*, Guinea-pig liver microsomes were incubated for 40 min with 7-oxoLCA (1 μM) and glucose-6-phosphate (1 mM). BAs were extracted and quantitated by UPLC-MS/MS. Unconverted 7-oxoLCA is represented by black bars. Data (n=3) represent mean ± SD. *C*, Oxoreduction of cortisone by guinea-pig liver microsomes. *D*, Western blotting against 11β-HSD1 in guinea-pig (GPLm) and mouse liver microsomes (MLm)

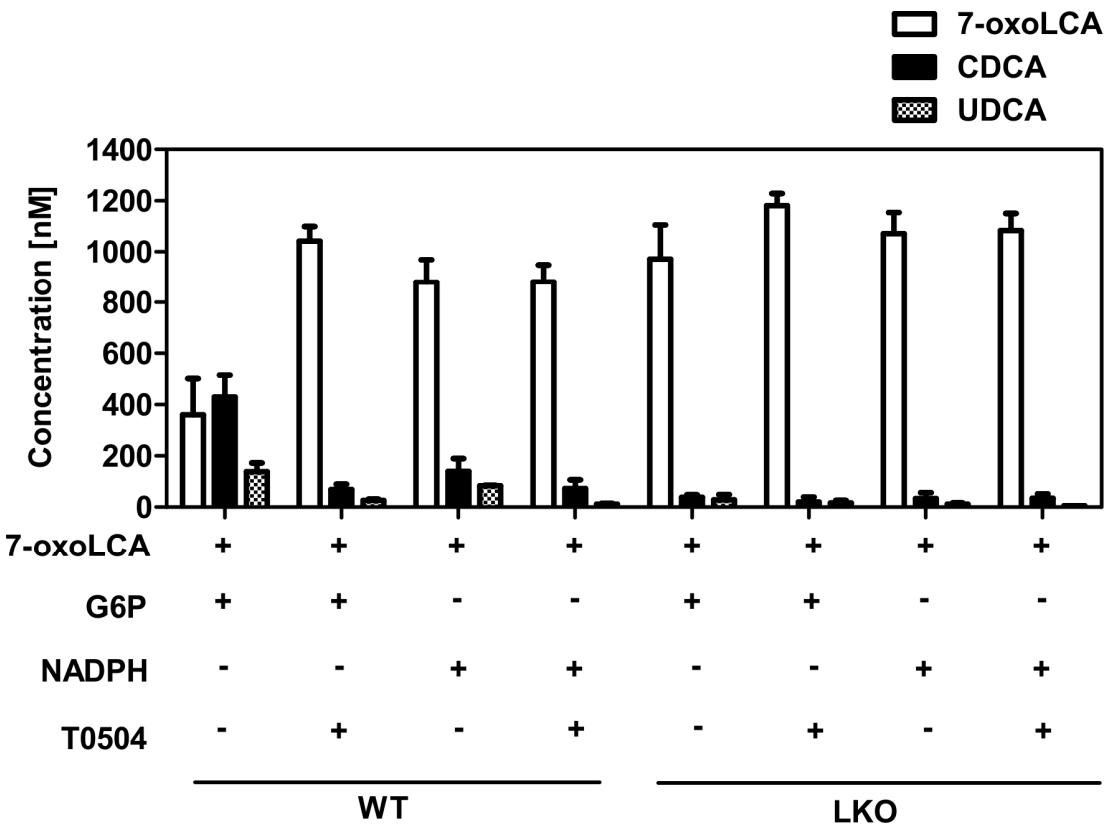

Figure 2. Wild-type or liver-specific 11β-HSD1 knockout (LKO) liver microsomes were incubated for 60 min with 7-oxoLCA (1 μM), hexose-6-phosphate (1 mM G6P) or NAPDH and 11β-HSD1 inhibitor T0504 (5 μM) as indicated. 7-oxoLCA is represented by white bars, CDCA and UDCA are represented by black and hatched bars, respectively. Data (n=3) represent mean ± SD. Reactions were terminated with acetonitrile extracted and measured by UPLC-MS/MS.

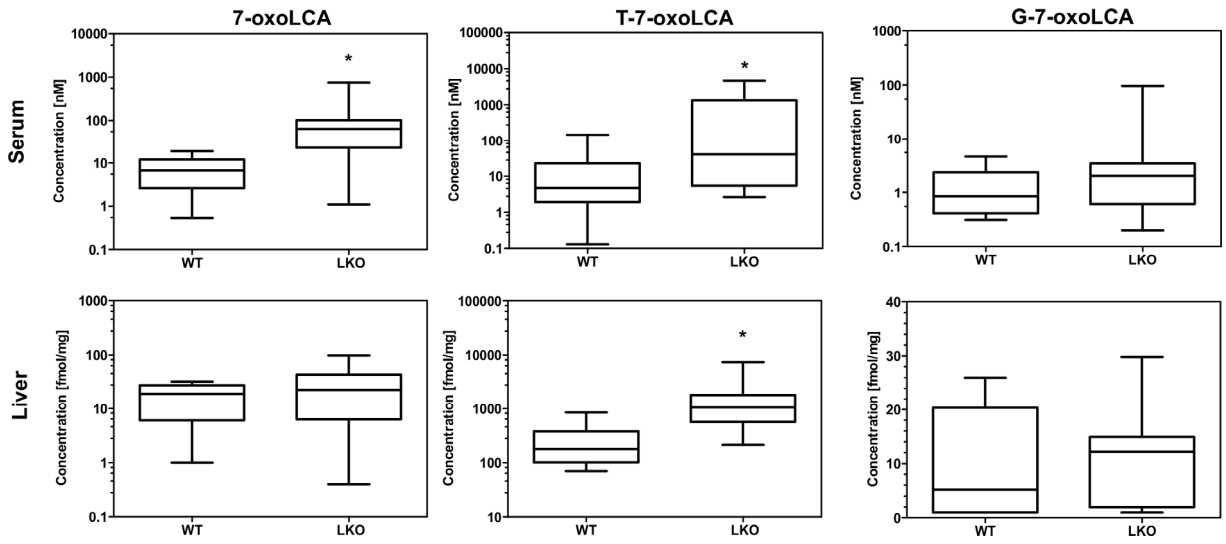

Figure 3. Circulating and intrahepatic concentrations of 7-oxoLCA, taurine-7-oxoLCA and glycine-7-oxoLCA of wild-type (WT) and liver-specific 11β-HSD1 deficient (LKO) mice. Data (n=16) represent mean ± SD. Statistics* for $p \leq 0.05$.

.

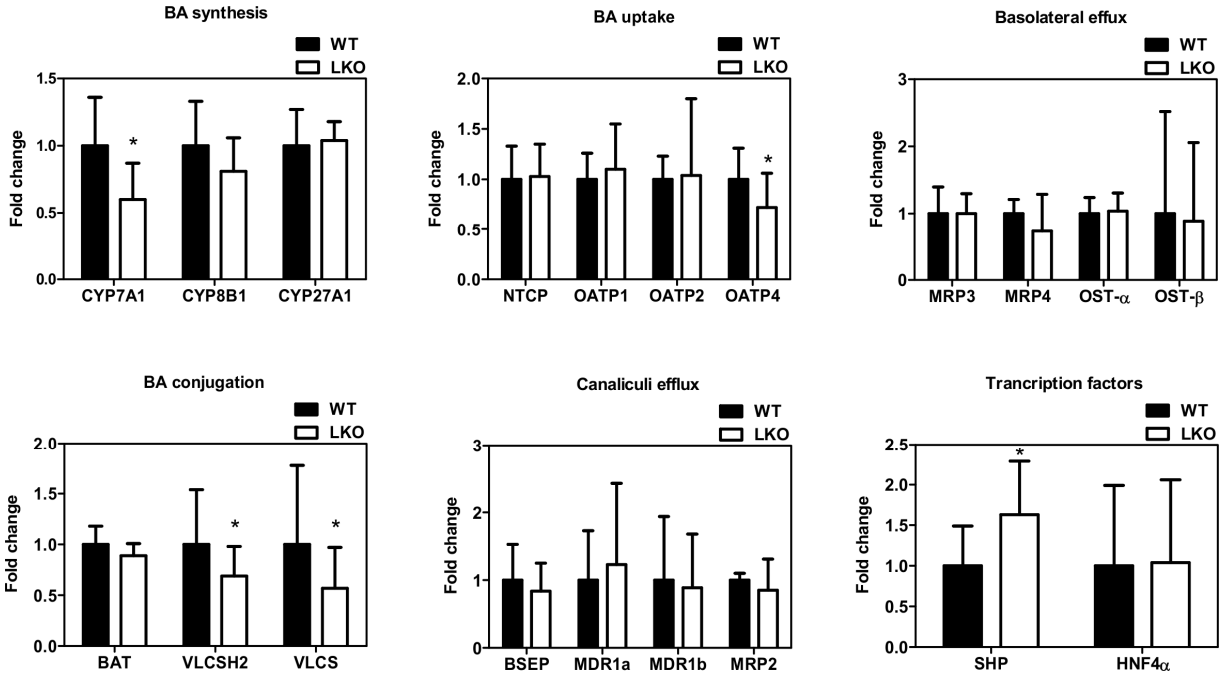

Figure 4. Gene expression profiles in liver of wild-type and liver-specific 11β-HSD1 deficient (LKO) mice: BA synthesis, basolateral uptake, BA efflux, BA conjugation, canaliculi efflux and transcription factors involved in BA homeostasis as indicated. Data (n=16) represent mean ± SD. Statistics: * for $p \leq 0.05$.

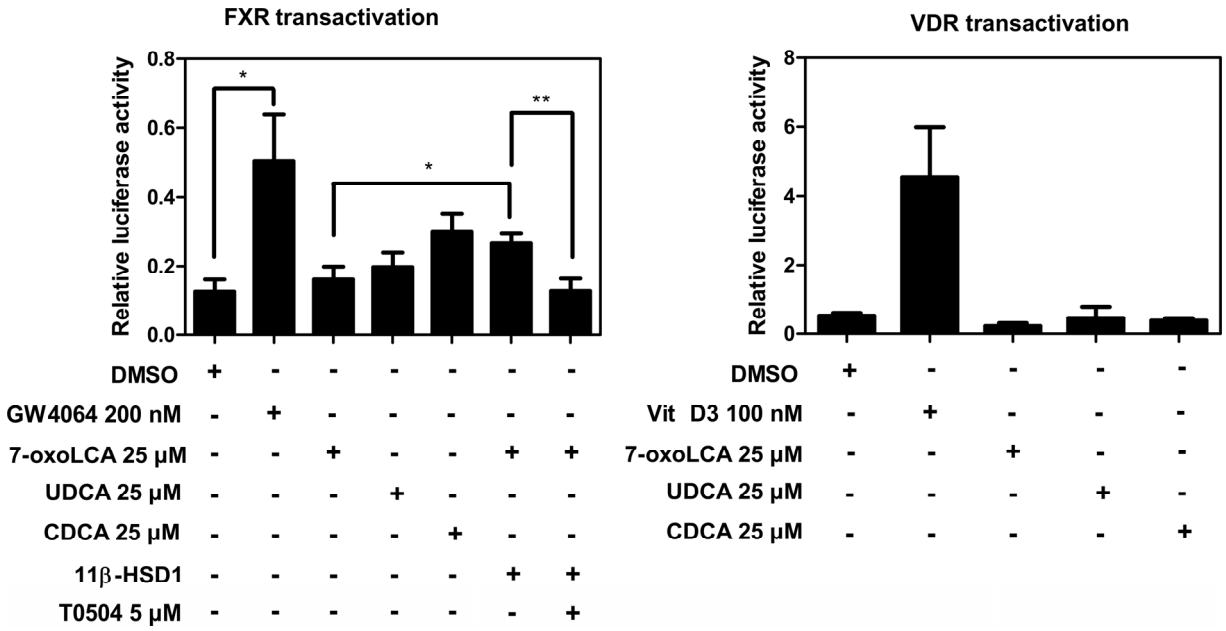

Supplemental Figure 1. FXR and VDR transactivation assays. *Right panel:* Huh7 cells were transfected with hOATP1b3 luciferase reporter construct together with FXR, RXRα and human 11β-HSD1 expression constructs. *Left panel:* Caco-2 cells were transfected with human PCFT promoter together with FXR, RXR expression constructs. Twelve hours after transfection, cells were treated with vehicle, ligands and 11β-HSD1 inhibitor (T0504) as indicated. Twenty-four hours after adding the ligands, cells were harvested and luciferase activity was measured.

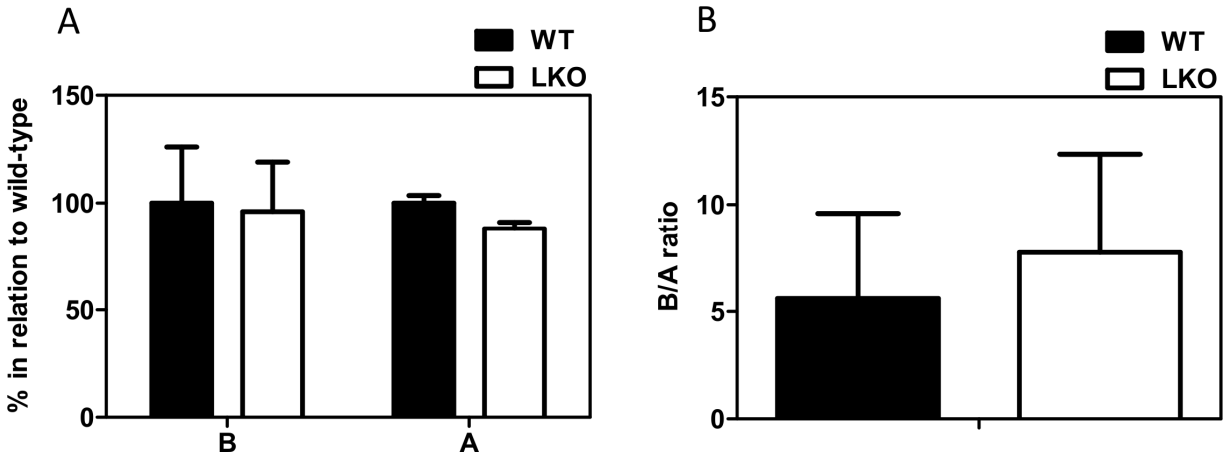

Supplemental Figure 2. *A*, Intrahepatic levels of corticosterone (B) and 11-dehydrocorticosterone (A) in wild-type (WT) and liver-specific 11β-HSD1 deficient (LKO) mice. *B*, B/A ratios in liver of wild-type (WT) and liver-specific 11β-HSD1 knockout (LKO). Data (n=16) represent mean ± SD.

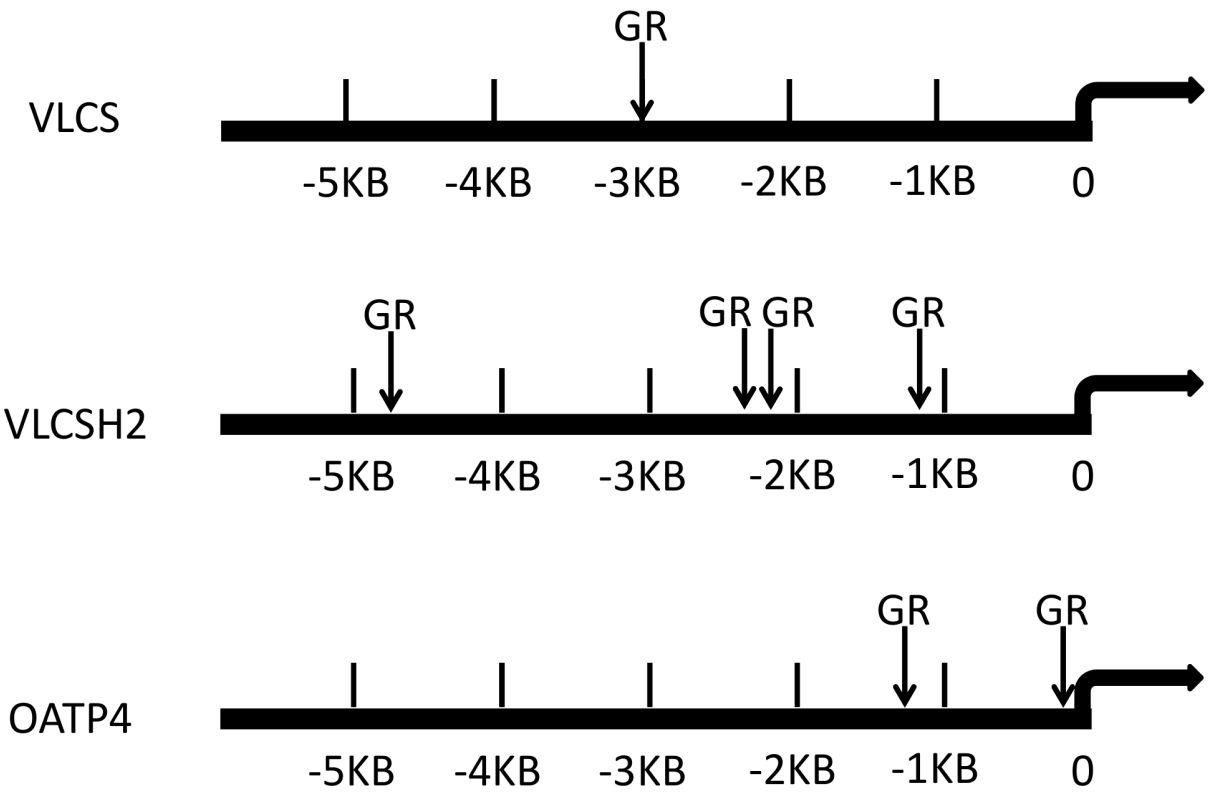

Supplemental Figure 3. In silico analysis of putative GR responsive elements in 6 KB of promoter/enhancer of mouse VLCS, VLCSH2 and OATP4 genes. Six KB of promoter/enhancer sequences of mouse VLCS and VLCSH2 were assessed from the genomic DNA database (www.ensembl.org). The DNA sequences were analysed by Alibaba2.1 (http://www.gene-regulation.com/pub/programs/alibaba2/).

TABLES

Table 1 Comparison of enzyme kinetic comparison of the oxoreduction of 7-oxoLCA and cortisone by recombinant 11β-HSD1 from six species.

	Oxoreduction of 7-oxoLCA		Oxoreduction of cortisone
Species	Km [μM]	Vmax [nmol×h-1×mg-1]	Vmax [nmol×h-1×mg-1]
Canine	1.9 ± 0.4	8.8 ± 1.0	2.2
Guinea-pig	-	-	8.0
Hamster	1.9 ± 0.2	23.9 ± 1.1	10.4
Human	1.2 ± 0.1	4.0 ± 0.2	3.9
Mouse	2.6 ± 0.4	27.1 ± 2.0	12.9
Rat	2.3 ± 0.5	11.6 ± 1.2	6.0

Table 2 Concentrations of 7-oxoLCA and its conjugates in serum from several species.

	Dog	Guinea-pig	Hamster	Human	Balb/c*[2]	C57BL/6*[2]	HW*[3]	SD*[3]
7-oxoLCA	41 ± 83	13593 ± 5482	11 ± 9	3 ± 1	20 ± 12	6 ± 4	4 ± 5	22 ± 28
T-7-oxoLCA	9 ± 11	3 ± 2	3 ± 1	1 ± 0.1	8 ± 2	32 ± 14	2 ± 0.2	4 ± 1
G-7-oxoLCA	1 ± 0.2	13005 ± 21535	1 ± 1	1 ± 0.1	5 ± 3	N.D.	N.D.	1 ± 2

The results are expressed in nM as mean ± standard deviation (n=8). Underlined values represent below lower limit of quantification. *[2] Mouse (Balb/c, C57BL/6); *[3] Rats (Sprague-Dawley (SD), Han Wistar (HW)); N.D.: not detected.

Table 3 Comparison of bile acid profiles in serum from wild-type and liver-specific 11β-HSD1 deficient mice.

	WT	LKO	Fold change
CA	528 ± 359	3232 ± 4704*	6
CDCA	20 ± 21	71 ± 86*	4
DCA	186 ± 178	425 ± 607	2
7-oxoDCA	239 ± 302	2846 ± 3688*	12
HDCA	36 ± 31	64 ± 73	2
LCA	N.D.	N.D.	
α-MCA	67 ± 71	1089 ± 1602*	16
β-MCA	904 ± 597	1293 ± 1866	1
ω-MCA	888 ± 614	1842 ± 2133	2
UDCA	92 ± 66	145 ± 188	2
Sub-total	2960	11006	4
T-CA	5255 ± 15320	17334 ± 26835	3
T-CDCA	247 ± 709	859 ± 1340	3
T-DCA	383 ± 825	1302 ± 2568	3
T-LCA	2 ± 4	19 ± 47	8
T-α-MCA	2365 ± 8363	8648 ± 15518	4
T-β-MCA	2861 ± 5229	7579 ± 16824	3
T-ω-MCA	1463 ± 2761	9342 ± 18918	6
T-UDCA	130 ± 262	414 ± 1016	3
Sub-total	12707	45497	4
G-CA	19 ± 40	104 ± 981	5
G-CDCA	N.D.	N.D.	
G-DCA	N.D.	N.D.	
G-LCA	N.D.	N.D.	
G-UDCA	N.D.	N.D.	
Total BAs	15686	56607	4

The results are expressed in nM as mean ± standard deviation (n=16). N.D.: not detected. Statistics: * for $p \leq 0.05$., WT, wild-type and LKO, liver-specific 11β-HSD1 deficient mice.

Table 4 Comparison of bile acid profiles in liver of wild-type and liver-specific 11β-HSD1 deficient mice.

	WT	LKO	Fold change
CA	1002 ± 1250	2794 ± 2542*	3
CDCA	9 ± 8	13 ± 12	2
DCA	33 ± 46	48 ± 64	1
7-oxoDCA	492 ± 939	3239 ± 3358*	7
HDCA	18 ± 18	41 ± 47*	2
LCA	N.D.	N.D.	
α-MCA	178 ± 188	1342 ± 1498*	8
β-MCA	1346 ± 1276	1211 ± 1023	1
ω-MCA	634 ± 734	1589 ± 1526*	3
UDCA	51 ± 53	124 ± 105*	2
Sub Total	3764	10401	3
T-CA	29827 ± 32975	33235 ± 23505	1
T-CDCA	1177 ± 1060	1333 ± 1071	1
T-DCA	1921 ± 3756	1184 ± 1469	0.6
T-LCA	26 ± 26	20 ± 17	0.8
T-α-MCA	2762 ± 3178	7324 ± 7928*	3
T-β-MCA	12584 ± 10870	7652 ± 5608	0.6
T-ω-MCA	16473 ± 12523	14000 ± 9936	0.8
T-UDCA	1377 ± 1060	472 ± 1005*	0.3
Sub Total	66147	65224	1
G-CA	116 ± 155	110 ± 140	0.9
G-CDCA	7 ± 3	7 ± 3	1.0
G-DCA	10 ± 9	6 ± 3	0.6
G-LCA	2 ± 3	1 ± 0.2	0.3
G-UDCA	7 ± 7	3 ± 4	0.5
Sub Total	142	128	0.9
Total	70053	75750	1

The results are expressed in fmol/mg of tissue as mean ± standard deviation (n=16). N.D.: not detected. Statistics: * for $p \leq 0.05$. WT, wild-type and LKO, liver-specific 11β-HSD1 deficient mice.

Supplemental Table 1: Extraction efficiency of selected BAs in liver tissue.

Bile acid	Extraction Efficiency (%)
CA	95 ± 2
α-MCA	99 ± 1
G-CDCA	92 ± 1
T-CA	92 ± 1
T-α-MCA	92 ± 1

Supplemental Table 2: Precision of selected BAs in liver tissue.

	Precision (CV%)			
Bile acid	Endogenous	QC low	QC middle	QC high
CA	9.7	7.6	5.2	5.2
CDCA	8.7	9.0	11.1	12.3
DCA	16.2	14.0	6.3	10.0
LCA	n.d.	15.4	13.6	7.7
α-MCA	12.0	8.3	7.0	5.0
G-CDCA	11.5	12.6	7.1	14.0
G-UDCA	14.9	13.1	8.1	6.4
T-CA	10.2	14.4	11.3	11.7

Supplemental Table 3: Accuracy of selected BAs in liver tissue.

	Accuracy (%)		
Bile acid	QC low	QC middle	QC high
CA	91	96	93
CDCA	95	111	106
DCA	101	106	114
LCA	105	104	109
α-MCA	93	95	90
G-CDCA	88	94	90
G-UDCA	103	95	95
T-CA	95	97	98

Supplemental Table 4 Comparison of bile acid profiles among various species.

	Canine	Guinea-pig	Hamster	Human	Balb/c	C57bL/6	Han Wistar	Sprague-Dawley
CA	701 ± 892	2286 ± 745	2480 ± 956	20 ± 10	57 ± 101	422 ± 387	593 ± 747	2896 ± 1982
CDCA	196 ± 264	36548 ± 11560	642 ± 420	67 ± 59	39 ± 16	58 ± 39	210 ± 270	706 ± 582
DCA	193 ± 281	618 ± 317	833 ± 459	138 ± 55	68 ± 34	590 ± 273	174 ± 82	1236 ± 1180
7-oxoDCA	36 ± 50	45 ± 46	54 ± 21	3 ± 1	3 ± 12	14 ± 21	1 ± 1	85 ± 69
HDCA	N.D.	581 ± 297	17 ± 15	5 ± 4	19 ± 12	28 ± 15	626 ± 374	1743 ± 1125
LCA	29 ± 36	1443 ± 762	107 ± 108	15 ± 7	1 ± 1.2	8 ± 4	5 ± 5	24 ± 24
α-MCA	N.D.	184 ± 126	N.D.	7 ± 3	6 ± 13.5	71 ± 106	70 ± 101	56 ± 41
β-MCA	N.D.	186 ± 161	N.D.	N.D.	63 ± 76	210 ± 229	164 ± 170	367 ± 227
ω-MCA	2 ± 4	104 ± 133	6 ± 6	4 ± 3	51 ± 43	133 ± 145	89 ± 90	454 ± 209
UDCA	145 ± 180	6662 ± 3290	49 ± 31	32 ± 19	11 ± 9	83 ± 61	57 ± 60	206 ± 164
T-CA	251 ± 300	18 ± 14	75 ± 28	24 ± 27	143 ± 75	197 ± 47	226 ± 57	723 ± 454
T-CDCA	3 ± 4	41 ± 24	2 ± 0.5	97 ± 67	5 ± 1.5	24 ± 16	15 ± 4	19 ± 11
T-DCA	235 ± 331	41 ± 51	57 ± 24	35 ± 35	166 ± 136	105 ± 66	N.D.	521 ± 201
T-LCA	51 ± 83	14 ± 9.5	23 ± 6	2 ± 2	N.D.	3 ± 3	6 ± 5	4 ± 5
T-α-MCA	24 ± 25	5 ± 3.6	N.D.	4 ± 5	30 ± 14	206 ± 41	179 ± 36	408 ± 238
T-β-MCA	5 ± 6	2 ± 1.8	N.D.	5 ± 7	107 ± 33	182 ± 57	166 ± 47	561 ± 322
T-UDCA	12 ± 12	5 ± 2.7	1 ± 0.3	5 ± 3	25 ± 12	19 ± 9	4 ± 0.7	4 ± 2.5
G-CA	N.D.	484 ± 326	367 ± 207	162 ± 106	N.D.	87 ± 97	82 ± 87	3 ± 2
G-CDCA	1 ± 0.5	11688 ± 11037	217 ± 159	1052 ± 584	7 ± 4	1 ± 0.2	4 ± 1.2	66 ± 61
G-DCA	1 ± 1.9	102 ± 101	219 ± 138	341 ± 291	N.D.	7 ± 4	7 ± 4.2	N.D.
G-LCA	N.D.	297 ± 135	110 ± 62	15 ± 14	N.D.	N.D.	N.D.	7 ± 9
G-UDCA	N.D.	1045 ± 605	N.D.	144 ± 101	1 ± 0.8	N.D.	N.D.	4 ± 5

The results are expressed in nM as mean ± standard deviation (n=8). N.D.: not detected. Underlined values represent below lower limit of quantification.

Supplemental Table 5: Primers used for gene expression studies.

Gene	Forward	Reverse	Provider
Abcb11	ATTAACCTTGGTGATTCTCG	ATACCTTTCCACCTCCTTATTC	Sigma
Abcb1a	AGGACAAAAGAAGGAACTTG	GATAAGGAGAAAAGCTGCAC	Sigma
Abcb1b	CTGTTGGCGTATTTGGGATGT	CAGCATCAAGAGGGGAAGTAATG	primerbank
Abcc2	CGTATATAAGAAGGCACTAACC	CAATCTGTAAAACACTGGACC	Sigma
Abcc3	CACTTTGCTAATCCAGTACG	GATCCAAGATTTTACCCTCTG	Sigma
Abcc4	AAACAAAGTCATCCTGTTCG	CAGAAAGTTCTTGATCCTCC	Sigma
Baat	GGAAACCTGTTAGTTCTCAGGC	GTGGACCCCCATATAGTCTCC	primerbank
CYP7A1	CTTGAGGATGGTTCCTATAAC	TTAAAAGTCAAAGGGTCTGG	Sigma
CYP8B1	AAGAAGTCGTTCACTTTCAC	ACATAATCCTCCTGTACCAC	Sigma
Cyp27a1	AAAGCTGTGATTAAGGAGAC	CAAACTGTGTATTCTTGGGG	Sigma
HNF4a	GTGGCGAGTCCTTATGACACG	GCTGTTGGATGAATTGAGGTTGG	primerbank
Nr0b2	CGATCCTCTTCAACCCAG	GAGATCTACCAGAAGGGTG	Sigma
Osta	TTTTCTCCATCTTGGCTAAC	AGTTCATCACTTGAGACCTG	Sigma
Ostb	TGGCAAACAGAAATCGAAAG	GCAGAAAGACAAGTGATGAG	Sigma
Slc10a1	CACTGTTCTTCTTTCCTCTC	TTTTGTTTGGTCCTTCTGAG	Sigma
Slc27a2	TCCTCCAAGATGTGCGGTACT	TAGGTGAGCGTCTCGTCTCG	primerbank
Slc27a5	CTACGCTGGCTGCATATAGATG	CCACAAAGGTCTCTGGAGGAT	primerbank
Slco1a1	ACAGATTCAGGCACATTTAC	GATTAGAATGAAGACTGCGG	Sigma
Slco1a4	GCTTTTCCAAGATCAAGGCATTT	CGTGGGGATACCGAATTGTCT	primerbank
Slco1b2	CAACCTGACTGGTTTTCTATG	AAGTGAAGGATCCAATGAAG	Sigma

6 CONCLUSIONS AND OUTLOOK

This PhD thesis aimed at understanding the role of 11β-HSD1 in BA homeostasis. To the best of our knowledge, this has not yet been addressed and is of pivotal importance for the development of therapeutic 11β-HSD1 inhibitors (Rosenstock, Banarer et al. 2010; Thomas and Potter 2011). Using a model of liver-specific 11β-HSD1 knockout mice, we found an altered BA homeostasis. A significant increase of several unconjugated BAs was observed in serum and liver of liver-specific 11β-HSD1 knockout mice, while intrahepatic conjugated BAs levels were rather decreased, suggesting a reduced BA conjugating machinery which was confirmed by the reduced expression levels of *VLCS* and *VLCSH2*, two enzymes presenting BA coenzyme A synthetase activity (Figure 4) (also known as BACS). On the other hand, conjugated BA levels in serum were not significantly changed, results which were in line with the unaltered expression levels of bile acid transporters. The toxicological consequences of the intrahepatic accumulation of BAs in liver-specific 11β-HSD1 knockout mice and also in 11β-HSD1 full knockout mice remain to be further investigated. Moreover, *in vivo* experiments aiming at challenging liver-specific 11β-HSD1 knockout and 11β-HSD1 full knockout mice with lithogenic diets, the administration of cholestatic drugs (e.g., cyclosporine A) and bile duct ligation models will contribute to clarify the importance of 11β-HSD1 and consequently normal glucocorticoids regeneration on BA homeostasis. It is important to reinforce that 11β-HSD1 inhibition is aimed at treating diabetic and obese patients, thus long-term and chronic interventions are expected. Moreover, these patients often are exposed to more than one therapeutic regimen; therefore the careful safety assessment of relevant co-treatment on BA homeostasis warrants further investigation. In addition, we suggest that the liver-specific 11β-HSD1 disruption might be a more physiologically relevant animal model to assess the effects of glucocorticoids in BA homeostasis, since the altered concentrations of active glucocorticoids, rather than the systemic concentrations are likely responsible for the dysregulation of BA (Figure 4). Moreover, liver-specific 11β-HSD1 knockout mice lack serious metabolic abnormalities, indicating that the impact of glucocorticoid and GR on the gluconeogenic pathway in this model is minimal. Furthermore, the role 11β-

HSD1 is not only limited to GR-dependent BA homeostasis but also, on the conversion of the secondary 7-oxoLCA. 7-oxoLCA and particularly its taurine conjugated form were markedly elevated in the serum of liver-specific 11β-HSD1 deficient mice and therefore may be potentially applied as biomarker to assess the efficacy of 11β-HSD1 inhibitors by the pharmaceutical industry. Importantly, T-7-oxoLCA was approximately 47-fold significantly enriched in serum of liver-specific 11β-HSD1 deficient mice, whereas the concentrations of all other taurine-conjugates BAs studied were not statistically different, suggesting its elevation is caused primarily due to the absence of 7-oxo reductase activity. Nevertheless, the potential of 7-oxo BAs as functional biomarker has to be further evaluated in animals and humans using selective 11β-HSD1 inhibitors. In this context, due to the fact that humans mainly conjugate BAs with glycine, G-7-oxoLCA is expected to accumulate in the plasma.

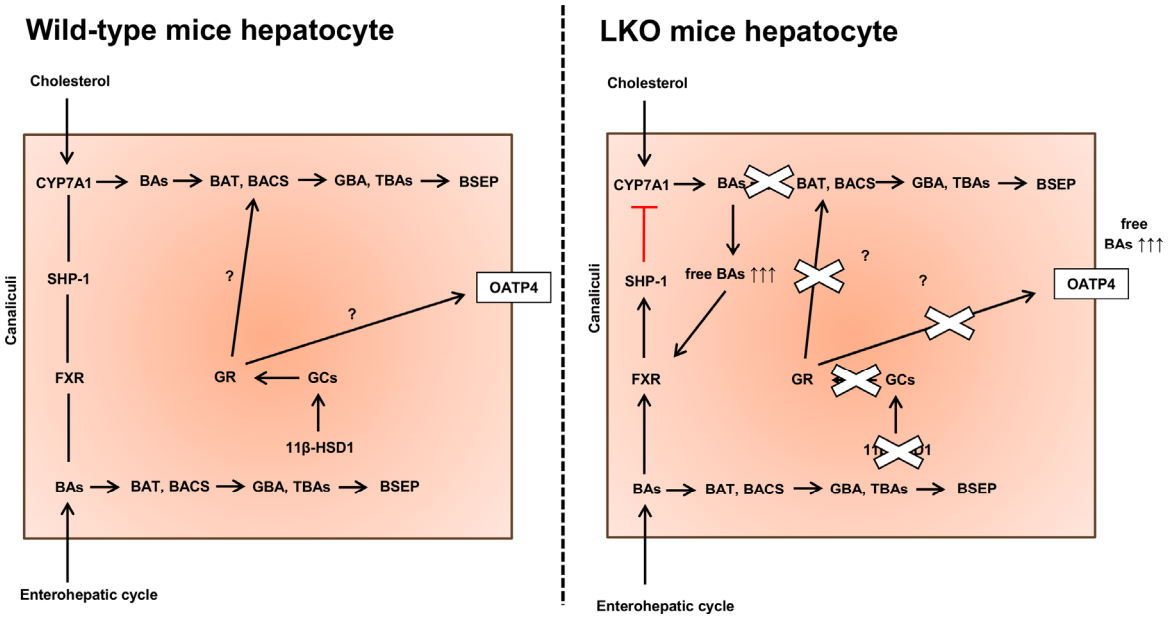

Figure 4 Possible mechanistic explanation for the effect of liver-specific 11β-HSD1 deficiency (LKO) in BA accumulation in mice hepatocytes. Arrows indicate activation, X and whiskers represent blocked or pathways with reduced activity; question markers indicate unclear gene expression mechanisms; GBA: glyco-BA; TBA: tauro-BA; GCs: active glucocorticoids; BACS: BA coenzyme A synthetase; BAT: BA coenzyme A: amino acid N-acyltransferase; BSEP: bile-salt export pump; OATP4: organic anion transporters 4; FXR: Farnesoid X receptor; SHP-1: short heterodimer partner 1.

7 REFERENCES

Abrahams, L., N. M. Semjonous, et al. (2012). "Biomarkers of hypothalamic–pituitary–adrenal axis activity in mice lacking 11β-HSD1 and H6PDH." Journal of Endocrinology 214(3): 367-372.

Akita, H., H. Suzuki, et al. (2002). "Transport Activity of Human MRP3 Expressed in Sf9 Cells: Comparative Studies with Rat MRP3." Pharmaceutical Research 19(1): 34-41.

Amery, L., M. Fransen, et al. (2000). "Mitochondrial and peroxisomal targeting of 2-methylacyl-CoA racemase in humans." Journal of Lipid Research 41(11): 1752-1759.

Ananthanarayanan, M., O. C. Ng, et al. (1994). "Characterization of cloned rat liver Na(+)-bile acid cotransporter using peptide and fusion protein antibodies." American Journal of Physiology - Gastrointestinal and Liver Physiology 267(4): G637-G643.

Andersson, S., D. L. Davis, et al. (1989). "Cloning, structure, and expression of the mitochondrial cytochrome P-450 sterol 26-hydroxylase, a bile acid biosynthetic enzyme." Journal of Biological Chemistry 264(14): 8222-8229.

Andrews, R. C. and B. R. Walker (1999). "Glucocorticoids and insulin resistance: old hormones, new targets." Clinical Science 96(5): 513-523.

Angeletti, R. H., P. M. Novikoff, et al. (1997). "The choroid plexus epithelium is the site of the organic anion transport protein in the brain." Proceedings of the National Academy of Sciences 94(1): 283-286.

Arampatzis, S., B. Kadereit, et al. (2005). "Comparative enzymology of 11β-hydroxysteroid dehydrogenase type 1 from six species." Journal of Molecular Endocrinology 35(1): 89-101.

Baes, M., S. Huyghe, et al. (2000). "Inactivation of the Peroxisomal Multifunctional Protein-2 in Mice Impedes the Degradation of Not Only 2-Methyl-branched Fatty Acids and Bile Acid Intermediates but Also of Very Long Chain Fatty Acids." Journal of Biological Chemistry 275(21): 16329-16336.

Ballatori, N., W. V. Christian, et al. (2005). "OSTα-OSTβ: A major basolateral bile acid and steroid transporter in human intestinal, renal, and biliary epithelia." Hepatology 42(6): 1270-1279.

Ballatori, N., F. Fang, et al. (2008). "Ostα-Ostβ is required for bile acid and conjugated steroid disposition in the intestine, kidney, and liver." American Journal of Physiology - Gastrointestinal and Liver Physiology 295(1): G179-G186.

Båvner, A., S. Sanyal, et al. (2005). "Transcriptional corepression by SHP: molecular mechanisms and physiological consequences." Trends in Endocrinology & Metabolism 16(10): 478-488.

Belinsky, M. G., P. A. Dawson, et al. (2005). "Analysis of the In Vivo Functions of Mrp3." Molecular Pharmacology 68(1): 160-168.

Bergwerk, A. J., X. Shi, et al. (1996). "Immunologic distribution of an organic anion transport protein in rat liver and kidney." American Journal of Physiology - Gastrointestinal and Liver Physiology 271(2): G231-G238.

Bhalla, S., C. Ozalp, et al. (2004). "Ligand-activated Pregnane X Receptor Interferes with HNF-4 Signaling by Targeting a Common Coactivator PGC-1α: FUNCTIONAL IMPLICATIONS IN HEPATIC CHOLESTEROL AND GLUCOSE METABOLISM." Journal of Biological Chemistry 279(43): 45139-45147.

Bookout, A. L., Y. Jeong, et al. (2006). "Anatomical Profiling of Nuclear Receptor Expression Reveals a Hierarchical Transcriptional Network." Cell 126(4): 789-799.

Boyle, C. D. and T. J. Kowalski (2009). "11β-hydroxysteroid dehydrogenase type 1 inhibitors: a review of recent patents." Expert Opinion on Therapeutic Patents 19(6): 801-825.

Brendel, C., K. Schoonjans, et al. (2002). "The Small Heterodimer Partner Interacts with the Liver X Receptor α and Represses Its Transcriptional Activity." Molecular Endocrinology 16(9): 2065-2076.

Brereton, P. S., R. R. van Driel, et al. (2001). "Light and Electron Microscopy Localization of the 11β-Hydroxysteroid Dehydrogenase Type I Enzyme in the Rat." Endocrinology 142(4): 1644-1651.

Carter, R. N., J. M. Paterson, et al. (2009). "Hypothalamic-Pituitary-Adrenal Axis Abnormalities in Response to Deletion of 11β-HSD1 is Strain-Dependent." Journal of Neuroendocrinology 21(11): 879-887.

Cattori, V., B. Hagenbuch, et al. (2000). "Identification of organic anion transporting polypeptide 4 (Oatp4) as a major full-length isoform of the liver-specific transporter-1 (rlst-1) in rat liver." FEBS Letters 474(2–3): 242-245.

Chatterjee, B., I. Echchgadda, et al. (2005). Vitamin D Receptor Regulation of the Steroid/Bile Acid Sulfotransferase SULT2A1. Methods in Enzymology. S. Helmut and P. Lester, Academic Press. Volume 400: 165-191.

Chen, F., L. Ma, et al. (2003). "Liver Receptor Homologue-1 Mediates Species- and Cell Line-specific Bile Acid-dependent Negative Feedback Regulation of the Apical Sodium-dependent Bile Acid Transporter." Journal of Biological Chemistry 278(22): 19909-19916.

Cheng, X., D. Buckley, et al. (2007). "Regulation of hepatic bile acid transporters Ntcp and Bsep expression." Biochemical Pharmacology 74(11): 1665-1676.

Clarke, J. L. and P. J. Mason (2003). "Murine hexose-6-phosphate dehydrogenase: a bifunctional enzyme with broad substrate specificity and 6-phosphogluconolactonase activity." Archives of Biochemistry and Biophysics 415(2): 229-234.

Cole, T. J., J. A. Blendy, et al. (1995). "Targeted disruption of the glucocorticoid receptor gene blocks adrenergic chromaffin cell development and severely retards lung maturation." Genes & Development 9(13): 1608-1621.

Cowles, R. L., J.-Y. Lee, et al. (2002). "Dietary Stearic Acid Alters Gallbladder Bile Acid Composition in Hamsters Fed Cereal-Based Diets." The Journal of Nutrition 132(10): 3119-3122.

Craddock, A. L., M. W. Love, et al. (1998). "Expression and transport properties of the human ileal and renal sodium-dependent bile acid transporter." American Journal of Physiology - Gastrointestinal and Liver Physiology 274(1): G157-G169.

Csanaky, I. L., H. Lu, et al. (2011). "Organic anion–transporting polypeptide 1b2 (Oatp1b2) is important for the hepatic uptake of unconjugated bile acids: Studies in Oatp1b2-null mice." Hepatology 53(1): 272-281.

Cui, Y. J., L. M. Aleksunes, et al. (2009). "Compensatory Induction of Liver Efflux Transporters in Response to ANIT-Induced Liver Injury Is Impaired in FXR-Null Mice." Toxicological Sciences 110(1): 47-60.

Dahlbäck, H. and I. Holmberg (1990). "Oxidation of 5β-cholestane-3α,7α,12α-triol into 3α,7α,12α-trihydroxy-5β-cholestanoic acid by cytochrome P-45026 from rabbit liver mitochondria." Biochemical and Biophysical Research Communications 167(2): 391-395.

Dawson, P. A., J. Haywood, et al. (2003). "Targeted Deletion of the Ileal Bile Acid Transporter Eliminates Enterohepatic Cycling of Bile Acids in Mice." Journal of Biological Chemistry 278(36): 33920-33927.

Denk, G. U., C. J. Soroka, et al. (2004). "Multidrug resistance-associated protein 4 is up-regulated in liver but down-regulated in kidney in obstructive cholestasis in the rat." Journal of Hepatology 40(4): 585-591.

Denson, L. A., E. Sturm, et al. (2001). "The Orphan Nuclear Receptor, shp, Mediates Bile Acid-Induced Inhibition of the Rat Bile Acid Transporter, ntcp." Gastroenterology 121(1): 140-147.

Elferink, R. P., G. N. Tytgat, et al. (1997). "Hepatic canalicular membrane 1: The role of mdr2 P-glycoprotein in hepatobiliary lipid transport." The FASEB Journal 11(1): 19-28.

Eloranta, J. J., D. Jung, et al. (2006). "The Human Na+-Taurocholate Cotransporting Polypeptide Gene Is Activated by Glucocorticoid Receptor and Peroxisome Proliferator-Activated Receptor-γ Coactivator-1α, and Suppressed by Bile Acids via a Small Heterodimer Partner-Dependent Mechanism." Molecular Endocrinology 20(1): 65-79.

Eloranta, J. J. and G. A. Kullak-Ublick (2005). "Coordinate transcriptional regulation of bile acid homeostasis and drug metabolism." Archives of Biochemistry and Biophysics 433(2): 397-412.

Eloranta, J. J., Z. M. Zaïr, et al. (2009). "Vitamin D3 and Its Nuclear Receptor Increase the Expression and Activity of the Human Proton-Coupled Folate Transporter." Molecular Pharmacology 76(5): 1062-1071.

Falany, C. N., H. Fortinberry, et al. (1997). "Cloning, expression, and chromosomal localization of mouse liver bile acid CoA:amino acid N-acyltransferase." Journal of Lipid Research 38(6): 1139-1148.

Falany, C. N., M. R. Johnson, et al. (1994). "Glycine and taurine conjugation of bile acids by a single enzyme. Molecular cloning and expression of human liver bile acid CoA:amino acid N-acyltransferase." Journal of Biological Chemistry 269(30): 19375-19379.

Fukiya, S., M. Arata, et al. (2009). "Conversion of cholic acid and chenodeoxycholic acid into their 7-oxo derivatives by Bacteroides intestinalis AM-1 isolated from human feces." FEMS Microbiology Letters 293(2): 263-270.

Furster, C., J. Zhang, et al. (1996). "Purification of a 3β-Hydroxy-Δ5-C27-steroid Dehydrogenase from Pig Liver Microsomes Active in Major and Alternative Pathways of Bile Acid Biosynthesis." Journal of Biological Chemistry 271(34): 20903-20907.

Gao, B., B. Stieger, et al. (1999). "Localization of the Organic Anion Transporting Polypeptide 2 (Oatp2) in Capillary Endothelium and Choroid Plexus Epithelium of Rat Brain." Journal of Histochemistry & Cytochemistry 47(10): 1255-1263.

Garcia-Canaveras, J. C., M. T. Donato, et al. (2012). "Targeted profiling of circulating and hepatic bile acids in human, mouse and rat using an UPLC-MRM-MS-validated method." Journal of Lipid Research.

Gerk, P. M. and M. Vore (2002). "Regulation of Expression of the Multidrug Resistance-Associated Protein 2 (MRP2) and Its Role in Drug Disposition." Journal of Pharmacology and Experimental Therapeutics 302(2): 407-415.

Goodwin, B., S. A. Jones, et al. (2000). "A Regulatory Cascade of the Nuclear Receptors FXR, SHP-1, and LRH-1 Represses Bile Acid Biosynthesis." Molecular Cell 6(3): 517-526.

Gradhand, U., T. Lang, et al. (2007). "Variability in human hepatic MRP4 expression: influence of cholestasis and genotype." Pharmacogenomics J 8(1): 42-52.

Groothuis, G. M., M. J. Hardonk, et al. (1982). "Autoradiographic and kinetic demonstration of acinar heterogeneity of taurocholate transport." American Journal of Physiology - Gastrointestinal and Liver Physiology 243(6): G455-G462.

Guertin, F., A. Loranger, et al. (1995). "Bile formation and hepatic plasma membrane composition in guinea-pigs and rats." Comparative Biochemistry and Physiology Part B: Biochemistry and Molecular Biology 111(4): 523-531.

Hadoke, P. W. F., J. Iqbal, et al. (2009). "Therapeutic manipulation of glucocorticoid metabolism in cardiovascular disease." British Journal of Pharmacology 156(5): 689-712.

Hagenbuch, B., B. F. Scharschmidt, et al. (1996). "Effect of antisense oligonucleotides on the expression of hepatocellular bile acid and organic anion uptake systems in Xenopus laevis oocytes." Biochem. J. 316(3): 901-904.

Han, S. and J. Y. L. Chiang (2009). "Mechanism of Vitamin D Receptor Inhibition of Cholesterol 7α-Hydroxylase Gene Transcription in Human Hepatocytes." Drug Metabolism and Disposition 37(3): 469-478.

Harno, E. and A. White (2010). "Will treating diabetes with 11β-HSD1 inhibitors affect the HPA axis?" Trends in Endocrinology & Metabolism 21(10): 619-627.

Harris, H. J., Y. Kotelevtsev, et al. (2001). "Intracellular Regeneration of Glucocorticoids by 11β-Hydroxysteroid Dehydrogenase (11β-HSD)-1 Plays a Key Role in Regulation of the Hypothalamic-Pituitary-Adrenal Axis: Analysis of 11β-HSD-1-Deficient Mice." Endocrinology 142(1): 114-120.

He, J., S. Nishida, et al. (2011). "PXR Prevents Cholesterol Gallstone Disease by Regulating Biosynthesis and Transport of Bile Salts." Gastroenterology 140(7): 2095-2106.

Hennebert, O., S. Le Mée, et al. (2007). "5α-Androstane-3β,7α,17β-triol and 5α-androstane-3β,7β,17β-triol as substrates for the human 11β-hydroxysteroid dehydrogenase type 1." Steroids 72(13): 855-864.

Hennebert, O., C. Pernelle, et al. (2007). "7α- and 7β-hydroxy-epiandrosterone as substrates and inhibitors for the human 11β-hydroxysteroid dehydrogenase type 1." The Journal of Steroid Biochemistry and Molecular Biology 105(1–5): 159-165.

Hofmann, A. F. (2002). "Rifampicin and treatment of cholestatic pruritus." Gut 51(5): 756-757.

Holt, J. A., G. Luo, et al. (2003). "Definition of a novel growth factor-dependent signal cascade for the suppression of bile acid biosynthesis." Genes & Development 17(13): 1581-1591.

Houten, S. and J. Auwerx (2004). "The enterohepatic nuclear receptors are major regulators of the enterohepatic circulation of bile salts." Annals of Medicine 36(7): 482-491.

Hughes, K. A., S. P. Webster, et al. (2008). "11-Beta-hydroxysteroid dehydrogenase type 1 (11β-HSD1) inhibitors in Type 2 diabetes mellitus and obesity." Expert Opinion on Investigational Drugs 17(4): 481-496.

Hult, M., B. Elleby, et al. (2004). "Human and rodent type 1 11ß-hydroxysteroid dehydrogenases are 7ß-hydroxycholesterol dehydrogenases involved in oxysterol metabolism." Cellular and Molecular Life Sciences 61(7): 992-999.

Hult, M., C. S. I. Nobel, et al. (2001). "Novel enzymological profiles of human 11β-hydroxysteroid dehydrogenase type 1." Chemico-Biological Interactions 130–132(0): 805-814.

Hylemon, P. B. and J. Harder (1998). "Biotransformation of monoterpenes, bile acids, and other isoprenoids in anaerobic ecosystems." FEMS Microbiology Reviews 22(5): 475-488.

Inagaki, T., M. Choi, et al. (2005). "Fibroblast growth factor 15 functions as an enterohepatic signal to regulate bile acid homeostasis." Cell Metabolism 2(4): 217-225.

Inoue, Y., A.-M. Yu, et al. (2004). "Hepatocyte Nuclear Factor 4α Is a Central Regulator of Bile Acid Conjugation." Journal of Biological Chemistry 279(4): 2480-2489.

Ishibashi, S., M. Schwarz, et al. (1996). "Disruption of Cholesterol 7α-Hydroxylase Gene in Mice: I. POSTNATAL LETHALITY REVERSED BY BILE ACID AND VITAMIN SUPPLEMENTATION." Journal of Biological Chemistry 271(30): 18017-18023.

Jemnitz, K., K. Heredi-Szabo, et al. (2010). "ABCC2/Abcc2: a multispecific transporter with dominant excretory functions." Drug Metabolism Reviews 42(3): 402-436.

John, S., T. A. Johnson, et al. (2009). "Kinetic Complexity of the Global Response to Glucocorticoid Receptor Action." Endocrinology 150(4): 1766-1774.

Jones, A. L., G. T. Hradek, et al. (1980). "Autoradiographic evidence for hepatic lobular concentration gradient of bile acid derivative." American Journal of Physiology - Gastrointestinal and Liver Physiology 238(3): G233-G237.

Jung, D., A. C. Fantin, et al. (2004). "Human ileal bile acid transporter gene ASBT (SLC10A2) is transactivated by the glucocorticoid receptor." Gut 53(1): 78-84.

Jung, D., M. Podvinec, et al. (2002). "Human organic anion transporting polypeptide 8 promoter is transactivated by the farnesoid X receptor/bile acid receptor." Gastroenterology 122(7): 1954-1966.

Kakyo, M., H. Sakagami, et al. (1999). "Immunohistochemical distribution and functional characterization of an organic anion transporting polypeptide 2 (oatp2)." FEBS Letters 445(2–3): 343-346.

Kannenberg, F., P. Ellinghaus, et al. (1999). "Aberrant Oxidation of the Cholesterol Side Chain in Bile Acid Synthesis of Sterol Carrier Protein-2/Sterol Carrier Protein-x Knockout Mice." Journal of Biological Chemistry 274(50): 35455-35460.

Kenneke, J. F., C. S. Mazur, et al. (2008). "Mechanistic Investigation of the Noncytochrome P450-Mediated Metabolism of Triadimefon to Triadimenol in Hepatic Microsomes." Chemical Research in Toxicology 21(10): 1997-2004.

Khan, A. A., E. C. Y. Chow, et al. (2009). "Expression and regulation of the bile acid transporter, OSTα-OSTβ in rat and human intestine and liver." Biopharmaceutics & Drug Disposition 30(5): 241-258.

Klaassen, C. D. and L. M. Aleksunes (2010). "Xenobiotic, Bile Acid, and Cholesterol Transporters: Function and Regulation." Pharmacological Reviews 62(1): 1-96.

Klaassen, C. D. and S. A. Reisman (2010). "Nrf2 the rescue: Effects of the antioxidative/electrophilic response on the liver." Toxicology and Applied Pharmacology 244(1): 57-65.

Kliewer, S. A. and T. M. Willson (2002). "Regulation of xenobiotic and bile acid metabolism by the nuclear pregnane X receptor." Journal of Lipid Research 43(3): 359-364.

Kock, K. and K. L. R. Brouwer (2012). "A Perspective on Efflux Transport Proteins in the Liver." Clin Pharmacol Ther 92(5): 599-612.

Kong, B., L. Wang, et al. (2012). "Mechanism of tissue-specific farnesoid X receptor in suppressing the expression of genes in bile-acid synthesis in mice." Hepatology 56(3): 1034-1043.

Kotelevtsev, Y., M. C. Holmes, et al. (1997). "11β-Hydroxysteroid dehydrogenase type 1 knockout mice show attenuated glucocorticoid-inducible responses and resist hyperglycemia on obesity or stress." Proceedings of the National Academy of Sciences 94(26): 14924-14929.

Kotti, T. J., K. Savolainen, et al. (2000). "In Mouse α-Methylacyl-CoA Racemase, the Same Gene Product Is Simultaneously Located in Mitochondria and Peroxisomes." Journal of Biological Chemistry 275(27): 20887-20895.

Kullak-Ublick, G. A. (1999). "Regulation of organic anion and drug transporters of the sinusoidal membrane." Journal of Hepatology 31(3): 563-573.

Kullak-Ublick, G. E. R. D. A., B. R. U. N. O. Stieger, et al. (2000). "Hepatic Transport of Bile Salts." Semin Liver Dis 20(03): 273-292.

Lam, P., R. Wang, et al. (2005). "Bile Acid Transport in Sister of P-Glycoprotein (ABCB11) Knockout Mice†." Biochemistry 44(37): 12598-12605.

Lavery, G. G., A. E. Zielinska, et al. (2012). "Lack of Significant Metabolic Abnormalities in Mice with Liver-Specific Disruption of 11β-Hydroxysteroid Dehydrogenase Type 1." Endocrinology 153(7): 3236-3248.

Lemke, U., A. Krones-Herzig, et al. (2008). "The Glucocorticoid Receptor Controls Hepatic Dyslipidemia through Hes1." Cell Metabolism 8(3): 212-223.

Li-Hawkins, J., M. Gafvels, et al. (2002). "Cholic acid mediates negative feedback regulation of bile acid synthesis in mice." The Journal of Clinical Investigation 110(8): 1191-1200.

Lin, M. C., W. Kramer, et al. (1990). "Identification of cytosolic and microsomal bile acid-binding proteins in rat ileal enterocytes." Journal of Biological Chemistry 265(25): 14986-14995.

Lu, Y., Z. Zhang, et al. (2012). "Glucocorticoids Promote Hepatic Cholestasis in Mice by Inhibiting the Transcriptional Activity of the Farnesoid X Receptor." Gastroenterology 143(6): 1630-1640.e1638.

Lund, E., I. Björkhem, et al. (1993). "24-, 25- and 27-hydroxylation of cholesterol by a purified preparation of 27-hydroxylase from pig liver." Biochimica et Biophysica Acta (BBA) - Lipids and Lipid Metabolism 1166(2–3): 177-182.

Macdonald, I., C. Williams, et al. (1975). "NAD- and NADP-dependent 7alpha-hydroxysteroid dehydrogenases from bacteroides fragilis." Biochimica et Biophysica Acta (BBA) - Molecular Basis of Disease 384(1): 12-24.

Macdonald, I. A., D. M. Hutchison, et al. (1983). "Metabolism of primary bile acids by Clostridium perfringens." Journal of Steroid Biochemistry 18(1): 97-104.

Makishima, M., T. T. Lu, et al. (2002). "Vitamin D Receptor As an Intestinal Bile Acid Sensor." Science 296(5571): 1313-1316.

Makishima, M., A. Y. Okamoto, et al. (1999). "Identification of a Nuclear Receptor for Bile Acids." Science 284(5418): 1362-1365.

Martin, H.-J., U. Breyer-Pfaff, et al. (2006). "Purification and characterization of AKR1B10 from human liver: Role in carbonyl reduction of xenobiotics " Drug Metabolism and Disposition 34(3): 464-470.

Martin, K. O., A. B. Reiss, et al. (1997). "7 alpha-hydroxylation of 27-hydroxycholesterol: biologic role in the regulation of cholesterol synthesis." Journal of Lipid Research 38(5): 1053-1058.

Maser, E. and G. Bannenberg (1994). "11β-hydroxysteroid dehydrogenase mediates reductive metabolism of xenobiotic carbonyl compounds." Biochemical Pharmacology 47(10): 1805-1812.

Mason, J. I. and G. S. Boyd (1978). "The suppressive effect of the catatoxic steroid, pregnenolone-16alpha-carbonitrile, on liver microsomal cholesterol-7alpha-hydroxlyase." Steroids 31(6): 849-854.

Masuzaki, H., J. Paterson, et al. (2001). "A Transgenic Model of Visceral Obesity and the Metabolic Syndrome." Science 294(5549): 2166-2170.

Masuzaki, H., H. Yamamoto, et al. (2003). "Transgenic amplification of glucocorticoid action in adipose tissue causes high blood pressure in mice." The Journal of Clinical Investigation 112(1): 83-90.

McCarthy, T. C., X. Li, et al. (2005). "Vitamin D Receptor-dependent Regulation of Colon Multidrug Resistance-associated Protein 3 Gene Expression by Bile Acids." Journal of Biological Chemistry 280(24): 23232-23242.

Meier, P. J. (1995). "Molecular mechanisms of hepatic bile salt transport from sinusoidal blood into bile." American Journal of Physiology - Gastrointestinal and Liver Physiology 269(6): G801-G812.

Meier, P. J., U. Eckhardt, et al. (1997). "Substrate specificity of sinusoidal bile acid and organic anion uptake systems in rat and human liver." Hepatology 26(6): 1667-1677.

Meier, P. J. and B. Stieger (2000). "Molecular Mechanisms in Bile Formation." Physiology 15(2): 89-93.

Meier, P. J. and B. Stieger (2002). "Bile Salt Transporters " Annual Review of Physiology 64(1): 635-661.

Mennone, A., C. J. Soroka, et al. (2006). "Mrp4−/− mice have an impaired cytoprotective response in obstructive cholestasis." Hepatology 43(5): 1013-1021.

Mihalik, S. J., S. J. Steinberg, et al. (2002). "Participation of Two Members of the Very Long-chain Acyl-CoA Synthetase Family in Bile Acid Synthesis and Recycling." Journal of Biological Chemistry 277(27): 24771-24779.

Moi, P., K. Chan, et al. (1994). "Isolation of NF-E2-related factor 2 (Nrf2), a NF-E2-like basic leucine zipper transcriptional activator that binds to the tandem NF-E2/AP1 repeat of the beta-globin locus control region." Proceedings of the National Academy of Sciences 91(21): 9926-9930.

Morton, N. M., M. C. Holmes, et al. (2001). "Improved Lipid and Lipoprotein Profile, Hepatic Insulin Sensitivity, and Glucose Tolerance in 11β-Hydroxysteroid Dehydrogenase Type 1 Null Mice." Journal of Biological Chemistry 276(44): 41293-41300.

Morton, N. M., J. M. Paterson, et al. (2004). "Novel Adipose Tissue–Mediated Resistance to Diet-Induced Visceral Obesity in 11β-Hydroxysteroid Dehydrogenase Type 1–Deficient Mice." Diabetes 53(4): 931-938.

Moschetta, A., A. L. Bookout, et al. (2004). "Prevention of cholesterol gallstone disease by FXR agonists in a mouse model." Nat Med 10(12): 1352-1358.

Muller, C., D. Pompon, et al. (2006). "Inter-conversion of 7α- and 7β-hydroxy-dehydroepiandrosterone by the human 11β-hydroxysteroid dehydrogenase type 1." The Journal of Steroid Biochemistry and Molecular Biology 99(4–5): 215-222.

Nashev, L. G., C. Chandsawangbhuwana, et al. (2007). "Hexose-6-phosphate Dehydrogenase Modulates 11β-Hydroxysteroid Dehydrogenase Type 1-Dependent Metabolism of 7-keto- and 7β-hydroxy-neurosteroids." PLoS ONE 2(6): e561.

Nathanson, M. H. and J. L. Boyer (1991). "Mechanisms and regulation of bile secretion." Hepatology 14(3): 551-566.

Nishida, S., J. Ozeki, et al. (2009). "Modulation of Bile Acid Metabolism by 1α-Hydroxyvitamin D3 Administration in Mice." Drug Metabolism and Disposition 37(10): 2037-2044.

Odermatt, A., P. Arnold, et al. (1999). "The N-terminal Anchor Sequences of 11β-Hydroxysteroid Dehydrogenases Determine Their Orientation in the Endoplasmic Reticulum Membrane." Journal of Biological Chemistry 274(40): 28762-28770.

Odermatt, A., A. G. Atanasov, et al. (2006). "Why is 11β-hydroxysteroid dehydrogenase type 1 facing the endoplasmic reticulum lumen?: Physiological relevance of the membrane topology of 11β-HSD1." Molecular and Cellular Endocrinology 248(1–2): 15-23.

Odermatt, A., T. Da Cunha, et al. (2011). "Hepatic reduction of the secondary bile acid 7-oxolithocholic acid is mediated by 11beta-hydroxysteroid dehydrogenase 1." The Biochemical journal 436(3): 621-629.

Odermatt, A. and C. Gumy (2008). "Glucocorticoid and mineralocorticoid action: Why should we consider influences by environmental chemicals?" Biochemical Pharmacology 76(10): 1184-1193.

Odermatt, A. and L. G. Nashev (2010). "The glucocorticoid-activating enzyme 11β-hydroxysteroid dehydrogenase type 1 has broad substrate specificity: Physiological and toxicological considerations." The Journal of Steroid Biochemistry and Molecular Biology 119(1–2): 1-13.

Oelkers, P., L. C. Kirby, et al. (1997). "Primary bile acid malabsorption caused by mutations in the ileal sodium-dependent bile acid transporter gene (SLC10A2)." The Journal of Clinical Investigation 99(8): 1880-1887.

Panwala, C. M., J. C. Jones, et al. (1998). "A Novel Model of Inflammatory Bowel Disease: Mice Deficient for the Multiple Drug Resistance Gene, mdr1a, Spontaneously Develop Colitis." The Journal of Immunology 161(10): 5733-5744.

Parks, D. J., S. G. Blanchard, et al. (1999). "Bile Acids: Natural Ligands for an Orphan Nuclear Receptor." Science 284(5418): 1365-1368.

Pascussi, J.-M., L. Drocourt, et al. (2000). "Dexamethasone Induces Pregnane X Receptor and Retinoid X Receptor-α Expression in Human Hepatocytes: Synergistic Increase of CYP3A4 Induction by Pregnane X Receptor Activators." Molecular Pharmacology 58(2): 361-372.

Pascussi, J.-M., S. Gerbal-Chaloin, et al. (2000). "Dexamethasone Enhances Constitutive Androstane Receptor Expression in Human Hepatocytes: Consequences on Cytochrome P450 Gene Regulation." Molecular Pharmacology 58(6): 1441-1450.

Paterson, J. M., N. M. Morton, et al. (2004). "Metabolic syndrome without obesity: Hepatic overexpression of 11β-hydroxysteroid dehydrogenase type 1 in transgenic mice." Proceedings of the National Academy of Sciences of the United States of America 101(18): 7088-7093.

Penno, C. A., D. Arsenijevic, et al. (2013). "Quantification of Multiple Bile Acids in Uninephrectomized Rats Using Ultra-Performance Liquid Chromatography-Tandem Mass Spectrometry." Analytical Methods.

Pikuleva, I. A., A. Babiker, et al. (1998). "Activities of Recombinant Human Cytochrome P450c27 (CYP27) Which Produce Intermediates of Alternative Bile Acid Biosynthetic Pathways." Journal of Biological Chemistry 273(29): 18153-18160.

Pircher, P. C., J. L. Kitto, et al. (2003). "Farnesoid X Receptor Regulates Bile Acid-Amino Acid Conjugation." Journal of Biological Chemistry 278(30): 27703-27711.

Ramamoorthy, S. and J. Cidlowski (2013). "Exploring the Molecular Mechanism of Glucocorticoid Receptor Action from Sensitivity to Resistance." Hormone Resistance and Hypersensitivity 24 41-56.

Rao, A., J. Haywood, et al. (2008). "The organic solute transporter α-β, Ostα-Ostβ, is essential for intestinal bile acid transport and homeostasis." Proceedings of the National Academy of Sciences 105(10): 3891-3896.

Reichel, C., B. Gao, et al. (1999). "Localization and function of the organic anion–transporting polypeptide Oatp2 in rat liver." Gastroenterology 117(3): 688-695.

Ricketts, M. L., J. M. Verhaeg, et al. (1998). "Immunohistochemical Localization of Type 1 11β-Hydroxysteroid Dehydrogenase in Human Tissues." Journal of Clinical Endocrinology & Metabolism 83(4): 1325-1335.

Ridlon, J. M., D.-J. Kang, et al. (2006). "Bile salt biotransformations by human intestinal bacteria." Journal of Lipid Research 47(2): 241-259.

Rosales, R., M. R. Romero, et al. (2013). "FXR-dependent and -independent interaction of glucocorticoids with the regulatory pathways involved in the control of bile acid handling by the liver." Biochemical Pharmacology(0).

Rose, Adam J., Mauricio B. Díaz, et al. (2011). "Molecular Control of Systemic Bile Acid Homeostasis by the Liver Glucocorticoid Receptor." Cell metabolism 14(1): 123-130.

Rosenstock, J., S. Banarer, et al. (2010). "The 11-β-Hydroxysteroid Dehydrogenase Type 1 Inhibitor INCB13739 Improves Hyperglycemia in Patients With Type 2 Diabetes Inadequately Controlled by Metformin Monotherapy." Diabetes Care 33(7): 1516-1522.

Russell, D. W. (2003). "THE ENZYMES, REGULATION, AND GENETICS OF BILE ACID SYNTHESIS." Annual Review of Biochemistry 72(1): 137-174.

Russell, D. W. and K. D. R. Setchell (1992). "Bile acid biosynthesis." Biochemistry 31(20): 4737-4749.

Salen, G., D. Verga, et al. (1982). "Effect of 7-ketolithocholic acid on bile acid metabolism in humans." Gastroenterology 83(2): 341-347.

Schmidt, D. R., S. R. Holmstrom, et al. (2010). "Regulation of Bile Acid Synthesis by Fat-soluble Vitamins A and D." Journal of Biological Chemistry 285(19): 14486-14494.

Schwarz, M., E. G. Lund, et al. (1997). "Identification and Characterization of a Mouse Oxysterol 7α-Hydroxylase cDNA." Journal of Biological Chemistry 272(38): 23995-24001.

Schwarz, M., E. G. Lund, et al. (1996). "Disruption of Cholesterol 7α-Hydroxylase Gene in Mice: II. Bile acid deficiency is overcome by induction of oxysterol 7α-hydroxylase." Journal of Biological Chemistry 271(30): 18024-18031.

Schwarz, M., D. W. Russell, et al. (1998). "Marked reduction in bile acid synthesis in cholesterol 7α-hydroxylase-deficient mice does not lead to diminished tissue cholesterol turnover or to hypercholesterolemia." Journal of Lipid Research 39(9): 1833-1843.

Schwarz, M., D. W. Russell, et al. (2001). "Alternate pathways of bile acid synthesis in the cholesterol 7α-hydroxylase knockout mouse are not upregulated by either cholesterol or cholestyramine feeding." Journal of Lipid Research 42(10): 1594-1603.

Schweizer, R. A. S., M. Zürcher, et al. (2004). "Rapid Hepatic Metabolism of 7-Ketocholesterol by 11β-Hydroxysteroid Dehydrogenase Type 1." Journal of Biological Chemistry 279(18): 18415-18424.

Semjonous, N. M., M. Sherlock, et al. (2011). "Hexose-6-Phosphate Dehydrogenase Contributes to Skeletal Muscle Homeostasis Independent of 11β-Hydroxysteroid Dehydrogenase Type 1." Endocrinology 152(1): 93-102.

Senesi, S., B. Legeza, et al. (2010). "Contribution of Fructose-6-Phosphate to Glucocorticoid Activation in the Endoplasmic Reticulum: Possible Implication in the Metabolic Syndrome." Endocrinology 151(10): 4830-4839.

Seward, D. J., A. S. Koh, et al. (2003). "Functional Complementation between a Novel Mammalian Polygenic Transport Complex and an Evolutionarily Ancient Organic Solute Transporter, OSTα-OSTβ." Journal of Biological Chemistry 278(30): 27473-27482.

Sinha, J., F. Chen, et al. (2008). "β-Klotho and FGF-15/19 inhibit the apical sodium-dependent bile acid transporter in enterocytes and cholangiocytes." American Journal of Physiology - Gastrointestinal and Liver Physiology 295(5): G996-G1003.

Solaas, K., A. Ulvestad, et al. (2000). "Subcellular organization of bile acid amidation in human liver: a key issue in regulating the biosynthesis of bile salts." Journal of Lipid Research 41(7): 1154-1162.

Soroka, C. J., J. M. Lee, et al. (2001). "Cellular localization and up-regulation of multidrug resistance–associated protein 3 in hepatocytes and cholangiocytes during obstructive cholestasis in rat liver." Hepatology 33(4): 783-791.

Soroka, C. J., A. Mennone, et al. (2010). "Mouse organic solute transporter alpha deficiency enhances renal excretion of bile acids and attenuates cholestasis." Hepatology 51(1): 181-190.

Staudinger, J. L., B. Goodwin, et al. (2001). "The nuclear receptor PXR is a lithocholic acid sensor that protects against liver toxicity." Proceedings of the National Academy of Sciences 98(6): 3369-3374.

Stedman, C. A. M., C. Liddle, et al. (2005). "Nuclear receptors constitutive androstane receptor and pregnane X receptor ameliorate cholestatic liver injury." Proceedings of the National Academy of Sciences of the United States of America 102(6): 2063-2068.

Steinberg, S. J., S. J. Mihalik, et al. (2000). "The Human Liver-specific Homolog of Very Long-chain Acyl-CoA Synthetase Is Cholate:CoA Ligase." Journal of Biological Chemistry 275(21): 15605-15608.

Stieger, B., B. Hagenbuch, et al. (1994). "In situ localization of the hepatocytic Na+/Taurocholate cotransporting polypeptide in rat liver." Gastroenterology 107(6): 1781-1787.

Stieger, B., B. O´Neil, et al. (1992). "ATP-dependent bile-salt transport in canalicular rat liver plasma-membrane vesicles." Biochem. J. 284: 67-74.

Strautnieks, S. S., L. N. Bull, et al. (1998). "A gene encoding a liver-specific ABC transporter is mutated in progressive familial intrahepatic cholestasis." Nat Genet 20(3): 233-238.

Thomas, C., R. Pellicciari, et al. (2008). "Targeting bile-acid signalling for metabolic diseases." Nat Rev Drug Discov 7(8): 678-693.

Thomas, M. P. and B. V. L. Potter (2011). "Crystal structures of 11β-hydroxysteroid dehydrogenase type 1 and their use in drug discovery." Future Medicinal Chemistry 3(3): 367-390.

Thummel, K. E., C. Brimer, et al. (2001). "Transcriptional Control of Intestinal Cytochrome P-4503A by 1α,25-Dihydroxy Vitamin D3." Molecular Pharmacology 60(6): 1399-1406.

Tint, G. S., G. R. Xu, et al. (1990). "Ursodeoxycholic acid, chenodeoxycholic acid, and 7-ketolithocholic acid are primary bile acids of the guinea pig." Journal of Lipid Research 31(7): 1301-1306.

Tomlinson, J. W. and P. M. Stewart (2007). "Modulation of glucocorticoid action and the treatment of type-2 diabetes." Best Practice & Research Clinical Endocrinology & Metabolism 21(4): 607-619.

Trauner, M. and J. L. Boyer (2003). "Bile Salt Transporters: Molecular Characterization, Function, and Regulation." Physiological Reviews 83(2): 633-671.

Turncliff, R. Z., P. J. Meier, et al. (2004). "EFFECT OF DEXAMETHASONE TREATMENT ON THE EXPRESSION AND FUNCTION OF TRANSPORT PROTEINS IN SANDWICH-CULTURED RAT HEPATOCYTES." Drug Metabolism and Disposition 32(8): 834-839.

Usui, E., K. Okuda, et al. (1994). "Rat Hepatic 3α-Hydroxysteroid Dehydrogenase: Expression of cDNA and Physiological Function in Bile Acid Biosynthetic Pathway." Journal of Biochemistry 115(2): 230-237.

Van Veldhoven, P. P., G. Vanhove, et al. (1992). "Substrate specificities of rat liver peroxisomal acyl-CoA oxidases: palmitoyl-CoA oxidase (inducible acyl-CoA oxidase), pristanoyl-CoA oxidase (non-inducible acyl-CoA oxidase), and trihydroxycoprostanoyl-CoA oxidase." Journal of Biological Chemistry 267(28): 20065-20074.

Wamil, M., J. H. Battle, et al. (2011). "Novel Fat Depot–Specific Mechanisms Underlie Resistance to Visceral Obesity and Inflammation in 11β-Hydroxysteroid Dehydrogenase Type 1–Deficient Mice." Diabetes 60(4): 1158-1167.

Wang, H., J. Chen, et al. (1999). "Endogenous Bile Acids Are Ligands for the Nuclear Receptor FXR/BAR." Molecular Cell 3(5): 543-553.

Wang, R., H.-L. Chen, et al. (2009). "Compensatory role of P-glycoproteins in knockout mice lacking the bile salt export pump." Hepatology 50(3): 948-956.

Wang, R., M. Salem, et al. (2001). "Targeted inactivation of sister of P-glycoprotein gene (spgp) in mice results in nonprogressive but persistent intrahepatic cholestasis." Proceedings of the National Academy of Sciences 98(4): 2011-2016.

Wang, X., A. Spandidos, et al. (2012). "PrimerBank: a PCR primer database for quantitative gene expression analysis, 2012 update." Nucleic Acids Research 40(D1): D1144-D1149.

Washizu, T., Tomoda, I., Kaneko, JJ. (1991). "Serum bile acid composition of the dog, cow, horse and human." The Journal of Veterinary Medical Science 53(1): 81-86.

Weerachayaphorn, J., A. Mennone, et al. (2012). "Nuclear factor-E2-related factor 2 is a major determinant of bile acid homeostasis in the liver and intestine." American Journal of Physiology - Gastrointestinal and Liver Physiology 302(9): G925-G936.

Wieland, H. O. (1928). "The chemistry of the bile acids." Nobel Lecture December, 12, 1928.

Wikvall, K. (1981). "Purification and properties of a 3 beta-hydroxy-delta 5-C27-steroid oxidoreductase from rabbit liver microsomes." Journal of Biological Chemistry 256(7): 3376-3380.

Wilson, F. A., G. Burckhardt, et al. (1981). "Sodium-coupled Taurocholate Transport in the Proximal Convolution of the Rat Kidney In Vivo and In Vitro." The Journal of Clinical Investigation 67(4): 1141-1150.

Wistuba, W., C. Gnewuch, et al. (2007). "Lithocholic acid induction of the FGF19 promoter in instestinal cells is mediated by PXR " World Journal of Gastroenterology 13(31): 4230-4235.

Wong, M. H., P. Oelkers, et al. (1995). "Identification of a Mutation in the Ileal Sodium-dependent Bile Acid Transporter Gene That Abolishes Transport Activity." Journal of Biological Chemistry 270(45): 27228-27234.

Wsól, V. r., B. Szotáková, et al. (2003). "Stereochemical aspects of carbonyl reduction of the original anticancer drug oracin by mouse liver microsomes and purified 11β-hydroxysteroid dehydrogenase type 1." Chemico-Biological Interactions 143–144(0): 459-468.

Yamanishi, Y., Y. Nosaka, et al. (1985). "Sterol and bile acid metabolism after short-term prednisolone treatment in patients with chronic active hepatitis." Gastroenterologia Japonica 20(3): 246-251.

Zelcer, N., K. v. d. Wetering, et al. (2006). "Mice lacking Mrp3 (Abcc3) have normal bile salt transport, but altered hepatic transport of endogenous glucuronides." Journal of Hepatology 44(4): 768-775.

Zhang, M. and J. Y. L. Chiang (2001). "Transcriptional Regulation of the Human Sterol 12α-Hydroxylase Gene (CYP8B1): roles of hepatocyte nuclear factor 4α in mediating bile acid repression " Journal of Biological Chemistry 276(45): 41690-41699.

Zollner, G., P. Fickert, et al. (2003). "Role of nuclear bile acid receptor, FXR, in adaptive ABC transporter regulation by cholic and ursodeoxycholic acid in mouse liver, kidney and intestine." Journal of Hepatology 39(4): 480-488.

8 ACKNOWLEDGEMENTS

I thank to Professor Alex Odermatt for the opportunity to develop this thesis in his laboratory and to all members of the laboratory for the support. I thank to Novartis for the opportunity of conducting this joint PhD program and to all members of the department of Discovery and Investigative Safety (DIS, NIBR) who helped in many aspects the execution of this work, for instance, ordering materials and reagents, giving advices, sharing ideas and protocols, and so forth. Thanks to the scientists who have been directly involved in supplying materials, samples, chemicals, plasmids, and thus helped to directly materialize this work. Thanks to the Prodoc steering committee for the opportunity of obtaining the education in toxicology and to all Prodoc members. Thanks to the University of Basel, Biozentrum and Pharmazentrum staff and members for contributing for my education.

9 DECLARATION

I, Carlos Alberto Penno declare that I have written this thesis "**The Role of 11β-Hydroxysteroid Dehydrogenase Type 1 in Bile Acid Homeostasis**" with the help indicated and that I have only submitted it to the Faculty of Science of the University of Basel and to no other faculty or university.

Carlos Alberto Penno

Basel, 12.03.2013